Connectivity-Aware Routing Algorithms

for Cognitive Radio Networks

By

Mahmoud M. Gad

Thesis submitted to the

Faculty of Graduate and Postdoctoral Studies

in partial fulfillment of the requirements

for the Doctorate in Philosophy degree in Electrical and Computer Engineering

School of Electrical Engineering and Computer Science

Faculty of Engineering

University of Ottawa

Abstract

The increased demand on wireless applications, coupled with the current inefficiency in spectrum usage, mandate a new communication paradigm shift from fixed spectrum assignment to dynamic spectrum sharing which can be achieved using the cognitive radio technology. Cognitive radio allows unlicensed secondary nodes to form communication links over licensed spectrum bands on an opportunistic basis which increases the spectrum management efficiency. Cognitive radio networks (CRN), however, impose unique challenges due to the fluctuation in the available spectrum as well as the diverse quality of service requirements. One of the main challenges is the establishment and maintenance of routes in multi-hop CRNs. In this thesis, we critically investigate the problem of routing in multi-hop CRNs. The main objective of this research is to maximize network connectivity while limiting routing delay. We developed a general connectivity metric for single-band and multi-band CRNs based on the properties of the Laplacian matrix eigenvalues spectrum. We show through analytical and simulation results that the developed metric is more robust and has lower computational complexity than the previously proposed metrics. Furthermore, we propose a new position-based routing algorithm for large scale CRNs which significantly reduces the routing computational complexity with negligible performance degradation compared to the traditional full node search algorithm. In addition, the connectivity metric developed in this thesis is used to develop a connectivity-aware distributed routing protocol for CRNs. Finally, we use a commodity cognitive radio testbed to demonstrate the concept of CR Wi-Fi networks.

Acknowledgements

I would like to express my deepest gratitude to my supervisor Professor Hussein T. Mouftah for his outstanding guidance, support and motivation since I joined this program and throughout the writing of this dissertation. His meticulous supervision has not only educated me in research work but it will also serve as an inspiration and a model to follow in the future. Without his guidance and support, this dissertation would not have been possible.

Many thanks go to Dr. Ahmed Farid, my colleague at the School of Electrical Engineering and Computer Science, who spent a considerable amount of his time with me in brainstorming ideas and approaches.

Dedication

I would like to dedicate this thesis to my dear wife, Mai ElAmir, for her unlimited support and help to overcome the occasional hard times and moments of frustration that often happen during research work. With her invaluable advice and moral support, I was able to successfully complete my PhD.

My special thanks go to my parents who encouraged me to pursue my doctoral study. They have been the major driving force that led to my success.

Table of Contents

List of Figures

List of Acronyms

AC	Algebraic Connectivity
AF	Activity Factor
AODV	Ad hoc On-demand Distance Vector
AP	Access Point
BEP	Bandwidth Footprint Product
BPP	Binomial Point Process
CAODV	Cognitive Ad hoc On-demand Distance Vector
CCAC	Compact Cognitive Algebraic Connectivity
CCC	Common Control Channel
CDF	Cumulative Distribution Function
CE	Cognitive Engine
CNC	Cognitive Natural Connectivity
CNCR	Cognitive Natural Connectivity Routing
CORAL	COgnitive RAdio Learning Platform

CR	Cognitive Radio
CRAHN	Cognitive Radio Ad Hoc Network
CRN	Cognitive Radio Network
CR-NMS	Cognitive Radio Network Management System
CSMA	Carrier Sense Multiple Access
DARPA	Defense Advanced Research Projects Agency
DFR	Dual Frequency Routing
DORP	Delay motivated On-demand Routing Protocol
DSA	Dynamic Spectrum Access
ECAC	Expected value of Cognitive Algebraic Connectivity
ETX	Expected Transmission Count
FCC	Federal Communication Commission
FNR	Farthest-Neighbor Routing
ISM	Industrial, Scientific and Medical Band
MAC	Medium Access Control
MBCNC	Multi-band Cognitive Natural Connectivity

MILP	Mixed Integer Linear Programming
MINLP	Mixed Integer Non-Linear Programming
MMD	Minimum Multi-hop Delay
NC	Natural Connectivity
NNR	Nearest-Neighbor Routing
PDF	Probability Density Function
POFR	Probability of Finding a Route
PORC	Probability of Finding a Route in Cognitive Networks
PPP	Poisson Point Process
PU	Primary User
QoS	Quality of Service
RA	Route Availability
ROSA	ROuting and Spectrum Allocation
RREP	Route Reply
RREQ	Route REQuest
SAMER	Spectrum Aware Mesh Routing

SCNC	State Cognitive Natural Connectivity
SEARCH	SpEctrum Aware Routing protocol for Cognitive ad Hoc networks
SFR	Single Frequency Routing
SNR	Signal-to-Noise Ratio
SOP	Spectrum Opportunity
SPEAR	Spectrum Aware Routing
STOD-RA	Spectrum Tree On Demand Routing
SU	Secondary User
TDM	Time Division Multiplexing
USRP	Universal Software Radio Peripheral
WiFi-CR	WiFi-Cognitive Radio
WLAN	Wireless Local Area Network
WRAN	Wireless Regional Area Network

List of Symbols

N	Number of Secondary Users
λ_s	Secondary user density
λ_c	Critical density
G	Graph
d_i	Node degree
$A(\Delta)$	Cognitive Adjacent Matrix
λ_2	Algebraic Connectivity
R	PU transmission range
r	SU transmission range
f	Frequency
d_{ij}	Degree matrix element (i, j)
$a_{i,j}$	Adjacent matrix element (i, j)
L	Laplacian matrix
$\overline{\lambda}$	Natural connectivity
S	Source
D	Destination
L_{SD}	Source-Destination distance

Chapter 1

Introduction

1.1 Cognitive Radio Networks Overview

The limited available spectrum and the inefficiency in the spectrum usage mandate a new communication paradigm shift from fixed communication to dynamic communication. The basic idea of Cognitive Radio Networks (CRNs) is that the unlicensed devices (also known as cognitive radio nodes or secondary users) need to vacate the band once the licensed device (also known as a primary user) is detected. CRNs, however, impose unique challenges due to the high fluctuation in the available spectrum as well as the diverse quality of service (QoS) requirements. Specifically in Cognitive Radio Ad Hoc Networks (CRAHNs), the distributed multi-hop architecture, the dynamic network topology, and the time and location varying spectrum availability are some of the key distinguishing factors. These challenges necessitate novel design techniques that simultaneously address a wide range of communication problems spanning several layers of the protocol stack [AKY-09] and [MAR-12].

In CRNs, the existence of a communication link between two secondary users depends not only on the distance between them but also on the availability of the communication channel, i.e., the presence of a spectrum opportunity offered by the primary network. As a result, even in a static secondary network, communication links are time-varying due to the temporal dynamics

of spectrum opportunities. Thus the CRN connectivity affects the network's QoS level and requires designing special routing algorithms for CRNs which take into account the time-varying nature of CRN communication links.

Several routing solutions for CRNs were proposed in the literature. These algorithms may be sorted into different categories depending on the classification criteria. CRN routing algorithms may be categorized based on the availability of spectrum knowledge. They can also be categorized based on the main criteria which the routing metric uses to select best routes, e.g. delay, throughput, location, or power consumption. CRN routing algorithms can also be categorized depending on the mobility of the secondary users and the number of available spectrum bands, i.e. single or multi-band.

1.2 Motivation

While cognitive radio networks open the door for a tremendous amount of opportunities such as increased spectrum usage efficiency, they nonetheless impose unique challenges. In traditional wireless networks, a communication link exists between two nodes if they are within the transmission range of each other. However, in cognitive radio networks, the existence of a communication link depends also on the primary user activity. Thus, the connectivity of CRNs is a time-varying parameter. The problem gets more complicated when multi-hop cognitive radio networks are considered. For example, a route between two nodes in a CRN can be affected by different primary users in different spectrum bands. Thus, to evaluate the overall route quality, the activity factor of these PUs must be taken into consideration.

In the past few years, the connectivity of CRNs has been studied and a number of measures have been proposed to quantify it using different graph theory tools. These tools usually suffer either from numerical complexity or a lack of robustness when applied in different CRNs scenarios. In this thesis, we are addressing, in detail, the problem of measuring the connectivity of CRNs with multiple primary users operating on multiple frequency bands. The conclusions will be used later to design distributed connectivity-aware routing algorithms for CRNs.

There has recently been a growing interest in large scale CRNs for different applications. The increased demand for these CRNs poses enormous challenges in designing routing protocols for CRNs, a topic we will address in detail later.

1.3 Objectives

Our objective in this thesis is to study in-depth the challenges and opportunities in the area of routing for CRNs, to propose a new connectivity metric to measure the CRN connectivity under different scenarios, and to propose novel routing algorithms for single and multi-band CRNs. The main objective of this research is to maximize network connectivity while limiting routing delay. This promises to be immensely challenging due to the nature of spectrum availability in CRNs. Spectrum holes are available temporarily and must be used on an opportunistic basis. As a result, the routing decision should be both fast and robust. There is a limited time opportunity to use a given spectrum hole. This thesis focuses on designing robust and computationally inexpensive routing metrics and algorithms for CRNs.

1.4 Contributions

The main research contributions of this thesis are as follows:

- Developed a new connectivity metric for cognitive radio networks with multiple disjointed primary users operating in the same frequency band. The new connectivity metric, named *Cognitive Natural Connectivity (CNC)*, is a robust measure and has low computational complexity.
- Proposed a generalized connectivity metric for multi-band, multiple PU CRNs based on the CNC metric. The generalized metric can be used to analyze, design, and plan multi-band CRNs without any pre-conditions on the CRN node distribution as in previous studies.
- Proposed a location-based routing algorithm for large scale CRNs. This algorithm limits the routing delay, significantly reduces the problem complexity, and provides negligible performance degradation when compared to the performance of the complete network search space.
- Proposed a connectivity-aware distributed routing algorithm for CRNs which attempts to balance between long-term route stability and short-term performance measures such as end-to-end delay.
- Carried out an interference measurement experiment in the 2.4 GHz ISM band using the COgnitive Radio Learning platform (CORAL) and used it to demonstrate the applications of CRN in future Wi-Fi networks.

1.5 Thesis Outline

The thesis consists of seven chapters which may be briefly outlined as follows:

Chapter 1 is an Introduction in which the main purpose and direction of the thesis are set out. Chapter 2 offers a review of the state of the art in the field of routing for CRNs. It examines the multi-hop cognitive radio network connectivity problem as well as the routing algorithms for CRNs. In Chapter 3, a new connectivity metric for multi-primary-user CRNs is developed. In Chapter 4, the connectivity of multi-band CRNs is studied and a generalized connectivity metric is proposed. In Chapter 5, an efficient location-based routing algorithm for large scale CRNs is presented. In Chapter 6, a distributed connectivity-aware CRN routing algorithm is proposed followed by a discussion of the application of cognitive radio in future Wi-Fi networks. Finally, in Chapter 7, conclusions and future research directions are addressed.

1.6 List of Publications

Journal Papers

- Mahmoud Gad, Ahmed Farid, Hussein T. Mouftah, “New Connectivity Metric for Multi-Primary-Users Cognitive Radio Ad Hoc Networks”, Submitted to IEEE Transactions on Cognitive Communications and Networking.
- Mahmoud Gad, Ahmed Farid, Hussein T. Mouftah, “A Location-Based Routing Algorithm for Large-Scale Cognitive Radio Networks”, Submitted to Elsevier Ad Hoc Networks Journal.

Conference Papers

- Mahmoud Gad, Ahmed Farid, Hussein T. Mouftah, "On the Connectivity of Multi-band Cognitive Radio Ad Hoc Networks," Proceedings of the IEEE 27th Canadian Conference on Electrical and Computer Engineering (CCECE), pp.1-6, May 2014.
- Mahmoud Gad, Ahmed Farid, Hussein T. Mouftah, "A New Connectivity Metric for Cognitive Radio Networks," Proceedings of the IEEE 24th International Symposium on Personal Indoor and Mobile Radio Communications (PIMRC), pp.2893-2897, September 2013.
- Mahmoud Gad, Ahmed Farid, Hussein T. Mouftah, "A Reduced Search Space Routing Algorithm for Large-scale Cognitive Radio Wireless Networks," Proceedings of the 26th Annual IEEE Canadian Conference on Electrical and Computer Engineering (CCECE), pp.1-4, May 2013.
- Mahmoud Gad, Mostafa El-Khamy, Hussein T. Mouftah, "Dual Band Connectivity of Cognitive Radio Networks", CogART 2011, Barcelona, Spain, October 2011.

Posters

- Mahmoud Gad, and Hussein T. Mouftah, "Mining Wi-Fi Spectrum Usage Data: Techniques and Applications", 6th WiSense Workshop, Ottawa, August 2014.
- Mahmoud Gad, Ahmed Farid, Hussein T. Mouftah, "A Fast Position-Based Routing Algorithm for Large-Scale Wireless Cognitive Radio Networks", 5th WiSense Workshop, Ottawa, August 2013 (won the best poster award).
- Mahmoud Gad, and Hussein T. Mouftah, "A Genetic Algorithm Based Routing Protocol for Multi-Band Cognitive Radio Networks", 4th WiSense Workshop, Ottawa, September 2012.

- Mahmoud Gad, Mostafa El-Khamy, Hussein T. Mouftah, “On the Connectivity of Cognitive Wireless Sensor Networks”, 3rd WiSense Workshop, Ottawa, September 2011
- Mahmoud Gad, Hussein T. Mouftah, M. Bennai and John Sydor; “A MATLAB Toolbox for the CORAL Development Platform”, 3rd WiSense Workshop, Ottawa, September 2011 (won the 3rd place poster award).
- Mahmoud Gad and Hussein T. Mouftah, “Routing Protocols for Cognitive Wireless Sensor Networks”, presented at the 2010 WiSense Workshop, Queen’s University, Kingston, May 2010.
- Mahmoud Gad and Hussein T. Mouftah, “Cognitive Radio for Wireless Sensor Networks”, Poster presented at the 2009 WiSense Workshop, University of Ottawa, Ottawa, July 2009.

Chapter 2

State of the Art

2.1 Introduction to Cognitive Radio Networks

Today's wireless networks are regulated by a fixed spectrum assignment policy, i.e. the spectrum is regulated by governmental agencies and is assigned to license holders or services on a long term basis for large geographical regions. The spectrum usage is concentrated on certain portions of the spectrum while a significant amount of the spectrum remains underutilized. According to the Federal Communication Commission (FCC), temporal and geographical variations in the utilization of assigned spectrum range from 15% to 85% [FCC-03] and similar results are found in [PAT-11].

For many years, it has been believed that the spectrum shortage was due to the proliferation of wireless applications and their substantial bandwidth usage. However, spectrum measurements around different metropolitan areas show that vast portions of the licensed spectrum are not in use [McH-07, SEE-07]. This finding suggests that an improvement in spectrum utilization can solve the spectrum shortage problem.

The limited available spectrum and the inefficiency in the spectrum usage necessitate a new communication paradigm shift from fixed communication to dynamic communication. Dynamic spectrum access is considered a solution to the inefficient spectrum usage problems. The

approach of the Defense Advanced Research Projects Agency (DARPA) on dynamic spectrum access networks, aims at implementing a policy-based intelligent radio, widely known as cognitive radios [DAR-03]. The basic idea of cognitive radio networks is that the unlicensed devices (also known as cognitive radio or secondary users) need to vacate the band once the licensed device (also known as a primary user) is detected. CRNs, however, impose unique challenges due to the high fluctuation in the available spectrum as well as the diverse QoS requirements. Specifically in CRAHNs, the distributed multi-hop architecture, the dynamic network topology, the time varying, and the location varying spectrum availability are some of the key distinguishing factors. These challenges necessitate novel design techniques that would simultaneously address a wide range of communication problems spanning several layers of the protocol stack [AKY-09].

The concept of cognitive radio was first introduced by Mitola in his Ph.D. thesis [MIT-00] as a radio that can learn from its surrounding radio environment and adjust its parameters using this learning process. The FCC formally defines CR in [FCC-03] as follows: “A cognitive radio is a radio that can change its transmitter parameters based on interaction with the environment in which it operates”. It is worth noting that CR is a design concept rather than a communication system or standard. Cognitive radio can be used to improve the performance of the existing communication systems as well as a design concept for new systems solely based on dynamic spectrum access.

From the above definition we can identify two main characteristics of a CR: *cognitive capability* and *reconfigurability*. The cognitive capability refers to the ability of the radio technology to

capture the information from its radio environment. This capability requires the continuous sensing of the surrounding environment as well as the ability to characterize and learn about the transmission type in these bands. Through this capability, the portions of the spectrum that are unused at a specific time or location can be identified. Consequently, the best spectrum and appropriate operating parameters can be selected. Reconfigurability enables the radio to be dynamically programmed according to the radio environment. More specifically, a cognitive radio can be programmed to transmit and receive on a variety of frequencies and to use different transmission access technologies by its hardware design [JON-05].

Cognitive radio techniques provide the capability to use or share the spectrum in an opportunistic manner. Dynamic spectrum is one of the cognitive radio access techniques which allow a cognitive radio to operate in the best available channel. The ultimate objective of cognitive radio is to obtain the best available spectrum through cognitive capability and reconfigurability.

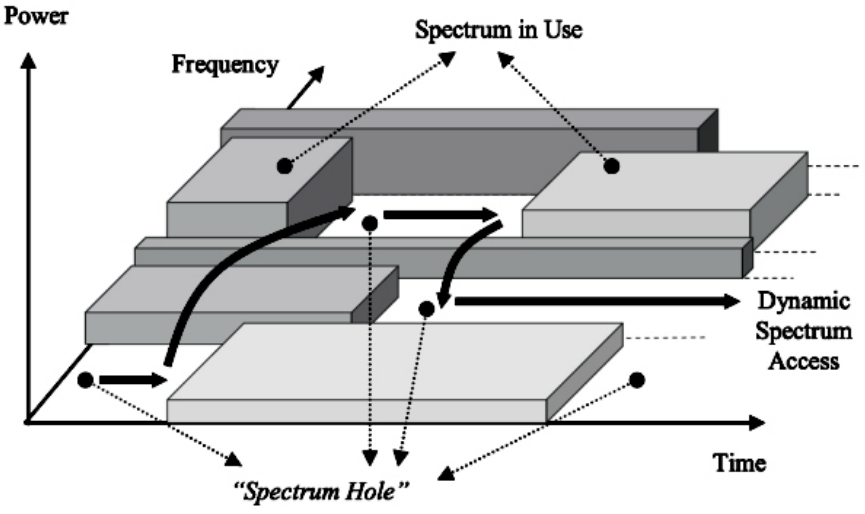

Figure 2.1: The spectrum holes concept [AKY-09].

Since most of the spectrum is already assigned, the most important challenge is to share the licensed spectrum without interfering with the transmission of the licensed users, as illustrated in Figure 2.1. Cognitive radio enables the usage of temporarily unused spectrum bands, which are referred to as *spectrum holes* or *white spaces*. If this band is to be used by a licensed user, the cognitive radio moves to another spectrum hole or stays in the same band waiting for an opportunity to transmit, as shown in Figure 2.1.

2.2 Classical Multi-hop Networks vs. Cognitive Radio Networks

Multi-hop CRNs have some unique features if compared to classical multi-hop wireless networks. The first difference is in the transmission spectrum. In CRNs, the available spectrum bands are distributed over a wide frequency range, which varies in time and space. Thus, each user has a different spectrum availability according to the PU activity. The key difference is that the PU must be guarded from the SU transmission.

The second difference is the multi-hop transmission. The end-to-end route in CRNs consists of multiple hops having different channels according to the spectrum availability. Thus, CRNs require collaboration between routing and spectrum assignment in order to establish these routes [WAN-06]. Taking the PU activity into consideration, the end-to-end QoS involves not only traffic load, but also the spectrum availability throughout the route. The third difference can be noticed in mobile CRNs. These networks have to distinguish between disturbances caused by node mobility (due to variation in the channel conditions) and those caused by the PU activity in order to correctly predict the best next hop.

2.3 Spectrum Management for Cognitive Radio Networks

Nodes in CRNs can be classified into two groups: primary users and secondary users. A CRN needs special functionality to share the licensed spectrum band with the PU nodes. In order to adapt to the dynamic spectrum environment, the CRNs require a spectrum-aware operation. The spectrum management framework discussed in [AKY-09] has 3 main functions: spectrum sensing, spectrum decision, and spectrum sharing. The first function is spectrum sensing in which the CR user monitors the available spectrum bands and then detects spectrum holes. Spectrum sensing is the most important function in CR networks and we will give more details about it in the next section. The second function is the spectrum decision in which the available spectrum bands are identified. It is essential that the CR nodes select the most appropriate band according to their QoS requirements. In order to design a decision algorithm that incorporates dynamic spectrum characteristics, we need to obtain *a priori* information regarding the PU activity. Furthermore, the spectrum decision involves undertaking spectrum selection and route formation. Finally, the third function is spectrum sharing between different SUs. Spectrum sharing provides the capability to share the spectrum resources opportunistically with multiple CR users. In this area, game theory was used to analyze the behavior of CR nodes and design MAC protocols that ensure fairness between different CR users, as in [LIA-11].

The performance of CRNs is highly affected by the used spectrum sensing method and its quality (in terms of the probability of detection and the probability of false alarm); and the frequency of the spectrum sensing operations. Two main categories of spectrum sensing techniques can be found in the literature: narrowband spectrum sensing techniques and

wideband spectrum sensing techniques. The narrowband techniques include: energy detector based sensing, waveform-based sensing, cyclostationarity-based sensing, and matched-filtering. Wide-band techniques include both Nyquist wideband sensing and sub-Nyquist wideband sensing [SUN-13].

Energy detector based approach is the most common method of spectrum sensing because of its low computational and implementation complexity. In addition, it is more generic as receivers do not need any knowledge of the primary users' signal. The signal is detected by comparing the output of the energy detector with a threshold which depends on the noise floor. Some of the problems facing energy detectors include the selection of the threshold for detecting primary users, the inability to differentiate interference from primary users and noise, and poor performance under low Signal-to-Noise Ratio (SNR) values. Moreover, energy detectors do not work efficiently in detecting spread spectrum signals [YUC-09].

Waveform-based sensing utilizes known patterns which are usually used in wireless systems to assist synchronization among other functions. Such patterns include preambles, pilot patterns, spreading sequences, etc. In the presence of a known pattern, sensing can be performed by correlating the received signal with a known copy of itself. This method is only applicable to systems with a known signal pattern.

Cyclostationary feature detection is a method used for detecting primary user transmissions by exploiting the cyclostationary features of the received signals. Cyclostationary features are caused by the periodicity in the signal or in its statistics. They can also be intentionally induced to assist spectrum sensing.

Matched-filtering based sensing is known as the optimum method for the detection of primary users when the transmitted signal is known.

A basic comparison of the different narrowband sensing methods, discussed above, is shown in Figure 2.2. For example waveform-based sensing is more accurate (in terms of the probability of detection and the probability of false alarms) than energy detector and cyclostationarity based methods because of the coherent processing that comes from using deterministic signal components. However, there should be *a priori* information about the primary user's characteristics and primary users should transmit known patterns or pilots.

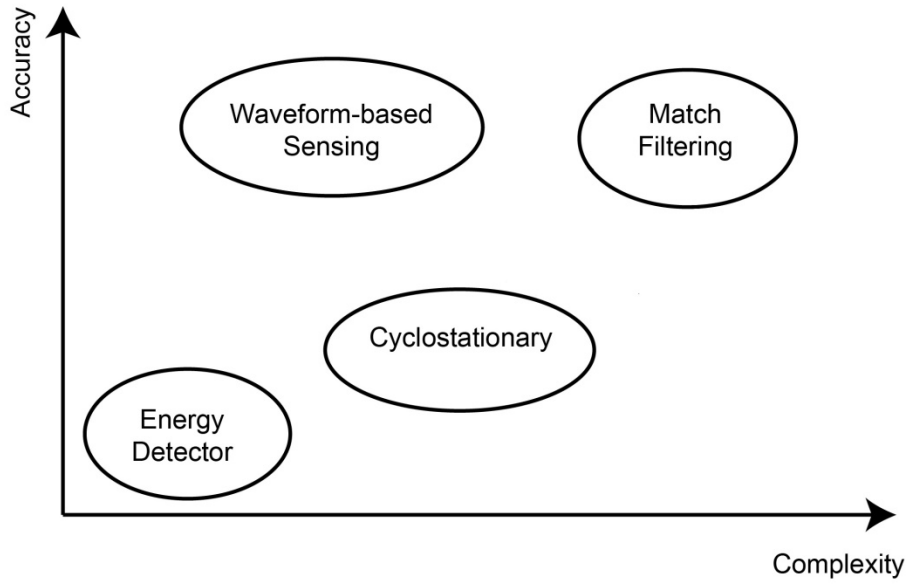

Figure 2.2: Comparison between different narrowband sensing methods in terms of their sensing accuracies and complexities [YUC-09].

In wideband Nyquist wideband sensing techniques, the signal is directly acquired using an analog to digital converter and then digital signal processing techniques are used to detect the availability of a spectrum opportunity. The drawback of these techniques is the analog to digital

converter's high sampling rate and the high implementation complexity. In sub-Nyquist wideband sensing techniques, wideband signals are acquired using sampling rates lower than the Nyquist rate and then spectral opportunities are detected using those partial measurements. Sub-Nyquist techniques can be classified into two main categories: compressive sensing-based wideband sensing and multi-channel sub-Nyquist wideband sensing.

2.4 Connectivity in Cognitive Radio Networks

The research in the connectivity of wireless networks, specially the scaling law, has received increasing interest in the research community since the work of Gupta and Kumar [GUP-00]. The capacity scaling laws of CR networks have been analyzed in [VU-07], [JEO-11], [JIA-14] and [FRA-08]. The scaling law of the multi-hop delay in homogeneous ad hoc networks has been extensively studied in the literature. The multi-hop delay for a specific routing algorithm is analyzed in [YIN-08b], [BAN-03], and [SHA-04], while the capacity-delay trade-off is studied under a given network and mobility model in [NEE-05], [SHA-07], and [LE-09]. The scaling law of the multi-hop delay with respect to the source-destination distance is established in [YIN-08a], [ZHE-06], and [XU-08].

In [REN-11], the authors analytically characterized the connectivity and multi-hop delay of the secondary network. They used a Poisson distributed secondary network overlaid with a Poisson distributed primary network in an infinite two-dimensional Euclidean space. The contribution of [REN-11] is that it analytically characterizes the connectivity of the secondary network, where the connectivity is defined by the finiteness of the Minimum Multi-hop Delay (MMD) between two randomly chosen secondary users.

Under the used Poisson model, the key parameter that characterizes the topological structure of the secondary network is the density λ_S of the secondary users. For a given transmission power and interference tolerance of the PU network, the key parameter that characterizes the impact of the primary network is the PU's density λ_{PT}. The connectivity of the secondary network can thus be characterized by a partition of the (λ_S, λ_{PT}) plane as shown in Figure 2.3.

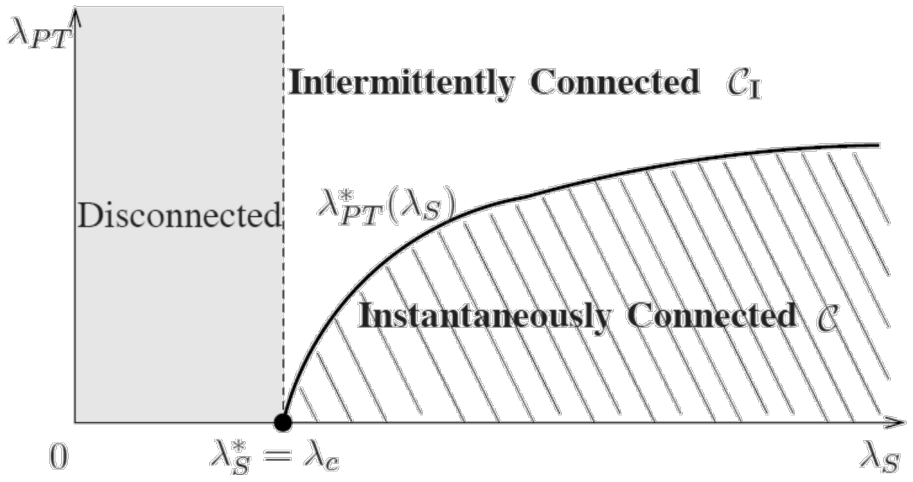

Figure 2.3: Connectivity regions of ad hoc cognitive radio networks

When $\lambda_S > \lambda_c$ (critical density), it is shown in [REN-11] that for any two secondary users in this infinite topologically connected component, the MDD is finite almost surely. While the secondary network is connected and the MDD is finite, whenever there are sufficient topological links (i.e., $\lambda_S > \lambda_c$), there may not be sufficient communication links to make the network instantaneously connected at any given time. The latter is determined by the traffic load of the primary network. As illustrated in Figure 2.3, for any given density λ_S of the secondary users with $\lambda_S > \lambda_c$, there exists a maximum density $\lambda^*_{PT}(\lambda_S)$ of the primary transmitters beyond which the secondary network is only intermittently connected. When the SU's network intermittently connected, messages can only traverse the topological path connecting two

secondary users by making stops in between to wait for spectrum opportunities. It is thus natural to expect that the MDD will behave differently in an instantaneously connected secondary network as compared to an intermittently connected secondary network.

While the work in [REN-11] defines three operation modes for multi-hop cognitive radio networks, it does not measure how well a CRN is connected under different situations including: different node distributions, non-equal PU and SU activity factors, and in multi-band CRNs. Moreover, the analysis in this work depends on the assumption that SU nodes are distributed following a Poisson distribution which is not the case in many practical scenarios. In addition, there is little work done so far in the area of connectivity in CRNs specially in the area of multi-band CRNs where the CR has the capability of working in different frequency bands (e.g. 700 MHz and ISM 2.4 GHz), and where the network topology depends on the used frequency band. We will discuss this problem in detail in Chapter 4.

2.5 Routing in CRNs: Challenges

The problem of routing in multi-hop CRNs targets the creation and the maintenance of wireless multi-hop paths among SUs by deciding both the relay nodes and the spectrum to be used on each link of the path. Such a problem exhibits similarities with routing in multi-channel, multi-hop ad hoc networks and mesh networks, but with the additional challenge of having to deal with the simultaneous transmissions of the PUs which dynamically change the Spectrum Opportunities (SOPs) availability. The main challenges for routing data throughout multi-hop CRNs, as discussed in [CES-10], are as follows:

The first challenge is the *spectrum-awareness* in which designing efficient routing solutions for multi-hop CRNs requires a coupling between the routing protocol and the spectrum management algorithms such that the routing protocol can be continuously aware of the surrounding physical environment to take more accurate decisions. There are three scenarios in this case. First, spectrum occupancy information can be provided to the routing protocol by an external entity (e.g., SUs may have access to a database of white spaces of TV towers [FCC-08]). Second, spectrum occupancy information is to be gathered locally by each SU through local and distributed sensing mechanisms. Third, spectrum occupancy information could be gathered using a hybrid solution of the two previous scenarios.

The second challenge is the setup of *quality* routes in a dynamic variable environment. The actual topology of multi-hop CRNs is highly influenced by PUs' behavior, and classical ways of measuring and assessing the quality of end-to-end routes (nominal bandwidth, throughput, delay, energy efficiency and fairness) should be coupled with novel measures on path stability, spectrum availability and PU presence. The used routing metrics would differ according to the PU's activity which ranges from low, moderate, to high [KHA-09].

The third challenge is the route maintenance and reparation in multi-hop CRNs. The sudden appearance of a PU in a given location may render a given channel unusable in a given area, thus resulting in unpredictable route failures, which may require frequent path rerouting either in terms of nodes or used channels.

2.6 Taxonomy of Routing Algorithms for CRNs

As we discussed earlier, several routing solutions are proposed in the literature. These algorithms can be categorized into two main classes depending on the assumptions made on the issue of spectrum-awareness: full spectrum knowledge based algorithms and local spectrum knowledge based algorithms [YOU-14], [CES-10].

2.6.1 Routing schemes based on full spectrum knowledge

The FCC has recently promoted the opportunistic use of white spaces in the spectrum below 900 MHz and in the 3 GHz bandwidth through the use of centrally-maintained spectrum data bases indicating over time and space the channel availabilities [FCC-08]. Before sending or receiving data, cognitive opportunistic devices will be required to access these databases to determine available channels. Under this scenario, the central availability of up-to-date information on spectrum occupancy completely decouples the spectrum assessment modules (sensing, sharing) from the routing decisions/policies which can be locally optimized. In this section we will summarize those routing approaches classified according to the mathematical tool used to design these protocols.

a. Graph-based routing approaches

In classical wired/wireless networks, graph theory tools have been used to study route design. Graph theory provides effective methodologies to model the multi-hop behavior of telecommunication networks, and flexible algorithms to compute multi-hop routes. The route design process in wireless multi-hop networks consists of two phases: graph abstraction and

route calculation. In the *graph abstraction* phase the physical network topology is used to generate a corresponding logical graph. The outcome of this phase is the graph structure *G = (N, V, f(V))*, where *N* is the number of nodes, *V* is the number of edges, and *f(V)* is the weight of each edge of the graph. The route calculation phase generally deals with designing a path in the graph connecting source–destination pairs. Classical approaches to route calculation widely used in wired and wireless network scenarios often use mathematical programming tools to model and design flows along multi-hop networks.

Routing through layered-graphs

The two-phase approach to route design, as previously discussed, has also been used for multi-hop CRNs. The authors of [XIN-05a,b] propose a framework to jointly address channel assignment and routing in semi-static multi-hop CRNs. In semi-static CRNs, the PU activity is assumed to be low enough for the channel assignment and the routing among SUs to be statically designed. This work focuses on the case where cognitive radio devices are equipped with a single half-duplex cognitive radio transceiver, which can be tuned to *M* available spectrum bands or channels. The framework is based on the creation of a layered graph with a number of layers equal to the number of available channels. Each SU device is represented in the layered graph with a node. The edges of the layered graph may be divided into three types: *access, horizontal, and vertical*. *Access edges* connect each node with all the corresponding sub-nodes. *Horizontal edges* between pairs of sub-nodes belonging to the same logical layer are added to the graph if the two corresponding CR devices can be connected with the corresponding channel. *Vertical edges* connect sub-nodes of different layers of a single

secondary device, and represent the capability of a secondary device to switch from one channel to another to forward incoming traffic. Figure 2.4.a shows an example of a simple four nodes network topology where A, B, and C can access both channels while node D can access channel 1 only. The corresponding layered graph architecture is shown in Figure 2.4.b.

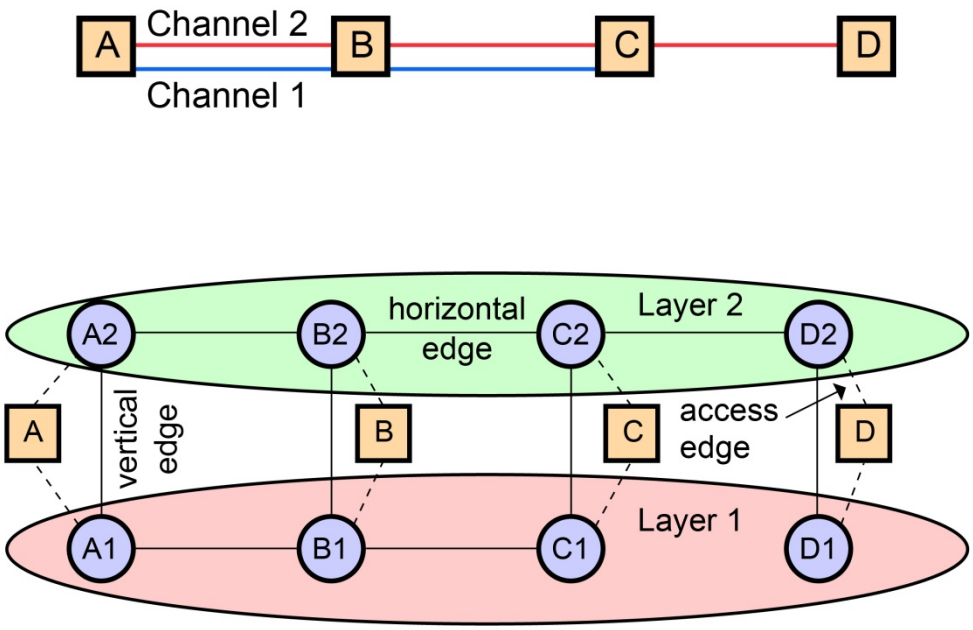

Figure 2.4: Layered-graph creation. (a) Network topology (upper), (b) Layered graph (lower)

The weight of horizontal edges could represent the specific quality of the wireless link, like bandwidth, link availability, link load, etc. The vertical edges could account for different quality parameters for different quality parameters including: the cost of switching between channels, or the improvement in the signal-to-noise ratio obtained by switching between the two given channels.

Once the graph is created and the metrics are assigned to each edge, the joint channel assignment and routing problem in the original network topology can be solved by finding

multi-hop paths between source–destination couples in the corresponding layered graph. In [XIN-05b], the authors used a metric for the horizontal links which is proportional to traffic load and interference. A centralized heuristic algorithm is proposed based on the calculation of the shortest paths in the layered graph. The proposed path-centric route calculation algorithm works iteratively by routing one source–destination flow at a time. Once a flow is routed, a new layered graph is calculated from the previous one by eliminating all unused incoming horizontal and vertical edges and re-calculating the weights assigned to the remaining edges to account for the routed traffic load.

The proposed layered graph framework is useful to jointly model channel assignment and routing in semi-static multi-hop CRNs, where the topology variability dynamics are low. On the down side, the proposed path-centric routing approach is fundamentally centralized requiring network-wide signaling support to generate the layered-graph. Moreover, the proposed iterative algorithm is suboptimal being based on a greedy approach. Finally, iterative path computation over graph abstractions may not scale well as the network dimensions increase.

Routing through colored-graphs

A similar approach based on graph structures is proposed in [ZHO-09], where a colored graph is used to represent the network topology. The colored graph $G_c = (N_c, V_c)$, where N_c is the vertex set (one vertex for each network device), and V_c is the edge set. Two vertices in the colored graph may be connected by a number of edges up to M, where M is the number of channels (colors) available for transmission on the specific link. Figure 2.5 shows an example of a five nodes network with three channels and the corresponding colored graph abstraction of the

physical network topology. The route calculation algorithm follows the same as the one proposed in [XIN-05b], using a centralized iterative approach. The shortest path is calculated for one source–destination pair on the colored graph resorting to metrics capturing the inter-link. Once a flow has been routed, the colored graph is updated by resetting the edge weights, then iterating for all the remaining traffic flows. This approach shares the same drawbacks of the layered graph approach.

User	Available Channels
A	Ch1 Ch3
B	Ch2 Ch3
C	Ch1 Ch2 Ch3
D	Ch1 Ch2
E	Ch1 Ch2

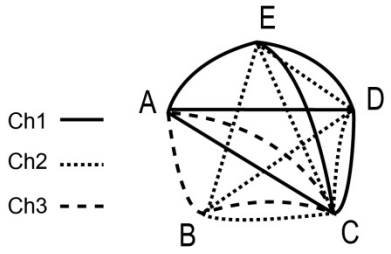

Figure 2.5: Channel assignment and the corresponding colored graph.

Routing and spectrum selection through conflict-graphs

The routing and spectrum selection problem in networks with single band cognitive radios is also addressed in [WAN-06]. The proposed solution decouples routing and channel assignment. In [WAN-06], given the network topology, all available routes between source–destination pairs are enumerated and all available channel assignment patterns are considered for each route. The *best* combination of routing and channel assignment is derived by running a centralized algorithm on a *conflict graph*. Each wireless link in the network is mapped to a vertex in the conflict graph. An edge is defined between two vertices if the corresponding wireless links

cannot be active at the same time. The conflict graph is used to derive a conflict-free channel assignment using a heuristic algorithm to calculate the maximum independent set.

This approach suffers from two problems: 1) it is not scalable; 2) this problem can be reduced to the problem of calculating the maximum independent set on a properly defined *conflict graph*, which is known to be NP-Hard.

b. Optimization approaches to routing design

Algorithms in this class assume *a priori* knowledge of the network topology and spectrum availabilities to optimally design routes in multi-hop CRNs. In [Hou-07] and [Hou-08], the authors focus on the problem of designing efficient spectrum sharing techniques for multi-hop CRNs. They introduce a Mixed Integer Non-Linear Programming (MINLP) formulation whose objective is to maximize the spectrum reuse factor throughout the network. This problem is equivalent to minimizing the overall bandwidth usage throughout the network. The proposed formulation captures different aspects of the multi-hop problem, i.e., link capacity, interference, and routing. The strengths of the works in [Hou-07] and [Hou-08] are that the proposed framework is effective in capturing many aspects of networking over multi-hop networks and that the proposed approaches provide nearly optimal solutions to the joint scheduling/routing problem for multi-hop CRNs. On the other hand, the proposed scheduling and routing algorithm is a centralized solution which assumes perfect knowledge of the network topology (presence, position and traffic pattern of the primary users, presence and position of the secondary users). Moreover, traffic splitting is allowed throughout the

secondary network. The assumption of having split traffic between secondary users may be unfeasible in practical secondary networks.

Mixed Integer Linear Programming (MILP) is also used in [MA-08], where authors introduced an MILP formulation for the problem of achieving throughput optimal routing and scheduling for secondary transmissions. The objective function aims at maximizing the source–destination pair achievable rate for small to medium size network scenarios.

2.6.2 Routing schemes based on local spectrum knowledge

This class of routing algorithms assumes the knowledge of only local spectrum information and they operate in a distributed fashion. The presented solutions are categorized according to the specific metric used to assess route quality. More details on routing metrics will be presented in Section 2.7.

a. Power-based routing algorithms

The main objective of the work in [PYO-07] is to design a routing algorithm that discovers minimum weight paths in CRNs. It assumes that the radio has access to different wireless systems (e.g. cellular or Wi-Fi) through different interfaces. It also assumes a dedicated Common Control Channel (CCC) between CR terminals to sustain cognitive radio network related functions. The weight of a link is defined as a function of the transmission power of the different wireless nodes an SU may use to communicate with a neighbor node with the assumption of free space propagation. The proposed routing protocol locally finds the path to

minimize the routing weight, which will minimize the transmission power, between a source and a destination.

It should be noticed that the model does not take into account the primary users, their behavior, or the interference caused by or to other CR nodes. The performance of the proposed system is highly dependent on the neighbor discovery procedure and its refresh rates, as there are no other maintenance or recovery procedures defined to react to PU activity.

b. Spectrum usage minimization

The authors in [SHI-08] present a distributed algorithm which addresses the scheduling, power control, and routing problems simultaneously. The routing algorithm is based on the Bandwidth Footprint Product (BFP) which refers the interference area of a node for a given transmission power. Since each node in the network uses a number of bands for transmission and each band has a certain footprint corresponding to its transmission power, the objective is to minimize the network-wide BFP, which is the sum of BFPs for all nodes in the network. It uses an iterative procedure to decide on the route selection, link scheduling, and the power allocation.

The authors show that the results of their iterative procedure are close to an upper bound derived from a MINLP formulation of the problem. However, this algorithm also requires that the spectral availability does not change throughout the algorithm operation (slow PU activity).

c. Controlled interference routing

In [XIE-10], the authors analyze the tradeoff between single-hop and multi-hop transmission for SUs constrained by the interference level that PUs can tolerate. The authors propose two

routing methods; Nearest-Neighbor Routing (NNR) and Farthest-Neighbor Routing (FNR). In the NNR scheme a transmitter attempts to find the nearest-neighbor inside a sector of a radius *D* depending on the considered QoS parameters and the positioning parameters of the SUs and PUs. Contrary to NNR, the FNR scheme searches for the farthest-neighbor within the range *D*. Performance results show that FNR achieves a better end-to-end channel utilization and reliability while NNR has better energy efficiency.

d. Delay-based solutions

The quality of routing solutions can be measured in terms of the delays to establish and maintain multi-hop routes, traffic transmission and propagation through the very same routes. Besides the classical delay components for transmitting information in wireless networks, novel components related to spectrum mobility, e.g. channel switching, link switching, should be taken into consideration in designing multi-hop CRNs. Delay-aware routing metrics are proposed in [MA-08], [CHE-07a, b] and [YAN-08], which consider different delay components including switching delay, MAC delay, and queuing delay. *Switching delay* is the delay that occurs when a node in a path switches from one frequency band to another. *Medium access delay* is based on the MAC access schemes used in a given frequency band. The queuing delay is based on the output transmission capacity of a node in a given frequency band. The novelty of work in [MA-08], [CHE-07a] is the introduction of a metric for multi-hop CRN which considers both the switching delay between frequency bands ($D_{\text{switching}}$) and back-off delay (MAC delay) within a given frequency band ($D_{\text{back-off}}$). These parameters depend on the CR hardware architecture which is different from one CR to another.

e. Throughput-based techniques

In this section a class of routing algorithms in which throughput maximization is the main objective will be reviewed.

In CRNs, a routing algorithm that completely ignores either the short-term local spectrum conditions or the global spectrum availability, can lead to sub-optimal solutions. The Spectrum Aware Mesh Routing (SAMER), proposed in [PEF-08], is a routing protocol that balances the long term route stability and the short term spectral availability. SAMER seeks to utilize the available spectrum blocks by routing data traffic over paths with higher spectrum availability, without ignoring instantaneous spectral conditions. SAMER builds a forwarding mesh which is adjusted periodically according to the spectrum dynamics, and opportunistically routes packets across this mesh. The mesh is centered around the long-term shortest path, calculated in terms of hop-count, but opportunistically expands or shrinks periodically to exploit spectrum availability. In short, SAMER takes a two-tier routing approach and balances between long-term optimality (in terms of hop count) and shortest opportunistic gain (in terms of higher spectrum availability).

SAMER is shown, in [PEF-08], to outperform the popular hop count metric and the Expected Transmission Time (the number of transmissions required to successfully deliver a packet) metric. Furthermore, simulation results suggest that SAMER avoids highly congested and unavailable links. However, the overhead associated with establishing and maintaining the forwarding mesh has not been considered in these simulations.

Another example of throughput-based routing algorithms is the ROuting and Spectrum Allocation (ROSA) algorithm introduced in [DIN-09]. The goal of this algorithm is to achieve high throughput efficiency. A generic node *i* performs the following actions:

1. It periodically searches for the list of potential next hops.
2. It calculates the capacity over the links toward all the potential neighbors.
3. It chooses the actual next hop, which maximizes the spectrum utility.

The routing algorithm is further coupled with a cooperative sensing technique. The exchange of the information is done using a local spectrum and power allocation algorithms.

f. Link quality/stability based solutions

Channel availability is significantly different in multi-hop CRNs than in traditional wireless multi-channel multi-hop networks. Indeed, nodes in multi-hop CRNs potentially have partially overlapping or non-overlapping sets of available channels, and the available channels are of time-varying nature. Consequently, network layer solutions in multi-hop CRNs should be able to cope with the necessity of re-routing in case specific portions of the currently active path are impaired by the presence of an activating PU. In this section we review the different routing solutions found in the literature which focus on designing stable and quality multi-hop routes.

Path recovery centered algorithms

SPEAR (SPEctrum-Aware Routing) is a routing algorithm proposed in [SAM-08] which aims at throughput maximization by combining end-to-end optimization with the flexibility of link-based approaches to address spectrum heterogeneity. The available spectrum is location

dependent and the introduction of primary users typically creates islands of different spectrum availability. As an example, in [SAM-08] it has been shown that the probability of finding a route between two nodes using a single frequency throughout the path is significantly lower than the probability of finding a route hopping on different channels. The SPEAR algorithm works in three directions: (1) integrating spectrum discovery with route discovery to cope with spectrum heterogeneity; (2) having a coordination of the channel assignments of a per-flow basis, by minimizing inter-flow interference; (3) reducing intra-flow interference.

To achieve these goals, SPEAR starts the route set-up by broadcasting and Ad hoc On-demand Distance Vector (AODV)-style route discovery which accumulates information about each node's available channels and their quality. At the end of the different paths toward the destination each Route Request (RREQ) contains a list with the node IDs, the nodes' spectrum availability and the links' quality. These parameters are combined at the destination to select the optimal route (by using graph coloring approaches as in [ZHO-09]). Unlike traditional on-demand route discovery protocols SPEAR discovers different paths. Redundant paths are not suppressed but are sent to the destination for the best path selection. The selected route is then reserved by using Route Reply (RREP) messages. Channel usage is scheduled at each node; a node can also locally change part of the channel assignment, in case of failures or node mobility, by keeping the local throughput unchanged.

Collaboration between route selection and spectrum decision is considered also in [ZHU-08]. Authors propose the Spectrum Tree On Demand Routing Protocol (STOD-RA) which consists of

a routing metric based on the PUs activities and the SUs QoS requirements, and a spectrum-tree structure which contains the sensed available channel.

The routing metric combines link stability (packet error rate, link rate, access technology) and spectrum availability (predicted link hold time). The idea behind this protocol is to predict the availability time of a spectrum band from the statistical history of PU activities.

Route stability centered algorithms

The link stability is considered also in [CUO-10] and [ABB-10], where this parameter is associated with the overall path connectivity via a mathematical model based on the Laplacian spectrum of graphs. Paths are measured in terms of their degree of connectivity that in a multi-hop CRN is highly influenced by the PUs behavior. The behavior of a PU is modeled by its average activity factor. This work considers N_p PUs randomly scattered in a region where N_s SUs exist as shown in Figure 2.6. Both SUs and PUs are assumed to be motionless. Each $PU_p, p = \{1, \dots, N_p\}$, represents a primary user network as shown in Figure 2.6. Each PU_p can be On or Off which is represented by a binary variable b_p such that:

$$b_p = \begin{cases} 1 & if\ PU_p\ is\ active \\ 0 & Otherwise \end{cases}$$

Consequently, each PU can be characterized by its average activity factor $a_p = E[b_p]$.

Cognitive graph G^c represents all the possible combinations of the PUs activity patterns. The number of all the possible combinations of these N_p binary variables is $M = 2^{N_p}$. For the m^{th} combination $m = \{1, \dots, M\}$ the graph G_m^c, the *cognitive eigenvalue* $\lambda_{2,m}^c$ is the second smallest eigenvalue of the Laplacian matrix driven from G_m^c

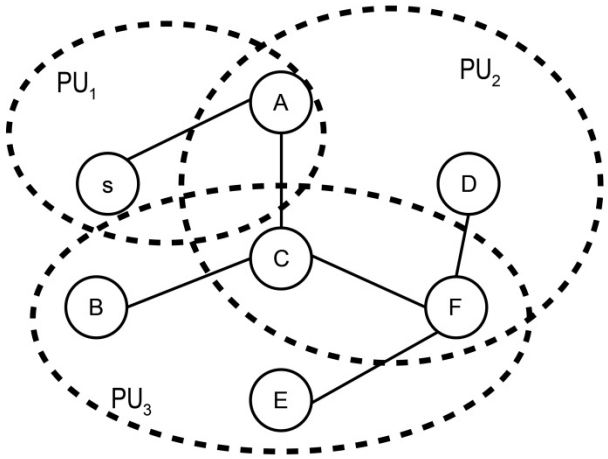

Figure 2.6: System model

The authors also define the average network connectivity (i.e. the *expected value of cognitive algebraic connectivity* (ECAC)). It represents a measure of the connectivity averaged over the random activity of the PUs. ECAC is defined as:

$$ECAC = E[\lambda_2^c] = \sum_{m=1}^{M} \Pr(m) \, . \, \lambda_{2,m}^c$$

where $\Pr(m)$ is the probability of the occurrence of the m^{th} combination. This probability is a function of the PUs' activity factors. Since the computation of the ECAC requires the computation of 2^{N_p} cognitive Laplacian matrices and for each of them the relevant second smallest eigenvalue, the authors introduced a methodology that reduces the computational complexity of this average measure and obtains a good estimation of ECAC. This parameter is named *Compact Cognitive Algebraic Connectivity* (CCAC) to underline that it is obtained from only one averaged Laplacian matrix. CCAC is shown to be a good approximation to the ECAC.

Based on this model, the authors have designed a routing scheme, named Gymkhana, which chooses paths that avoid those network zones that do not guarantee route stability and high

connectivity. Gymkhana uses a distributed protocol to collect some key parameters related to candidate paths from an origin to a destination. These parameters are then fed into the basic mathematical structure based on Laplacian matrixes which is used to compute efficient routing paths. Moreover, in addition to the routing purposes, the model can be used for measuring the connectivity of a multi-hop CRN which could also be used for network planning and dimensioning. This work was the first to introduce a routing algorithm for CRNs based on network connectivity metrics.

2.7 Routing Metrics in CRNs

In the following section, we summarize the different routing metrics designed for CRNs and used in the different routing algorithms discussed before.

Hop Count

SAMER protocol [PEF-08] uses the shortest path between a source and a destination as a base to build a long-term forwarding network. SEARCH [CHO-09] uses hop count as a deciding metric to switch from the original route to a maintenance route and back. CAODV [CAC-09] is a modified version of the AODV protocol that uses hop count as a filter to choose between different candidate routes.

Location-based metrics

Typically, cognitive radio nodes have access to location services either from the GPS system or form a network service. SEARCH [CHO-09] uses node locations to build a forwarding network between source and destination. LAUNCH [HAB-13] uses location information, among other

variables, to avoid high activity PU areas. In [XIE-10], two routing strategies are proposed, namely nearest-neighbor routing (NNR) and farthest-neighbor routing (FNR). Both depend on the location information of the SU nodes.

Spectrum availability

Spectrum availability can be used alone as a routing metric or it can be used with other variables to build a hybrid metric. In SAMER [PEF-08], the spectrum availability is used along with the available bandwidth and transmission time to define a routing metric.

Delay

The end-to-end delay in CRNs can be used as a routing metric. In the Delay motivated On-demand Routing Protocol (DORP) [CHE-07b], the channel switching time, the intra-flow interference, and the queuing delay are used to form a CRN routing metric. In SEARCH, the end-to-end delay, including the channel switching time, is used as a metric to select between different paths.

2.8 Conclusion

The limited available spectrum and the inefficiency in the spectrum usage necessitate a new communication paradigm shift from a fixed allocation of spectrum resources into to a dynamic spectrum allocation. Cognitive radio technology can efficiently address this challenge. The research in cognitive radio has evolved over the years from concentrating on the physical and the MAC layers, into to addressing the new challenges which generated by multi-hop CRNs. generated.

The time-varying nature of communication links in multi-hop CRNs creates a dependency between the CRN availability and the PU network activity factor. The connectivity of multi-hop CRNs has been studied for some special cases. In Chapters 3 and 4, we will introduce new connectivity metrics for single band CRNs and multi-band CRNs and their applications in designing routing algorithms for multi-hop CRNs.

Chapter 3

A New Connectivity Metric for Multi-Primary-Users Cognitive Radio Ad Hoc Networks

3.1 Introduction

In regular wireless networks, a communication link exists between two nodes if they are within the transmission range of each other. However, in cognitive radio networks, the existence of a communication link depends not only on relative positions but also on the PU activity. Thus, the connectivity of cognitive radio networks (CRNs) is a time-varying factor. In recent years, the connectivity problem of cognitive radio networks has been studied using three different approaches. First, from the information theory perspective, the scalability of CRNs is studied in [VU-07] as an extension to the sensor networks scalability problem presented in [GUP-00], [SHA-04]. Second, from the delay analysis perspective, the relation between network connectivity and the density of PUs and SUs is analyzed in [REN-10] and [REN-11]. This approach has also been used to study the relationship between the graph robustness and the network connectivity as in [JAM-07]. Third, from the routing perspective, different routing metrics have been proposed based on the network graph properties [ABB-12]. These metrics were used to design a routing algorithm that optimizes the network connectivity [CUO-10].

In the past few years, a number of measures have been proposed to quantify the connectivity and robustness of networks via graph analysis. The probability of finding a route between two random nodes can be used as a metric to the network connectivity as in [REN-11]. The k-vertex (edges) connectivity measure is one of the simplest measures. However, it only reflects the ability of graphs to retain connectedness after a vertex (or edge) deletion. Alternatively, super connectivity, conditional connectivity, and restricted connectivity [WU-12] provide improved measures. However, these measures are computationally expensive (NP-complete) and hence are not suitable for practical utilization.

One of the widely used measures for graph connectivity is the first non-zero ordered eigenvalue of the Laplacian matrix, which is conventionally known as the algebraic connectivity. The key feature of the algebraic connectivity is that its magnitude is proportional to how robust the graph is connected and hence the difficulty of dividing the graph into multiple disconnected sub-graphs. However, once a single node is isolated in the network, the algebraic connectivity is equal to zero although the rest of the graph may be connected.

Recently, [WU-12] showed that the concept of natural connectivity can be used to characterize the robustness of a network. The natural connectivity is proportional to the weighted number of closed walks of all lengths, and thus it can be used as a network connectivity measure for regular connected graphs and even graphs with isolated node(s).

This chapter is organized as follows. We start by reviewing previous work on the connectivity of CRNs and the different measures that can be used for connectivity analysis. Next, we present the system model and develop the proposed metric including the mathematical analysis and

proofs for the metric convexity. Then we present the extension to the case of multiple PUs and develop a new metric for network connectivity for multi-PUs. Next we present a number of simulations for both the single and multiple PUs cases including the application of the proposed metric to the problem of dual-band CRN connectivity. Finally, conclusions are presented.

3.2 Connectivity in CRNs

In wireless networks, a communication link exists between two nodes if they are within the transmission range of each other. However, in cognitive radio networks, which are characterized by their dynamic network topology, a communication link between two nodes depends not only on their mutual range but also on the PU activity where the links' availability, i.e., life time, is a time varying factor. When the two nodes are not within the transmission range of each other, intermediate nodes can be used to relay information to the destination. A wireless network is considered connected if a node can reach any arbitrary node within the network with a finite delay. Network connectivity depends on many network parameters such as node density, node transmission range, PU network activity and transmission range, and node distribution. Connectivity metric is a measure that reflects how well these nodes are connected to each other taking into account the effect of the above network parameters.

This section introduces the network and graph definitions that will be used throughout this work. Different connectivity metrics are defined including the probability of finding a route metric, the algebraic connectivity metric, and the natural connectivity metric.

3.2.1 Network and Graph Topology

Graph theory has been widely used in the analysis and design of wireless ad hoc network [BEN-14]. The topology of ad hoc networks with a set of nodes *V* (vertices) and a set of edges, *E* connecting these nodes is modeled as a graph *G(N, E)*, where *N* is the set of nodes where the cardinality of $N = |N|$.

A graph *G* is connected if for each pair of nodes in *G,* at least one path exists between them. It is possible to quantify the graph connectivity with two parameters: node connectivity and edge connectivity. The *node connectivity* of a graph *G*, denoted by $K_n(G)$, is equal to the minimum number of nodes whose deletion from *G* causes the graph to be disconnected or reduces it to a one-node graph. A graph *G* is *k*-node connected if $K_n(G) \geq k$. The *edge connectivity* of a graph *G*, denoted by $K_e(G)$, is equal to the minimum number of edges whose deletion from *G* causes the graph to be disconnected or reduces it to a one-node graph. A graph *G* is *k*-edge connected if $K_e(G) \geq k$.

The graph can be represented mathematically via two $N \times N$ matrices, the adjacent matrix $\mathbf{A}$ and the degree matrix $\mathbf{D}$, where $N = |V|$ and $|\cdot|$ denote set cardinality.

Given *G*, the $(i^{\text{th}}, j^{\text{th}})$ element, a_{ij}, of the adjacent matrix $\mathbf{A}$ is given as,

$$a_{ij} = \begin{cases} 1, & if\,(i,j) \in \mathrm{E}; \\ 0, & \text{otherwise.} \end{cases} \tag{3.1}$$

The adjacency matrix of simple graph is symmetric and has all diagonal elements equal to 0. The *degree* of any node *i* in a graph G, denoted by deg_i, is equal to the number of edges

incident on *i*; i.e., $deg_i = \sum_j a_{ij} = \sum_j a_{ji}$. The *N* × *N* matrix $\mathbf{D}$ contains the degree of each node. The generic element d_{ij} is defined as

$$d_{ij} = \begin{cases} deg_i & if\ i = j \\ 0 & otherwise \end{cases}$$

Different metrics have been proposed to characterize the connectivity of a network, i.e., how well the individual nodes are connected to each other. In this work, three measures will be considered for the sake of comparison, namely: the probability of finding a route; algebraic connectivity; and natural connectivity metrics.

3.2.2 Probability of Finding a Route

For a given network with *N* nodes, the probability of finding a route is defined as the probability that there exists a path between a node *i* and a node *j* for all $\{i, j\} \in \{1, 2, \cdots, N\}$. Different techniques can be used to compute the probability of finding a route. One of the most widely used techniques is Dijkstra's algorithm. By applying Dijkstra's algorithm to each node it is straightforward to determine the number of nodes connected to each other. The probability of finding a route is given by

$$\text{Prob(route)} = \mathcal{E}_{\mathbf{A}}\left[\frac{1}{N-1}\sum_{i=1}^{N} N_i\right] \tag{3.2}$$

where $N_i \le N-1$ is the number of nodes connected to node i through one or more hops and $\mathcal{E}_{\mathbf{A}}(\cdot)$ is the probabilistic expectation operator over matrix $\mathbf{A}$ realizations. Note that this probability can also be computed via the adjacent matrix $\mathbf{A}$. Node i and node j are connected together via *k* hops if the i^{th} and j^{th} element of $\mathbf{A}^k$ is nonzero. Let $\mathbf{B} = \mathcal{U}\left(\sum_{k=1}^{N} \mathbf{A}^k\right)$

where the operator $\mathcal{U}$ returns a matrix of entries equal to zeroes and ones, i.e., the i^{th} and j^{th} elements of $\mathbf{B}$ is $b_{ij} \in \{0,1\}$. Let $\overline{a}_{ij}$ represents the i^{th} and j^{th} elements of the summation $\sum_{k=1}^{N} \mathbf{A}^k$, then,

$$b_{ij} = \begin{cases} 0, & \overline{a}_{ij} = 0; \\ 1, & \overline{a}_{ij} > 0; \end{cases} \tag{3.3}$$

As a result, N_i can be obtained as follows

$$N_i = \sum_{j \neq i}^{N} b_{ij} \tag{3.4}$$

3.2.3 Algebraic Connectivity

The Laplacian matrix, $\mathbf{L}$, of a graph is defined as $\mathbf{L} = \mathbf{D} - \mathbf{A}$. Note that, $\mathbf{L}$ is symmetric and positive semi-definite matrix. Let $\lambda_1(\mathbf{L}) \leq \lambda_2(\mathbf{L}) \leq \cdots \leq \lambda_N(\mathbf{L})$ denote the ordered eigenvalues of $\mathbf{L}$ where the smallest eigenvalue $\lambda_1(\mathbf{L}) = 0$. One of the metrics used to characterize the connectivity of a graph is the *algebraic connectivity*, $\lambda_2(\mathbf{L})$, defined as the second smallest eigenvalue of $\mathbf{L}$. A further property is that for any bidirectional graph *G*, the second eigenvalue of its Laplacian is upper bounded by its node connectivity, which in turn is upper bounded by its edge connectivity

$$\lambda_2 \leq k_n(G) \leq k_e(G)$$

In [CUO-10], it is suggested that the concept of algebraic connectivity, suitably extended taking into account PUs' behavior, can be used to capture very fundamental aspects of CRNs characterized by dynamic topologies.

In fact, the algebraic connectivity does not properly reflect the robustness of a graph. It has been shown that the magnitude of the algebraic connectivity reflects how well the overall graph is connected, i.e., the larger the algebraic connectivity is the more difficult it is to divide a graph into sub-graphs [WU-12]. However, algebraic connectivity is equal to zero once a node or a group of nodes are disconnected from the network. As an example, given the network graph shown in Figure 3.1 with *N*=100 nodes, this graph has a single disconnected node resulting in $\lambda_2(\mathbf{L}) = 0$. However, a single edge that connects the isolated node to the graph as in Figure 3.2 results in $\lambda_2(\mathbf{L}) = 0.16$ although the rest of the two graphs, Figure 3.1 and Figure 3.2, are identical. Thus algebraic connectivity is not a suitable metric to use for graph connectivity comparisons.

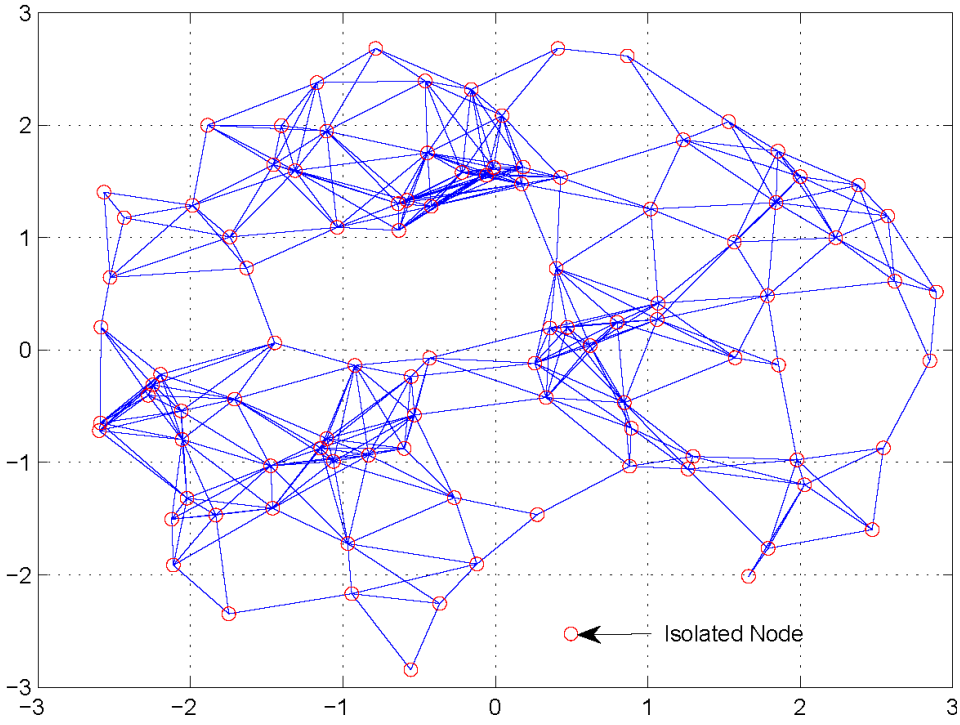

Figure 3.1: Graph connectivity example for *N=100* nodes: Disconnected graph λ_2=0

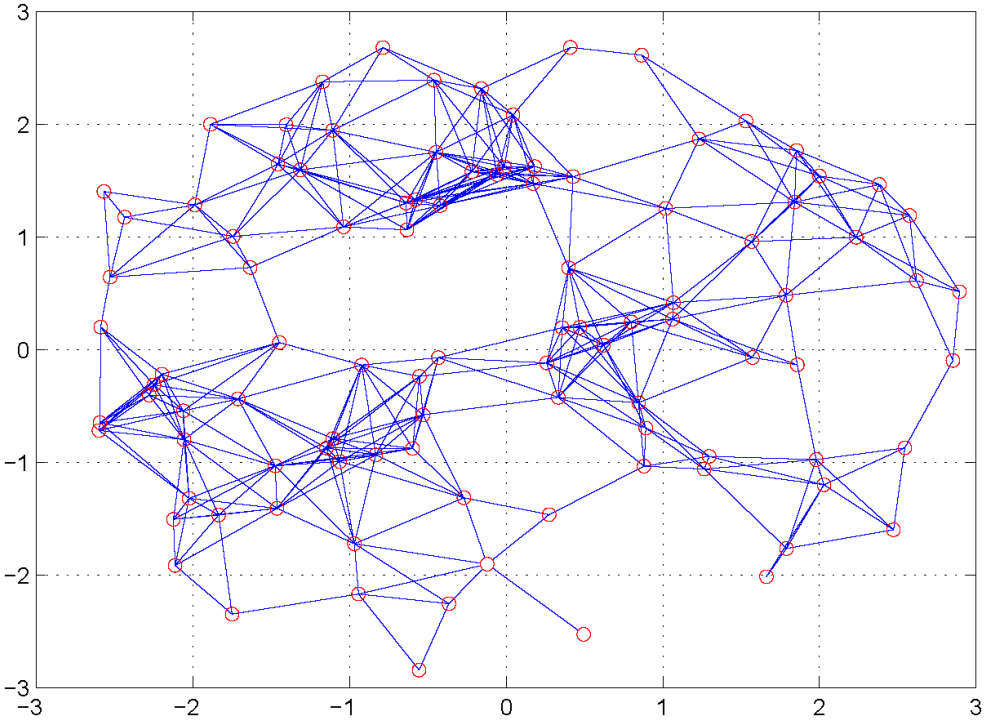

Figure 3.2: Graph connectivity example for *N=100* nodes: Connected graph λ_2=0.16

3.2.4 Estrada Index and Natural Connectivity

Assume a graph *G(N,E)*, without loops and multiple edges, and let $\lambda_1(\mathbf{L}) \le \lambda_2(\mathbf{L}) \le \cdots \le \lambda_N(\mathbf{L})$ denote the eigenvalues of the adjacency matrix of *G.* The *Estrada index* is defined in [EST-00] as

$$EE = \sum_{i=1}^{N} e^{\lambda_i} \tag{3.5}$$

Although it was first introduced in 2000, the Estrada index has already found numerous applications in many different fields.

In [PEN-07], the k^{th} spectral moment of the graph *G* is defined as $M_k = \sum_{k=0}^{\infty} (\lambda_i)^k$. Using the power-series expansion of e^x, the Estrada index can be defined as

$$EE(G) = \sum_{i=1}^{N} e^{\lambda_i} = \sum_{k=0}^{\infty} \frac{M_k(G)}{k!} \tag{3.6}$$

but $M_k(G)$ is equal to the number of self-returning walks of length k of the graph G [CVE-95]. A high Estrada index value indicates that more closed walk loops are available in G which means a highly connected graph.

In [WU-12], the natural connectivity is defined as the *average eigenvalue* and can be calculated using the Estrada index as in (3.7). It is shown that the natural connectivity provides a reliable measure of how well the graph is connected.

$$\overline{\lambda} = \log\left(\frac{1}{N} EE\right) \tag{3.7}$$

3.3 Analysis of the Cognitive Radio Networks Connectivity

3.3.1 System Model

Consider a system model that consists of two types of wireless networks, M primary users wireless networks and an *N* secondary users wireless network. Each primary user network consists of one PU transmitter, with a transmission range of *R*, and one or more PU receivers. The Secondary user network consists of *N* cognitive radios, *secondary users*, each with a transmission range r_θ as shown in Figure 3.3. The SUs are uniformly distributed over a square area of side length *L*. This model, and its variations, is widely used in studying the connectivity of CRNs as in [REN-11].

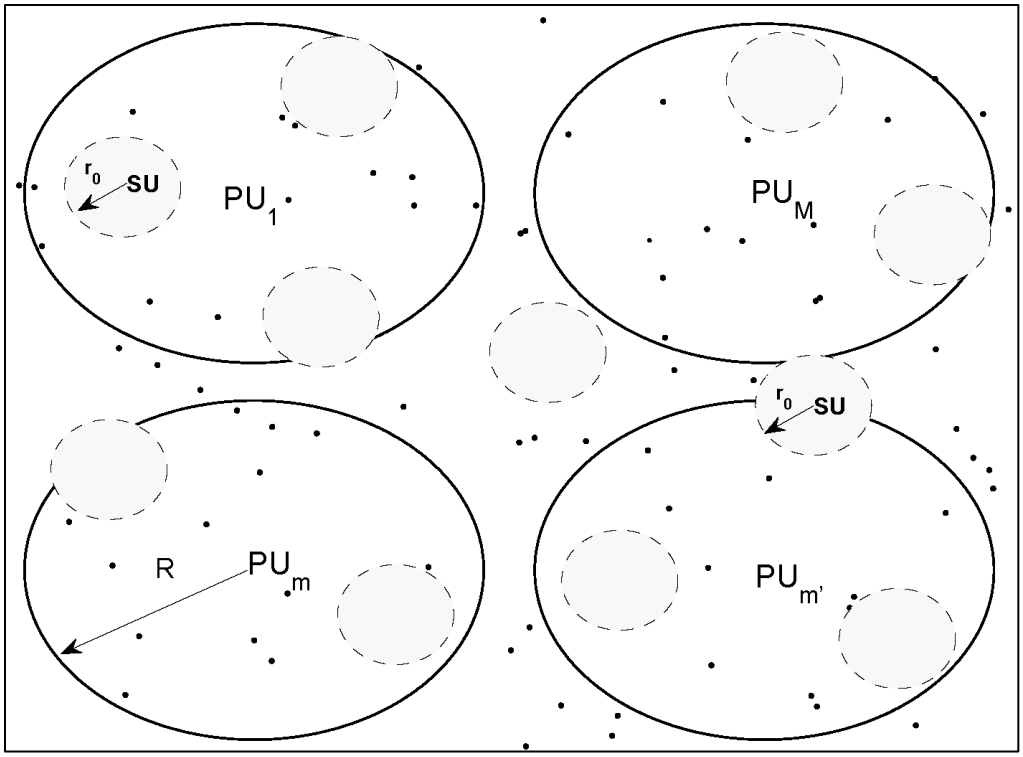

Figure 3.3: Schematic diagram for a cognitive radio network, with *M* primary users (PUs) networks with transmission radius *R*, and *N* secondary users (SUs) with transmission radius r_0 distributed uniformly over a square area of side *L*

As discussed earlier, the cognitive radio wireless network can be mapped to a graph of N nodes with the i^{th} node, v_i, is connected to the j^{th} node, v_j, via an edge e_{ij} of associated weight a_{ij} that represents the link quality. In this analysis, we consider the scenario where primary user networks, PU transmitter and receivers, and SU nodes utilize the same frequency, *f*, to establish communications links within the same network. Let $\mathbb{C}$ represents the set of all SU nodes within the network, $\mathbb{P}_m$ represents the set of nodes within the coverage area of the m^{th} primary users, and $\mathbb{Q}$ represents the set of nodes outside the primary users effect, i.e., $\mathbb{Q} = \mathbb{C} - \bigcup_{m=1}^{M} \mathbb{P}_m$. If all nodes lay inside the PUs effect, then $\mathbb{Q}$ is an empty set. The m^{th} PU's activity factor AF_m is defined as the percentage, in terms of time, that PU_m is actively

transmitting. Let $\Delta_m = 1 - AF_m$ represents the availability of a link that lies within the transmission range of PU_m and define a vector $\mathbf{\Delta} = [\Delta_1, \Delta_2, \cdots, \Delta_M]$. Let r_{ij} represents the Euclidean distance between node v_i and node v_j. The i^{th} and j^{th} element, a_{ij}, of the *cognitive adjacent matrix* denoted $\mathbf{A}(\mathbf{\Delta})$ is given by

$$a_{ij} = \begin{cases} 0, & r_{ij} > r_o \\ 1, & r_{ij} \le r_o, v_i \in \mathbb{Q} \text{ and } v_j \in \mathbb{Q} \\ \Delta_m, & r_{ij} \le r_o, v_i \in \mathbb{Q} \text{ and } v_j \in \mathbb{P}_m \\ \Delta_m \Delta_{m'}, & r_{ij} \le r_o, v_i \in \mathbb{P}_m \text{ and } v_j \in \mathbb{P}_{m'} \end{cases} \tag{3.8}$$

A simple illustrative example of $\mathbf{A}(\mathbf{\Delta})$ can be given by (3.9). In this scenario, the i^{th} *cognitive eigenvalues* of $\mathbf{A}(\mathbf{\Delta})$ is denoted as $\lambda_i(\mathbf{\Delta})$.

$$\mathbf{A}(\mathbf{\Delta}) = \begin{pmatrix} 0 & 1 & 0 & \Delta_1 & \cdots & 0 \\ 1 & 0 & 1 & \ddots & & \vdots \\ 0 & 1 & 0 & \Delta_m \Delta_{m'} & \ddots & \vdots \\ \Delta_1 & \ddots & \Delta_m \Delta_{m'} & 0 & 1 & \Delta_M \\ \vdots & & \ddots & 1 & 0 & 1 \\ 0 & \cdots & \cdots & \Delta_M & 1 & 0 \end{pmatrix} \tag{3.9}$$

3.3.2 Cognitive Natural Connectivity (CNC) Metric

In this section, the concept of Estrada index will be used to develop a new connectivity metric for single band cognitive radio networks, termed *cognitive natural connectivity* (CNC). The new metric is a generalization of the natural connectivity metric discussed above. Unlike the natural connectivity metric, in CNC the associated weight to each edge in the graph *G* may vary between 0 and 1 representing the link availability as will be discussed later in this chapter. The

associated weights are captured by the resulting *cognitive adjacent matrix* $\mathbf{A}(\mathbf{\Delta})$ as shown above. The cognitive natural connectivity metric is expressed as

$$\bar{\lambda}(\mathbf{\Delta}) = \log\left(\frac{1}{N}\sum_{i=1}^{N} e^{\lambda_i(\mathbf{\Delta})}\right) \tag{3.10}$$

Lemma 3.1

The cognitive natural connectivity metric $\bar{\lambda}(\mathbf{\Delta})$ is strictly non-decreasing with $\Delta_m \geq 0$.

Proof

Define a function $f(\mathbf{\Delta})$ as follows $f(\mathbf{\Delta}) = \sum_{i=1}^{N} e^{\lambda_i(\mathbf{\Delta})}$. It can be shown that (See Appendix A), $\partial f(\mathbf{\Delta}) / \partial \Delta_m \geq 0$. Meaning that, $f(\mathbf{\Delta})$ is a non-decreasing function with Δ_m. Since the $\log(\cdot)$ operator is monotonically increasing then it follows that $\bar{\lambda}(\mathbf{\Delta})$ is a non-decreasing function of $\Delta_m \geq 0$.

Lemma 3.2

$f(\mathbf{\Delta})$ is a convex function in Δ_m.

Proof

A necessary and sufficient condition for the convexity of $f(\Delta)$ is the non-negativity of its second derivative, i.e.,

$$\frac{\partial^2 f(\mathbf{\Delta})}{\partial \Delta_m^2} \geq 0$$

The first and second derivatives of $f(\mathbf{\Delta})$ with respect to Δ_m are given as follows

$$\frac{\partial f(\mathbf{\Delta})}{\partial \Delta_m} = \sum_{i=1}^{N} e^{\lambda_i} \frac{\partial \lambda_i}{\partial \Delta_m} \tag{3.11}$$

$$\frac{\partial^2 f(\mathbf{\Delta})}{\partial \Delta_m^2} = \sum_{i=1}^{N} \left[e^{\lambda_i} \frac{\partial^2 \lambda_i}{\partial \Delta_m^2} + e^{\lambda_i} \left(\frac{\partial \lambda_i}{\partial \Delta_m} \right)^2 \right] \tag{3.12}$$

Substituting (3.11) into (3.12) and considering the steps shown in Appendix A, it is straightforward to prove that $f(\mathbf{\Delta})$ is a convex function in Δ_m.

Theorem 3.1

The cognitive natural connectivity metric $\bar{\lambda}(\mathbf{\Delta})$ is a strictly increasing metric with edge availability $0 \le \Delta_m \le 1$. Since $f(\mathbf{\Delta})$ is a non-decreasing function (Lemma 3.1) and also a convex function (Lemma 3.2) in Δ_m, then it follows that $f(\mathbf{\Delta})$ is a strictly increasing function with $0 \le \Delta_m \le 1$. Since the $\log(\cdot)$ is a monotonically increasing function of its argument, then it follows that $\bar{\lambda}(\mathbf{\Delta})$ is a strictly increasing metric with $0 \le \Delta_m \le 1$.

As a result, $\bar{\lambda}$ can be utilized to measure the connectivity of cognitive networks since it is proportional to the networks links availabilities.

3.3.3 Multiple Primary Users

Consider the system model presented in Section 3.3.1. Let $s_m \in \{1, 0\}$ presents the On-Off state of the m^{th} primary user PU_m with probability of occurrence is given by

$$\text{Prob}(s_m) = \begin{cases} \Delta_m, & s_m = 0 \\ 1 - \Delta_m, & s_m = 1 \end{cases} \tag{3.13}$$

Define the set $\mathbb{S}_{\mathbb{M}}$ of all 2^M possible vectors $\mathbf{s}$ as follows

$$\mathbb{S}_{\mathbb{M}} = \left\{ \mathbf{s} : \mathbf{s} = [s_1, s_2, \cdots, s_M], s_m \in \{0,1\}, \mathbf{s} \in \{0,1\}^M \right\} \tag{3.14}$$

where $\mathbf{s} \in \mathbb{S}_{\mathbb{M}}$ represents a given realization for primary users On and Off states, i.e., $s_m = 1$ and $s_m = 0$ respectively.

The probability of occurrence of state $\mathbf{s}$ is given by

$$\text{Prob}(\mathbf{s}) = \left[\prod_{\substack{m=1 \\ \text{Given } s_m=0}}^{M} \Delta_m \right] \cdot \left[\prod_{\substack{m=1 \\ \text{Given } s_m=1}}^{M} (1-\Delta_m) \right] \tag{3.15}$$

Probability of Finding a Route in Cognitive Networks (PORC)

In this section, the probability of finding a route in cognitive radio network is presented. The approach applied here is an extension to the approach discussed in Section 3.2.2 with minor modifications. For each state vector *s*, there exists an associated adjacent matrix $\mathbf{A}_s$ consisting of 1's and 0's indicating which SU nodes are connected. Consequently, there are 2^M adjacent matrices denoted $\mathbf{A}_s$ and indexed by $s \in \{1, 2, \cdots, 2^M\}$. Recall Section 3.2.2 and let $N_i^s \leq N-1$ denote the number of nodes connected to node i via one or more hops at the state vector *s*. The probability of finding a route given the state vector *s* and network realization $\mathbf{A}$ is given by

$$\text{Prob}(\text{route}|\mathbf{A}, \mathbf{s}) = \frac{1}{N} \sum_{i=1}^{N} \frac{N_i^s}{N-1} \tag{3.16}$$

Hence the probability of finding a route in CRN is computed by averaging over all possible state vectors as

$$\text{Prob}(\text{route}|\mathbf{A}) = \sum_{\mathbf{s} \in \mathbb{S}_M} \text{Prob}(\text{route}|\mathbf{A}, \mathbf{s}) \cdot \text{Prob}(\mathbf{s}) \tag{3.17}$$

Then the average probability of finding a route (PORC) over network realizations is given by

$$\text{Prob}(\text{route}) = \mathcal{E}_{\mathbf{A}} \left[\text{Prob}(\text{route}|\mathbf{A}) \cdot \text{Prob}(\mathbf{A}) \right] \tag{3.18}$$

State Cognitive Natural Connectivity (SCNC)

In this section we define a metric termed *state cognitive natural connectivity* (SCNC) and represented by $\bar{\lambda}_S(\mathbf{\Delta})$. Unlike CNC where a single adjacent matrix, $\mathbf{A}(\mathbf{\Delta})$, is used to compute $\bar{\lambda}(\mathbf{\Delta})$, the SCNC metric considers 2^M adjacent matrices $\mathbf{A}_\mathbf{s}$. The CNC at state **s** is given by

$$\bar{\lambda}_\mathbf{s} = \log\left(\frac{1}{N}\sum_{i=1}^{N} e^{\lambda_i(\mathbf{A}_\mathbf{s})}\right) \tag{3.19}$$

where $\lambda_i(\mathbf{A}_\mathbf{s})$ is the i^{th} eigenvalue of $\mathbf{A}_\mathbf{s}$ and $i = 1, 2, \cdots, N.$

The *state cognitive natural connectivity* (SCNC) metric is the average of $\lambda_\mathbf{s}$ over the 2^M possible states *s* and is given by

$$\bar{\lambda}_S(\mathbf{\Delta}) = \sum_{s \in \mathbb{S}_M} \bar{\lambda}_\mathbf{s} \cdot \text{Prob}(\mathbf{s}) \tag{3.20}$$

3.4 Simulations

This section presents different simulations used to study and develop the CNC metric. A locally developed MATLAB simulation is used to analyse and study the CNC metric, and compare it to the POFR and the algebraic connectivity under different scenarios. These scenarios include single PU, two PUs, and multiple PU, all using a single frequency band. The system model in Section 3.3.1 was used in all simulations but with slight modifications in each case.

For each simulation, the parameters used are defined including the number of network realizations used for it. Since the execution time for all the simulations in this section was relatively short, the number of realizations were chosen so that the 95% confidence interval, as defined in Appendix B, is negligible.

3.4.1 Probability of finding a route and Cognitive Natural connectivity metrics for Different PU activity factors

Consider a circular area cognitive radio network of radius R_{Net} having a single primary user, $M = 1$, of transmission radius *R* and *N*=150 secondary users uniformly distributed over R_{Net} with a transmission radius $r_o = 0.2R_{\text{Net}}$. The PU center coincides with the network center and, without the loss of generality, is assumed to be at the origin and R_{Net}=1. Different PU activity factors $AF \in \{0, 0.1, 0.2, \cdots, 0.9, 1\}$ and different PU transmission radius $R = \{0.7, 0.8, 0.9, 1\}R_{\text{Net}}$ are considered.

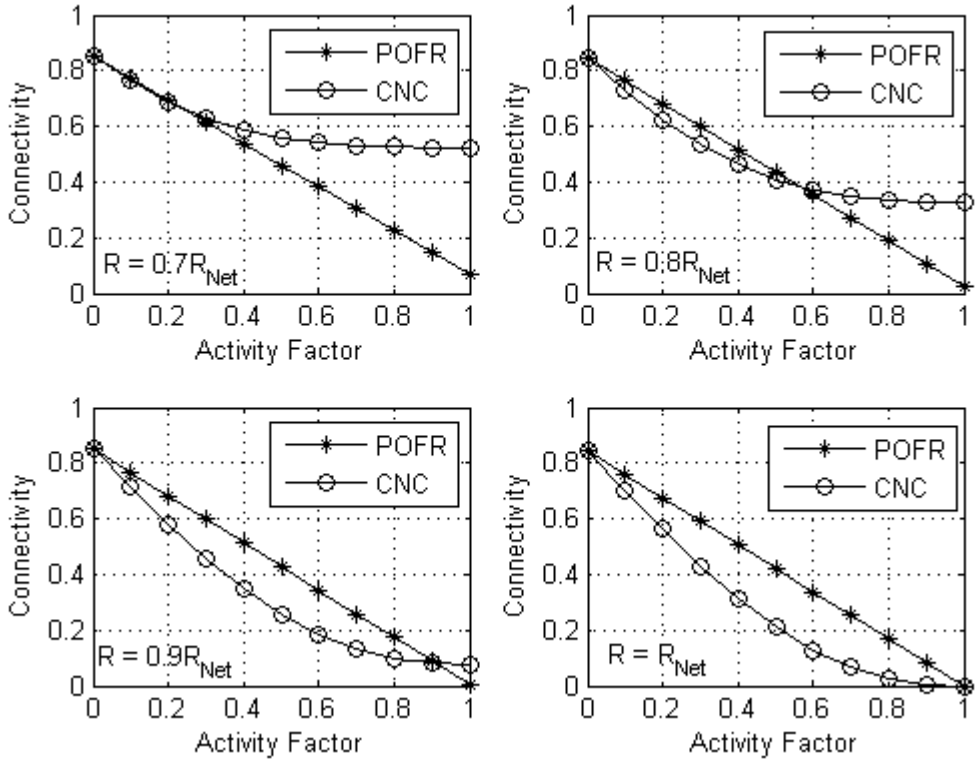

Figure 3.4: Probability of finding a route and normalized CNC versus PU activity factor for different PU transmission Radius *R*.

The probability of finding a route (POFR) is computed using Dijkstra's algorithm over 1000 different network realizations. For each network realization, Dijkstra's algorithm is used to find the shortest path between each node in the network as in Section 3.2.2. Results are shown in Figure 3.4. The cognitive natural connectivity (CNC) is also computed using 100 different network realizations for the same parameters and normalized to the POFR value which occurs at *AF*=0. Figure 3.4 demonstrates that the CNC metric can efficiently capture how well the network is connected.

3.4.2 Cognitive Natural Connectivity versus Algebraic Connectivity and Probability of finding a route

In this section we discuss and compare three connectivity metrics: *Probability of Finding a Route* (POFR); *Algebraic Connectivity* (AC); and *Natural Connectivity* (NC). In this context, route availability is defined as the probability of finding a route between two randomly chosen nodes in the network. Consider a cognitive radio network with a single primary user and the number of secondary users varies from *N*=30 to *N*=150. The nodes occupy a square area of side length *L* with PU transmission radius of $R = 0.4\,L$, and SU transmission range of r_o=0.3*R* and *R*=1.

The probability of finding a route versus the number of SUs nodes for different PU activity factors is shown in Figure 3.5. The probability of finding a route is computed as in Section 3.2.2 using 1000 network realizations. Clearly, as the number of SUs increases the probability of finding a route within the network also increases for all PU activity factors. In addition, for a given number of SU nodes, *N*, the larger the activity factor is, the smaller the probability to find a route.

In conclusion, the route availability metric appropriately captures the network connectivity since it considers any possible route between a source and a destination through the network. However, this method requires averaging over a large number of network realizations to achieve a good approximation for the network behavior.

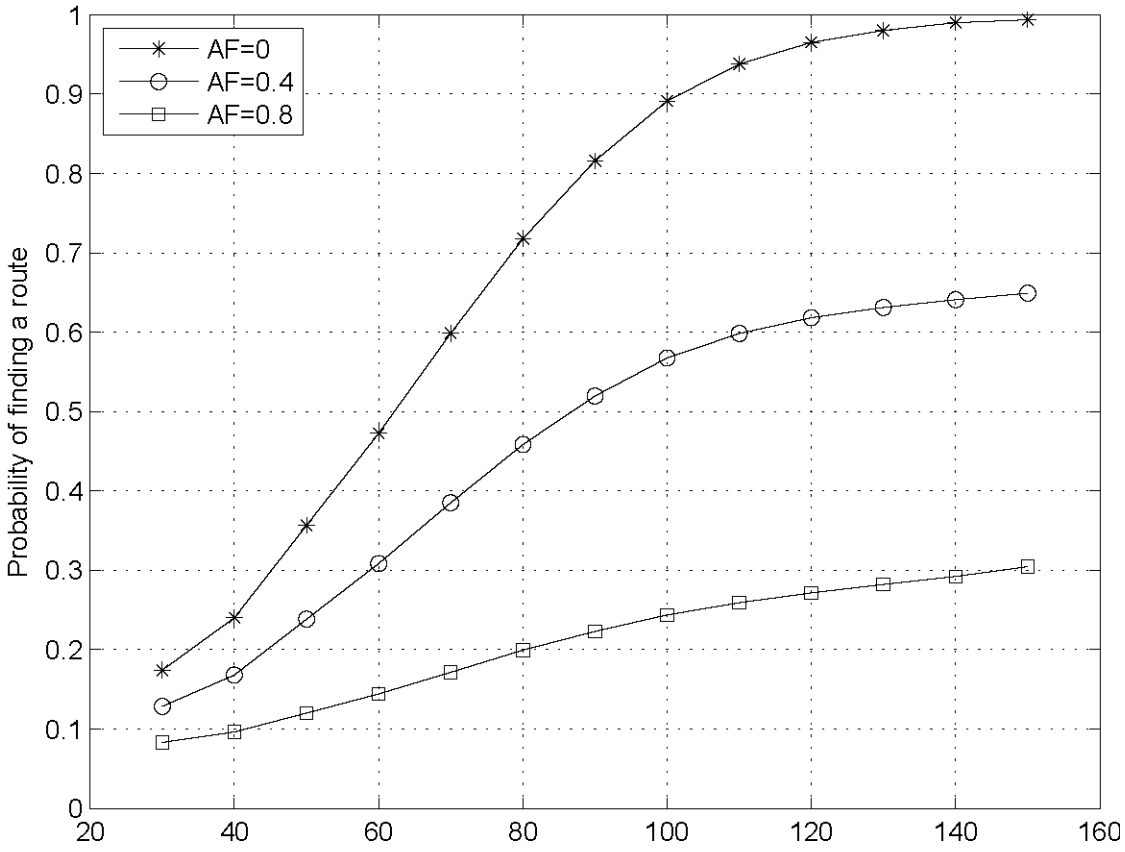

Figure 3.5: POFR versus the number of secondary users *N* for single PU and different activity factors.

The algebraic connectivity λ_2 is a more computationally inexpensive measure for network connectivity compared to the POFR metric. However, when studying network connectivity for cognitive radio networks the algebraic connectivity is denoted by $\lambda_2(\mathbf{\Delta})$ and is defined as the second smallest eigenvalue of $\mathbf{L}(\mathbf{\Delta}) = \mathbf{D}(\mathbf{\Delta}) - \mathbf{A}(\mathbf{\Delta})$ as discussed earlier. The algebraic connectivity versus the number of SUs nodes, *N*, for different activity factors is shown in

Figure 3.6. For each point, 100 network realizations were used. Note that $\lambda_2 = 0$ when $N \leq 80$ where in this case the network has one or more isolated node(s). When *N*>80 the algebraic connectivity $\lambda_2 > 0$ increases with the decrease of the PU activity factor, thus it can be used to measure the network connectivity in this region, i.e., *N*>80. The failure of the algebraic connectivity to measure network connectivity at small *N* is not the only drawback for this measure. It is also computationally expensive to find the critical number of SUs nodes $N > N_c$ where λ_2 can be used as a measure, i.e., $\lambda_2 > 0$. As a result, the algebraic connectivity is not a robust metric to measure network's connectivity especially for networks with low node density.

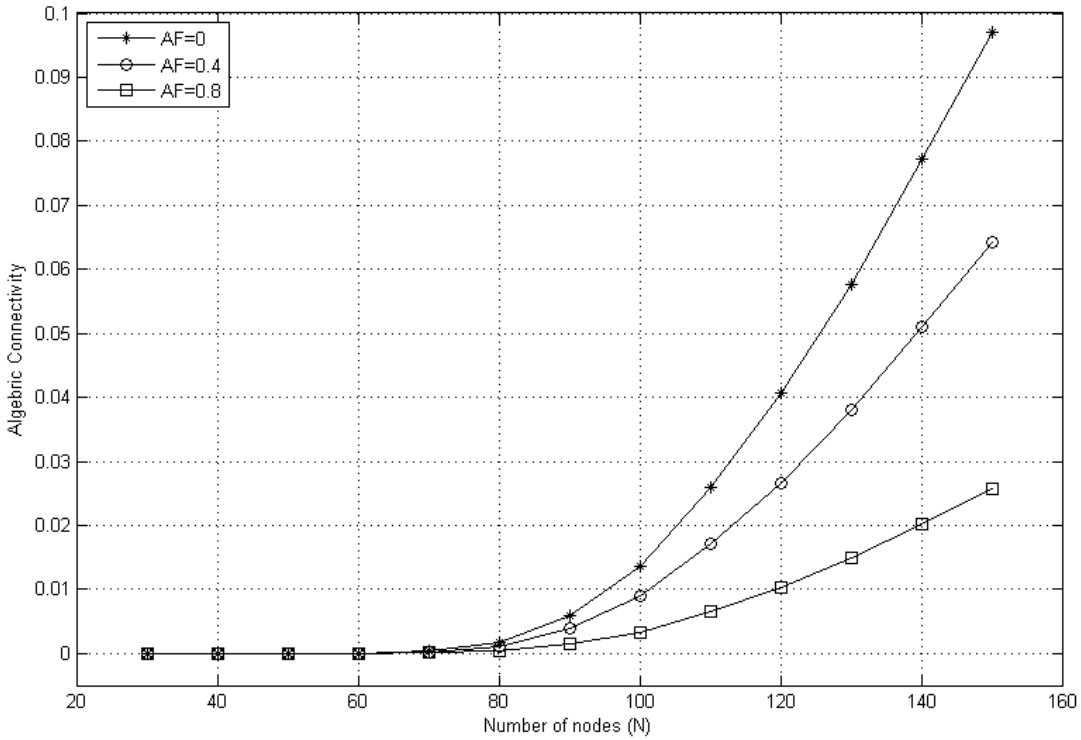

Figure 3.6: Algebraic connectivity versus the number of secondary users *N* for single PU and different activity factors.

The CNC metric versus the number of SU nodes *N* for different PU activity factors is shown in Figure 3.7 for 100 network realizations for each point. The metric increases as *N* increases for

different activity factors and does not overlap, i.e., for a given *N* the CNC metric is proportional to the PU activity factor.

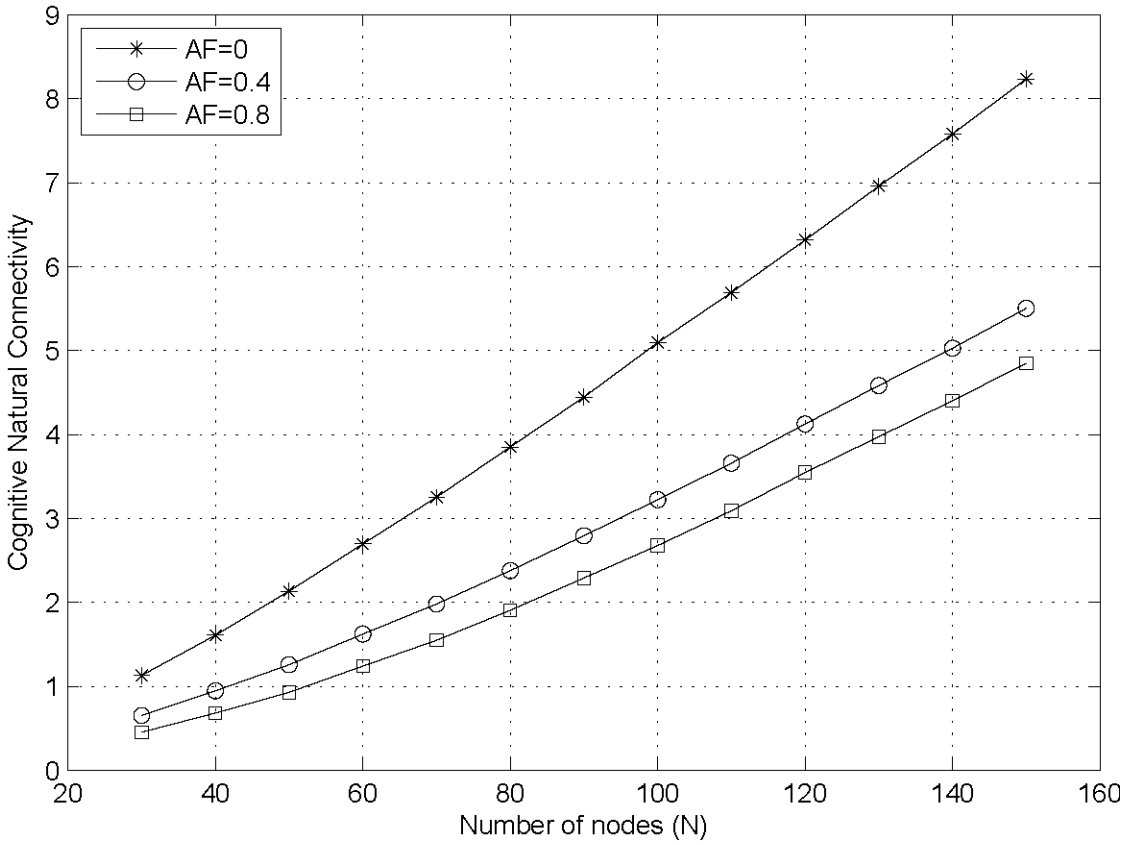

Figure 3.7: CNC versus the number of secondary users *N* for single PU and different activity factors.

Compared to the PORC metric, CNC provides a low computational complexity method to measure network connectivity. Furthermore, compared to Figure 3.5, the CNC metric can efficiently capture the network connectivity similar to the PORC metric, in particular at small *N*. In addition, CNC provides a remarkable computational complexity reduction since it does not need to calculate the probability of finding a route between each pair of nodes using the computationally expensive Dijkstra's algorithm. In addition, and unlike the algebraic connectivity metric, the CNC metric can efficiently capture the network connectivity at low node density networks, i.e., in networks with the possibility of isolated node(s).

3.4.3 Cognitive Natural Connectivity (CNC) for the Two PUs Scenario

Consider a rectangular network of size $2L \times L$ centered at the origin with two primary users PU_1 and PU_2 each with activity factor AF_1 and AF_2 respectively. Each PU has a transmission range $R = 0.4L$ and are centered at $(-L/2, 0)$ and $(L/2, 0)$ respectively. There exist $N = 200$ secondary users which are uniformly distributed over the network area and each with a transmission radius $r_o = 0.1L$. In this scenario, the cognitive natural connectivity $\bar{\lambda}(\boldsymbol{\Delta})$ is a function of two variables $\boldsymbol{\Delta} = [\Delta_1, \Delta_2]$ where $\Delta_m = 1 - AF_m$. Figure 3.8 presents a 3D plot for the cognitive natural connectivity versus AF_1 and AF_2 that are in the set $\{0, 0.1, \cdots, 0.9, 1\}$.

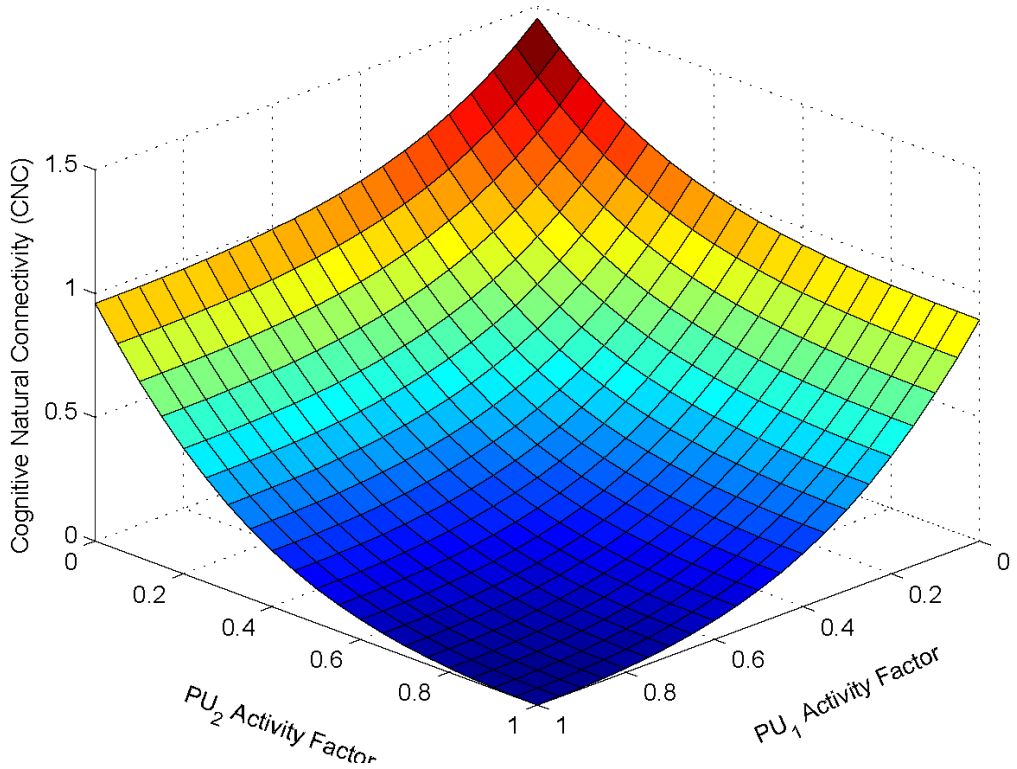

Figure 3.8: 3D plot for the cognitive natural connectivity (CNC) metric versus PU_1 and PU_2 activity factors. The Network size is $2L \times L$, with identical PU transmission radius R=0.4 L, and N=200 secondary users with a transmission radius r_o=0.1 L.

The numerical simulations shown in Figure 3.8 verify the analytical results presented in Theorem 3.1 where $\overline{\lambda}(\mathbf{\Delta})$ is a decreasing metric when either AF_1 and/or AF_2 increases. In order to provide more insights into these results, the contour of the 3D plot is shown in Figure 3.9. The non-overlapping contours indicate that $\overline{\lambda}(\mathbf{\Delta})$ is a monotonically decreasing function with AF_1 and AF_2. As a result, the cognitive natural connectivity metric can efficiently be used to measure the cognitive radio networks connectivity under different PUs activity factors scenarios.

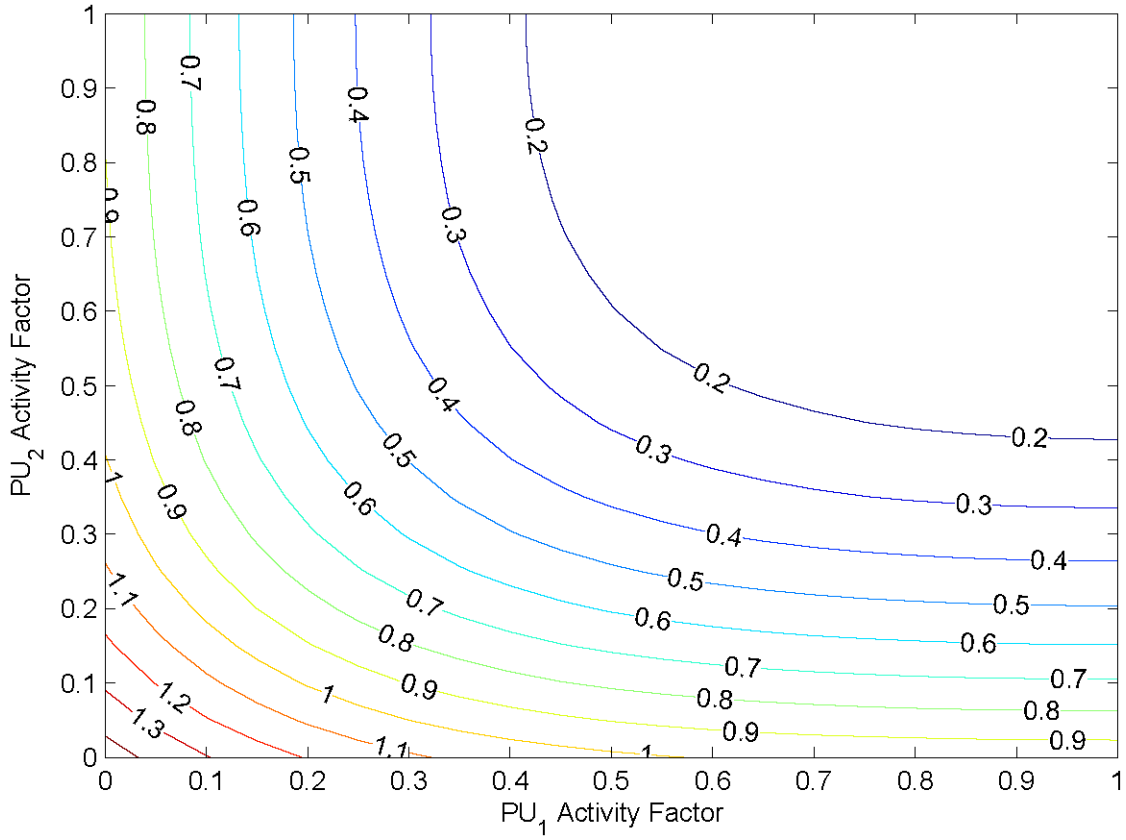

Figure 3.9: The contour plot for the 3D plot shown in Figure 3.8

3.4.4 Connectivity of Cognitive Networks under Multiple PUs

Consider a network of size $4L \times 4L$ centered at the origin, and $M = 4$ independent PUs each with a transmission radius $R_i = \{0, ..., L\}$ and centered at $(\pm L, \pm L)$. There are $N = 100$ SUs uniformly distributed each with a transmission radius of $r_o = 0.25L$. The activity factors of the three PUs are fixed to $AF_2 = AF_3 = AF_4 = 0.4$ while AF_1 varies from 0 to 1. The number of PUs and SUs are chosen for illustration purposes. The same procedure will work for any M and N.

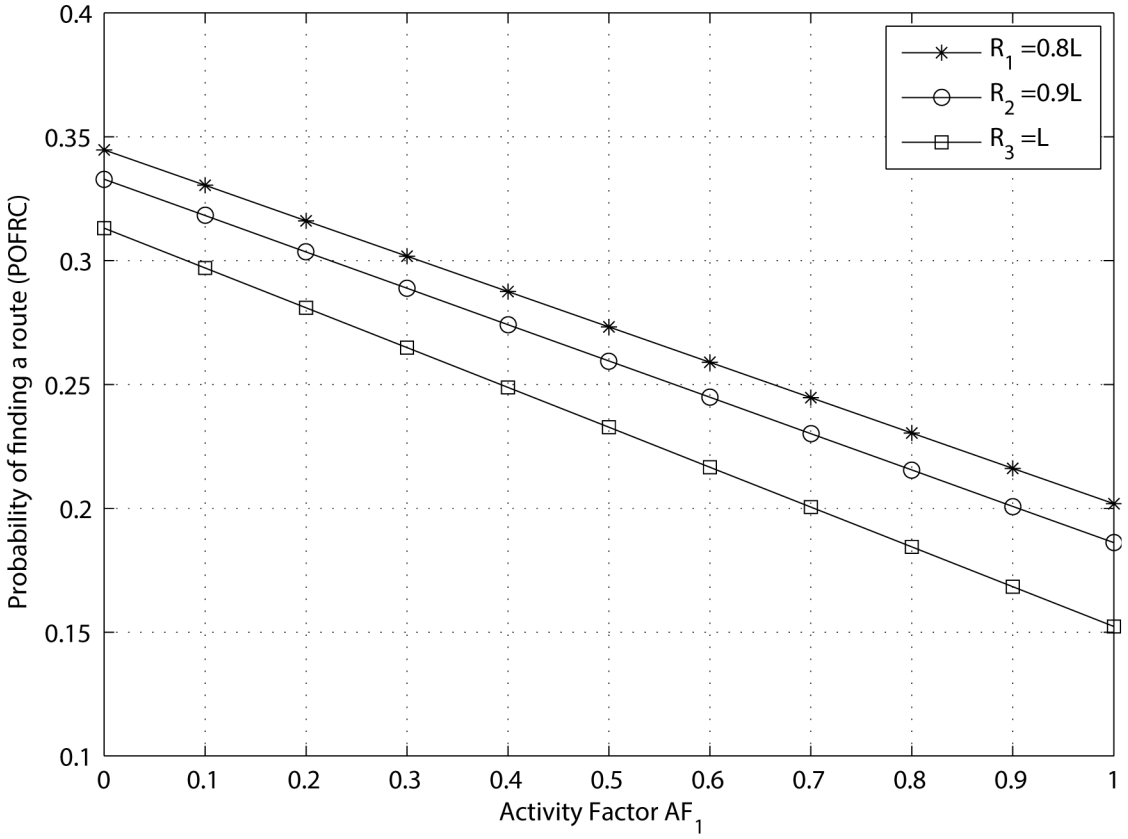

Figure 3.10: Probability of finding a route in cognitive network versus single PU activity factor for different PUs transmission radii.

The probability of finding a route in the cognitive network described above is computed using Equation (3.16) and is presented in Figure 3.10 versus PU_1 activity factor denoted AF_1 for

three PUs transmission radius equal to 0.8*L*, 0.9*L*, and *L* respectively, and for 1000 network realizations for each node.

As shown, when the activity factor increases the PORC decreases since the fraction of the time available to establish a communication path within the network decreases. Furthermore, when the PUs radius decreases the PORC increases since the number of nodes that lie outside the transmission range of all PUs increases and hence the probability that a path between any arbitrary nodes can be established increases as well.

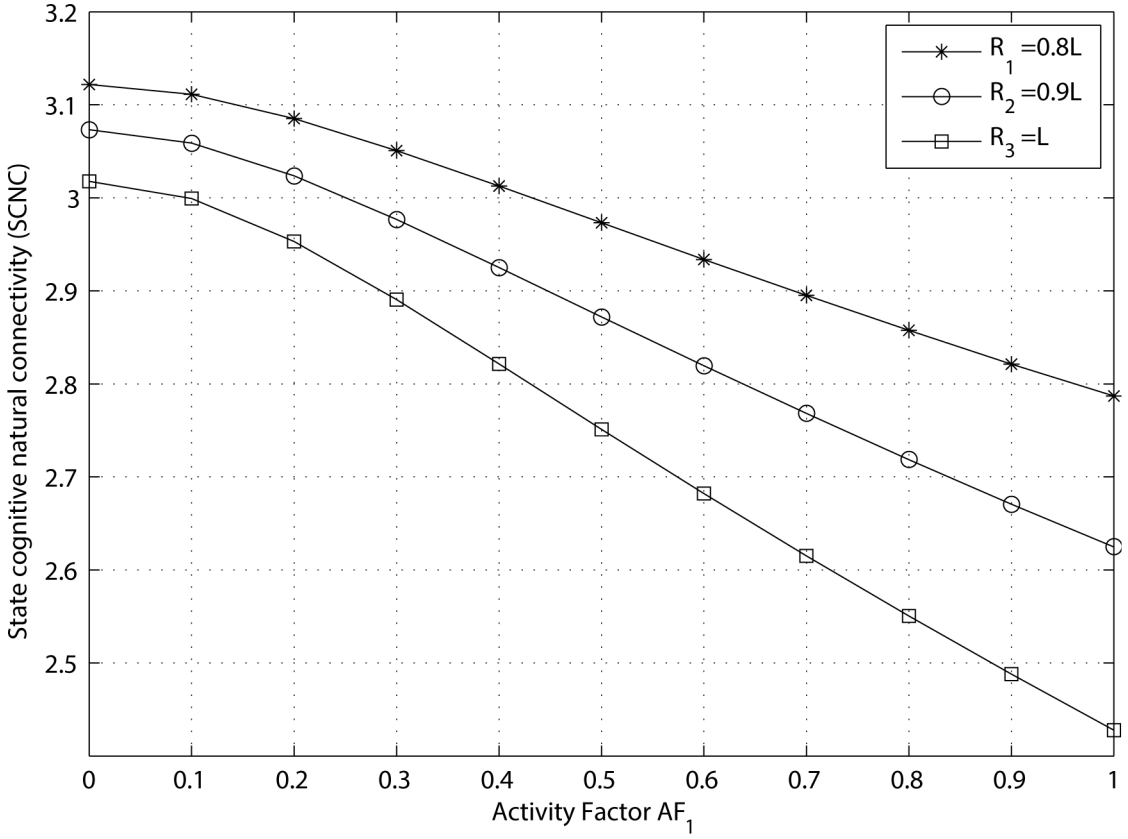

Figure 3.11: The SCNC metric versus single PU activity factor for different PUs transmission radii

The state cognitive natural connectivity metric (SCNC) is presented in Figure 3.11 versus the activity factor AF_1 for different PUs transmission radius equal to 0.8*L*, 0.9*L*, and *L* respectively. Clearly, SCNC decreases as the activity factor increases and for a given AF_1 it decreases with the

increase of the PUs radius when it varies from 0.8*L* to *L*. Note that, SCNC has the ability to characterize the network connectivity in a similar fashion as PORC under different scenarios.

Finally, the cognitive natural connectivity CNC metric is presented in Figure 3.12 versus PU activity factor AF_1 for different transmission radii $0.8L, 0.9L, \text{and } L$. Note that CNC exhibits a similar behavior as PORC where it decreases with the increase of AF_1 and also for a given AF_1 CNC decrease with the increase of the PUs radius. However, a significant computational complexity reduction is achieved compared to the SCNC metric where a single matrix $\mathbf{A}(\Delta)$ is used to compute the CNC metric instead of the 2^M matrices.

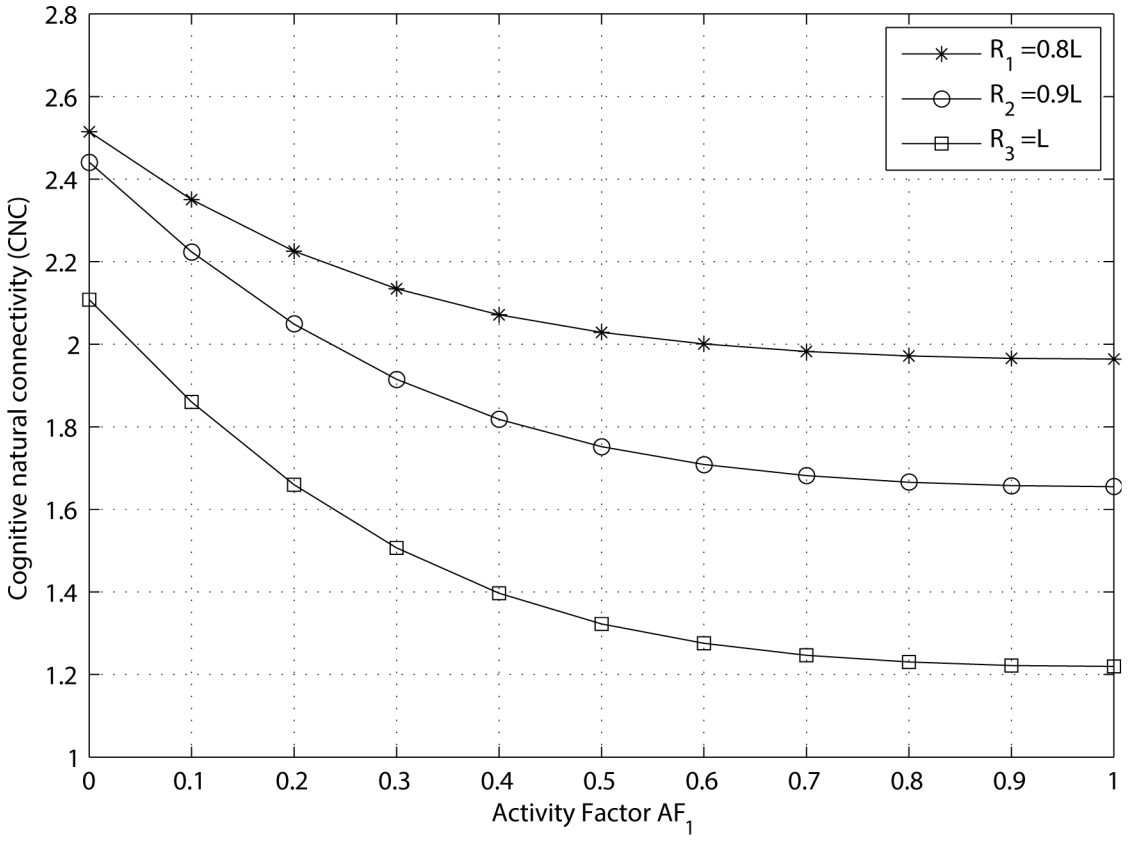

Figure 3.12: CNC versus single PU activity factor for different PUs transmission radii

3.5 Conclusion

In this chapter, a new connectivity metric–has been developed, named *Cognitive Natural Connectivity* (CNC), to measure the network connectivity in CRNs. This metric is shown to be a convex function of the links availability. The proposed metric is compared to the probability of finding a route and the algebraic connectivity metrics, both of which are commonly used to characterize network connectivity. It is shown that the metric provides a qualitative measure that has the same trend of the *probability of finding a route* metric with a significant complexity reduction. Furthermore, when compared to the algebraic connectivity metric, the CNC metric is a remarkably more robust measure for CRNs.

The characteristics of the CNC metric have been studied in both single and multi-PU scenarios using simulations. It is shown that the proposed connectivity metric provides a simple and robust method for determining the cognitive radio network connectivity under various scenarios.

Chapter 4

Multi-Band Connectivity in Cognitive Radio Networks

In this chapter, we extend our interest to studying the connectivity of multi-band CRNs. We start by analyzing the connectivity of a practical CRN scenario, i.e. dual band capable cognitive radio networks. Next, we show that the CNC metric can efficiently be utilized in the design of Dual-band cognitive radio networks. Finally, we propose a generalization of the CNC metric for the case of multi-band CRNs.

4.1 Dual band Cognitive Radio Networks

4.2.1 Problem Statement and System Model

A dual-band cognitive radio network is a network which consists of a single primary user (PU) operating at a frequency f_1 and N secondary users. Each cognitive radio node can setup a communication link with another SU node either using the primary user spectrum band f_1, in an opportunistic fashion, or using the unlicensed spectrum band f_2. In practical real-world scenarios $f_1<f_2$, therefore, a communication link operating at f_1 has better propagation characteristics and a longer transmission range compared to the link operating at f_2. As an example, f_1 can be a TV licensed band while f_2 can be the ISM band. In cognitive networks, unlicensed users would favor to use the frequency band f_1 for better communication characteristics; however, this spectrum is not always accessible by cognitive radio users. As a

result, a trade-off between range, i.e., network connectivity, and links availability, i.e., links life time, is presented. This trade-off plays a crucial role in the design of cognitive radio transmission strategy. The same work applies in cases where more than one unlicensed band is available for the SU's network.

The cognitive radio nodes can operate and communicate with each other in one of the following three scenarios: 1) *SU-band* : all secondary users operate at f_2, i.e., establishing stable short range communication links and hence a low network connectivity; 2) *Dual-band*: SUs located within the PU transmission range operate at f_2 and SUs located outside that range operate at f_1 leading to stable links with a relatively higher network connectivity compared to the former scenario; and 3) *PU-band*: all users operate at f_1 leading to a higher network connectivity and a smaller links availability.

In this section, the connectivity of dual-band capable CRNs is defined as the finiteness of the minimum multi-hop delay (MMD) between two randomly chosen secondary users. We will call it the Route Availability (RA) measure. The network is disconnected if the MMD between two randomly chosen secondary users is infinite almost surely.

Assume a two-dimensional network model, where *N* SU nodes are randomly distributed on a disc area of radius (*a*) following a Poisson distribution (uniform in radius and uniform in angle). The PU transmitter (e.g. TV tower) is at the center of that disc. As shown in Figure 4.1, a radial propagation model is assumed such that *b* and *c* are the transmission ranges of the PU transmitter and CR nodes respectively. Define *r=b/c* as the normalized PU transmission range

and *R=a/c* as the normalized network size. Define the PU's activity factor (*AF*) as the fraction of time the PU is transmitting.

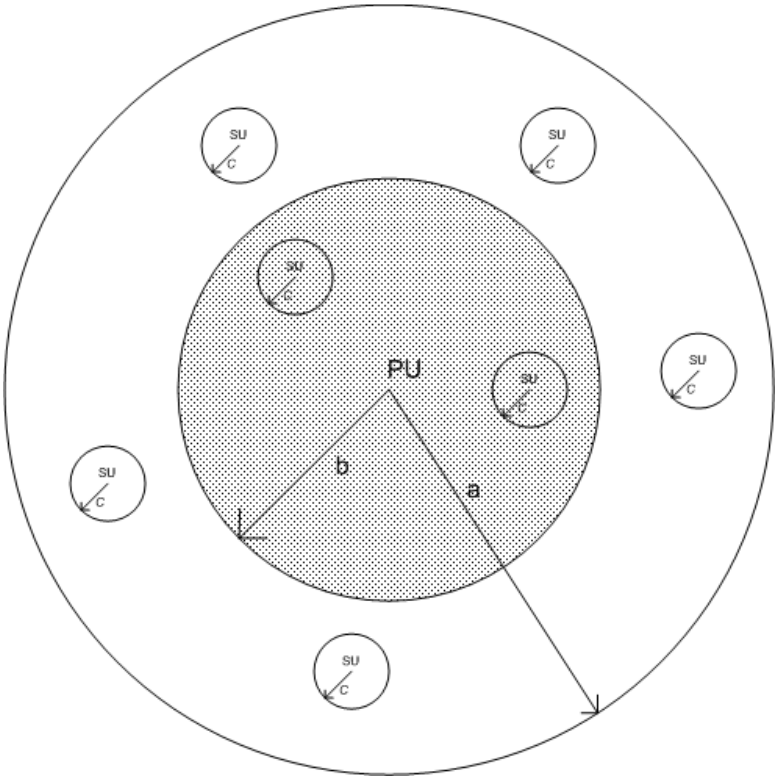

Figure 4.1: System Model

To demonstrate the effect of changing the CRN's parameters on the connectivity, we consider studying the effect of changing the CR node density (i.e. the number of CR nodes deployed in the test disc) and the CR node's transmission range, on the network connectivity. Figure 4.2 shows the effect of the available number of SU nodes and their transmission range on the route availability metric for $N \in \{10, \ldots, 50\}$ at different SU transmission ranges $\in \{1, \ldots, 10\}$ and 10,000 network realizations. We assume no PU activity. We can notice that as the SU's transmission range increases, and the network density increases, the network connectivity increases.

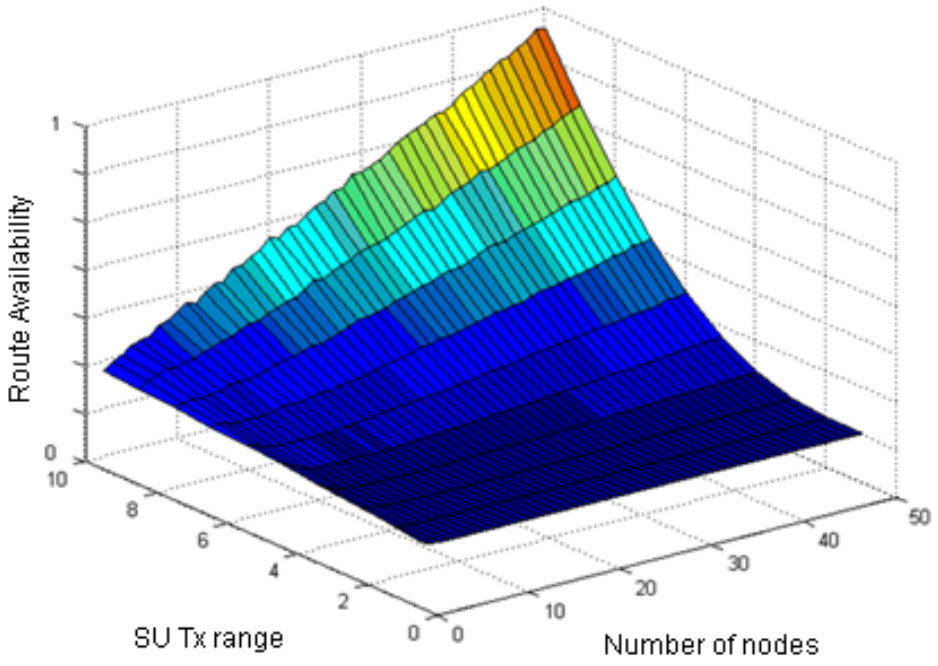

Figure 4.2: The effect of CRN node density and node transmission range on the network connectivity

4.2.2 Impact of the PU on the SU's network connectivity

In this section, we analyze the connectivity of a CRN operating in the PU band at different PU activity factors and compare it with the connectivity if the CRN was operating at the secondary band (e.g. ISM) only. In Figure 4.3, we assume r=5, f_1=2f_2, N=50 nodes. We investigate the CRN connectivity using different PU activity factors, AF= [0%, 50%, or 100%] and the results are averaged over 10,000 different network realizations.

First, we investigate the case when $R < r$, i.e. all CR nodes are located within the PU's transmission range. When the PU is always off (AF = 0%), comparing the connectivity when operating on f_1 or f_2, we conclude that the connectivity decreases at higher frequency bands. This is expected, as the propagation loss becomes higher as the frequency increases. When the

PU is always on (*AF* = 100%), we observe that network is disconnected on f_1. This is expected, as the CR nodes inside the PU's range cannot transmit on f_1. We note that the network connectivity on f_2 is unaffected by the PU's activity.

Next, we investigate the performance as the CR network size increases ($R > r$). In such a case, some nodes outside the PU range can connect on f_1 by finding routes outside the PU range. At PU *AF*=50%, CR nodes inside the PU range can establish communication links with each other through routes on the PU band f_1, for 50% of the time. This is illustrated in Figure 4.3, as the corresponding connectivity is half that calculated at zero PU *AF*.

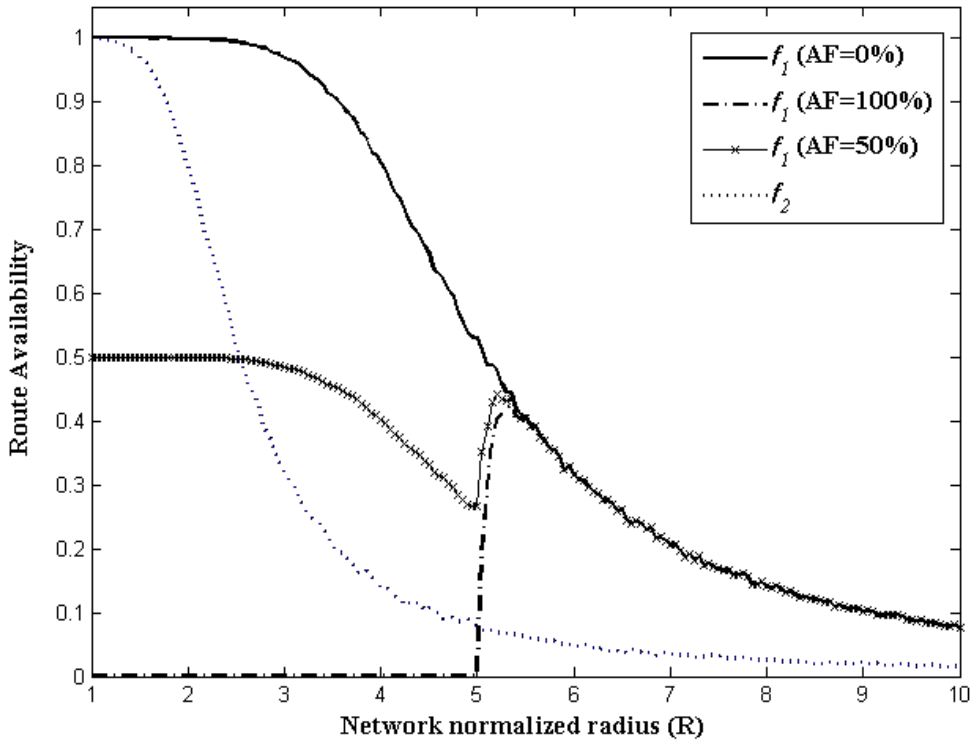

Figure 4.3: The effect of the operating frequency and the PU *AF* on the CRN connectivity for PU normalized transmission radius *r*=5

As R exceeds $r+\delta$, where δ is a small positive number, the effect of the PU's activity diminishes as most of the nodes are outside the PU's transmission range and the connectivity converges to the case where AF=0%. An interesting observation is the critical radius R_c, at which the connectivity on secondary band f_2 is, on average, equal to that on f_1 with 50% AF. If the PU's activity factor is 50%, and the normalized network size R is less than the critical radius R_c, it may better to operate on f_2 rather than on the PU band f_1, and vice versa.

4.2.3 Dual-Band Routing in Dual-Band CRNs

Now we move to the main question of how a dual band capable CRN can choose its operating frequency band to maximize its network connectivity. To answer this question, we propose two strategies to form a route between node i and node j. In the first strategy, all hops along the same route, between i and j, use the same frequency band, either f_1 or f_2. Thus, we name it S*ingle Frequency Routing (SFR)*. In the second strategy, the route could consist of links on f_1 and links on f_2. Thus, we name it *Dual Frequency Routing (DFR)*.

In SFR, the routing protocol will first attempt to establish the route between two CR nodes i and j on f_1. If the PU is active, and some of the links are within the PU range, then these links cannot be established on f_1 and the routing protocol will establish the whole route on f_2. In this strategy, the CRN tries to take advantage of the good propagation characteristics of f_1 and if f_1 is not available the CRN switches to f_2. Figure 4.4, shows that dual band capable CRNs with the SFR strategy have a higher network connectivity than both single band capable CRNs operating at f_1 only or f_2 only.

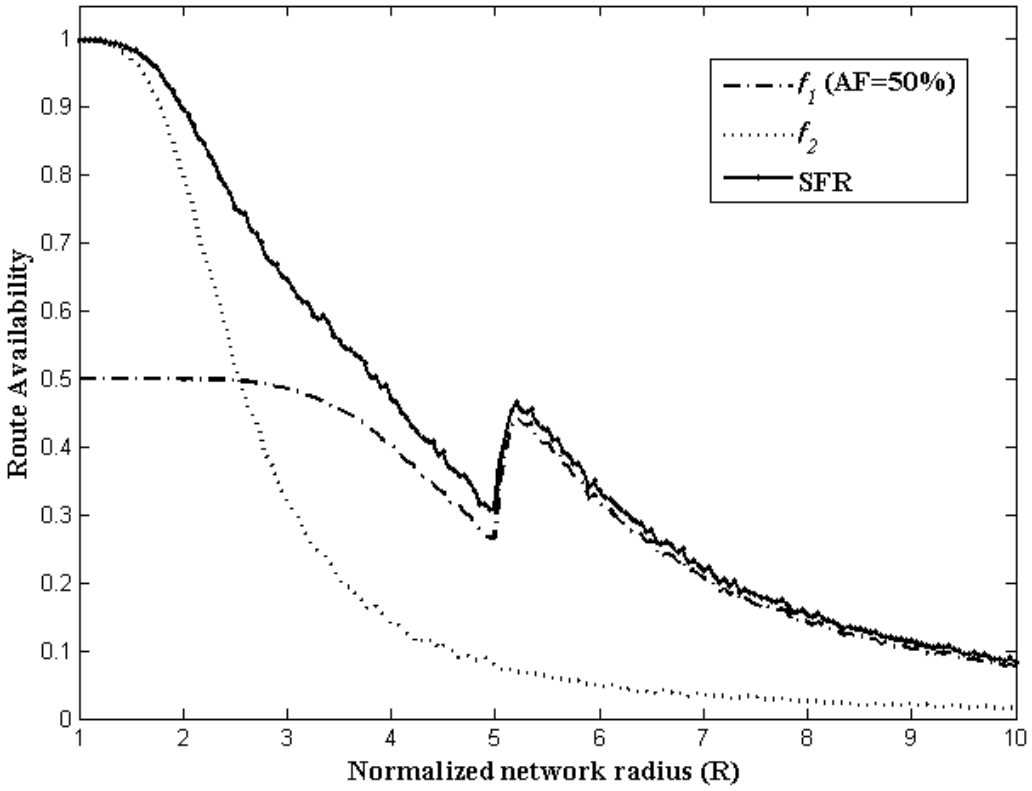

Figure 4.4: Route availability for the SFR protocol

In DFR strategy, the routing strategy establishes the route using links on f_1, except for the links which are not available due to PU activity which are established on f_2. Thus the route consists of a mix of links on f_1 and f_2.

The following simulation compares between the SFR and DFR. In this simulation, we used $f_1=2f_2$, AF=50%, 50 nodes, and 10,000 network realizations. Figure 4.5 shows that when all the SUs are inside the PU's range, (e.g. $R<5$), the two strategies perform the same. This is because all the links are affected by the PU's activity. When $R > r$, the dual frequency routing strategy performs slightly better than the single frequency strategy as it maximizes the use of the better frequency band f_1 whenever possible. Another advantage of DFR is that it minimizes the interference between adjacent nodes. The band switching head over is a drawback of the DFR.

Depending on the operating frequency band, the slight performance gain from DFR vs. the simplicity of SFR could be the deciding factor to choose one over the other.

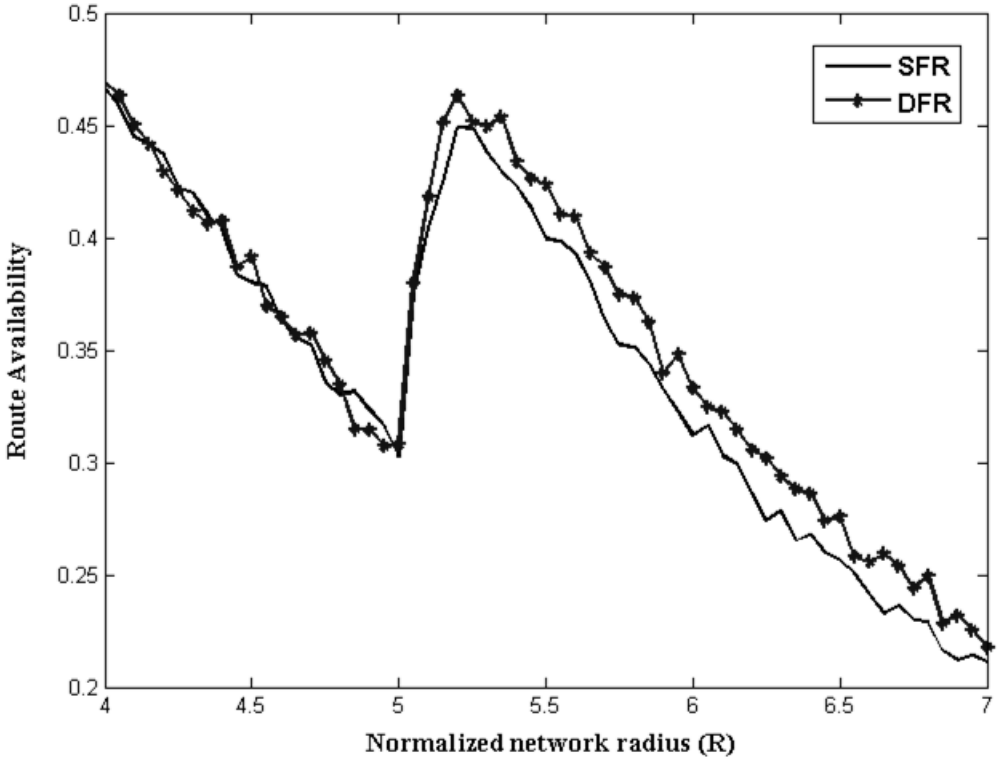

Figure 4.5: Comparison between SFR and DFR

4.2 Application of the Cognitive Natural Connectivity Metric in Dual Band CRNs

In this section, the cognitive natural connectivity (CNC) metric, developed in Chapter 3, is utilized in the design of Dual-band networks via selecting the scenario that would maximizes the network connectivity. Note that the optimal scenario depends on the network parameters such as number of SUs, transmission ranges, PU activity factor, etc.

A practical case in which $f_1=2f_2$ is considered throughout the following simulation. Consider N=60 SU nodes, uniformly distributed over a square area of size $L\times L$, each node has a transmission range r_o=0.8L. Two cases are considered for the PU transmission range R=0.35L and R=0.4L, with activity factor $AF \in [0,1]$. The results are averaged over 100 network realizations.

Figure 4.6 presents the cognitive natural connectivity CNC metric versus PU activity factor ranging from 0 to 1 using numerical simulations for the *SU-band*, *Dual-band*, and *PU-band* scenarios. Clearly, the CNC metric for the *Dual-band* scenario is greater than that for the *SU-band* scenario and both are independent of the PU activity factor. Note that the metric in the *SU-band* scenario is independent of the PU transmission range R (square marks). However, the metric in the *PU-band* scenario depends on the PU activity factor, AF , and the PU transmission radius, R , where the metric decreases as either AF or R increases.

Note that, at small values of AF , the *PU-band* scenario provides a higher network connectivity compared to the *Dual-band* scenario while the *Dual-band* scenario provides a higher connectivity at large values of AF . Clearly, there exists a critical value for the activity factor AF^* , which is a function of the network parameters, that is used to select between these two scenarios. In fact, comparing the operating AF to AF^* determines whether the Dual-band or the PU-band scenario should be considered in order to maximize the network connectivity. Qualitatively and as shown in Figure 4.6, the critical activity factor point is approximately $AF^* \approx 0.55$ for R=0.35L and $AF^* \approx 0.4$ for R=0.4L. Clearly, when $AF < AF^*$, all secondary users would transmit using the *PU-band* scenario, however, when $AF > AF^*$, the *Dual-band* scenario

would provide higher network connectivity. In conclusion, the cognitive natural connectivity metric provides a qualitative tool which can help cognitive radio networks to establish an efficient transmission scenario either by using the PU-band or the dual-band scenario to maximize network connectivity and hence network throughput.

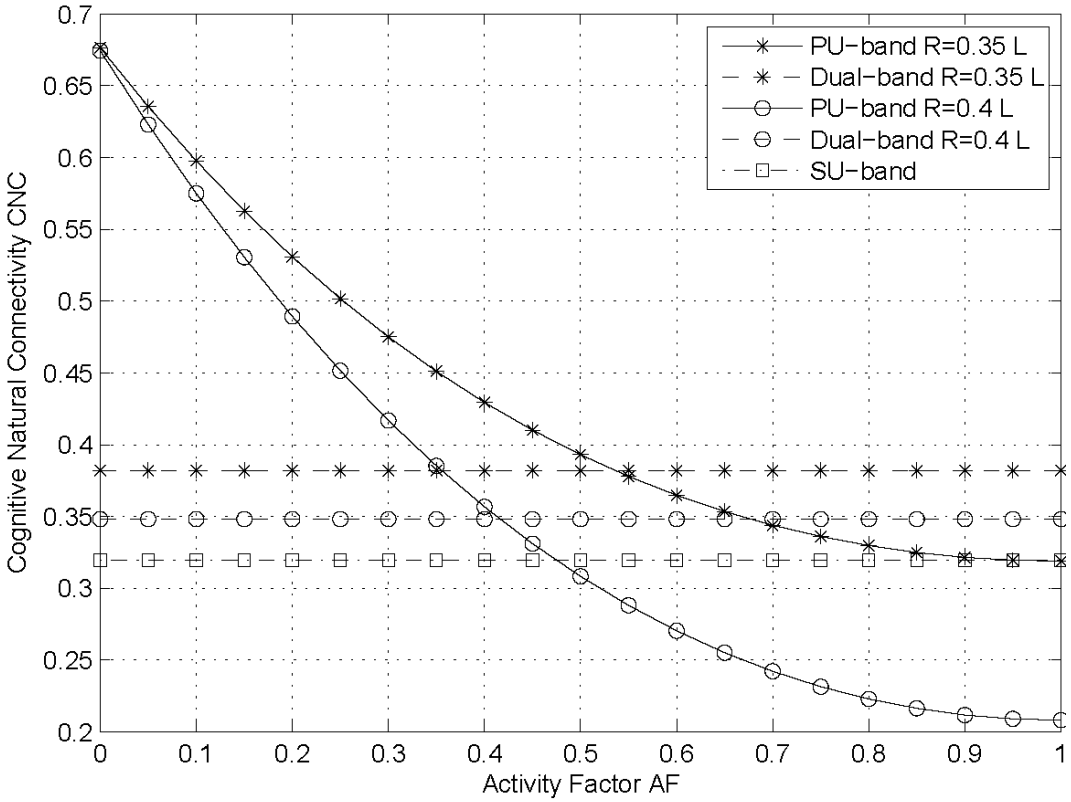

Figure 4.6: CNC metric versus PU activity factor for different PU transmission radii R=0.35L and R=0.4L considering the SU-band, Dual-band, and PU-band frequency assignment strategies

In terms of complexity, the simplest scenario is the SU-band where all SUs utilize a single frequency in the entire network without the need for a frequency switching process. In Dual-band scenario, a communication link connecting two SUs, one lying outside the PU range and the other lying within the PU range, requires that a frequency hand-over process at the PU edge be performed. Finally, the PU-band scenario has the highest complexity among the above scenarios where spectrum sensing and frequency switching are required.

4.3 Multi-Band Connectivity Metric for CRNs

In this section, the connectivity of multi-band cognitive radio networks is studied using the natural connectivity concept and a new connectivity metric for multi-band CRNs based on the cognitive natural connectivity (CNC) metric is developed. The metric is shown to be a convex function of the links availability which increases as the PUs activity decreases. The proposed metric has shown a remarkable complexity reduction compared to the probability of finding a route metric. The proposed metric is utilized to measure the connectivity of the multi-band cognitive radio networks.

4.3.1 System Model

Consider a multi-hop cognitive radio network with *M* primary users and *N* secondary users (nodes). Each node has the capability to setup a communication link with its neighbor nodes using one of *K* spectrum bands denoted $\{f_1,\cdots,f_K\}$. Each SU has a transmission range of r_k.

Let M_k represents the number of PUs operating at the band f_k with a total number of PUs given by $M=\sum_{k=1}^{K}M_k$. We assume that the M_k PUs are spatially-disjointed for all $k\in\{1,\cdots,K\}$ with transmission range R_{ik} for the i^{th} PU operating on the k^{th} frequency. Note that the transmission range of PUs and SUs is inversely proportional to the used frequency band. However, if adjacent frequencies are used then the effect of the frequency difference on the radius can be neglected.

The system model can be represented as a multi-layer system model with *K* layers, each representing a frequency band where each band contains M_k primary users. The system model is shown in Figure 4.7. It is assumed that SUs are uniformly distributed over a square area of side length *L*. This model is a generalization of the mode used in [REN-11] to study the connectivity in single band CRNs.

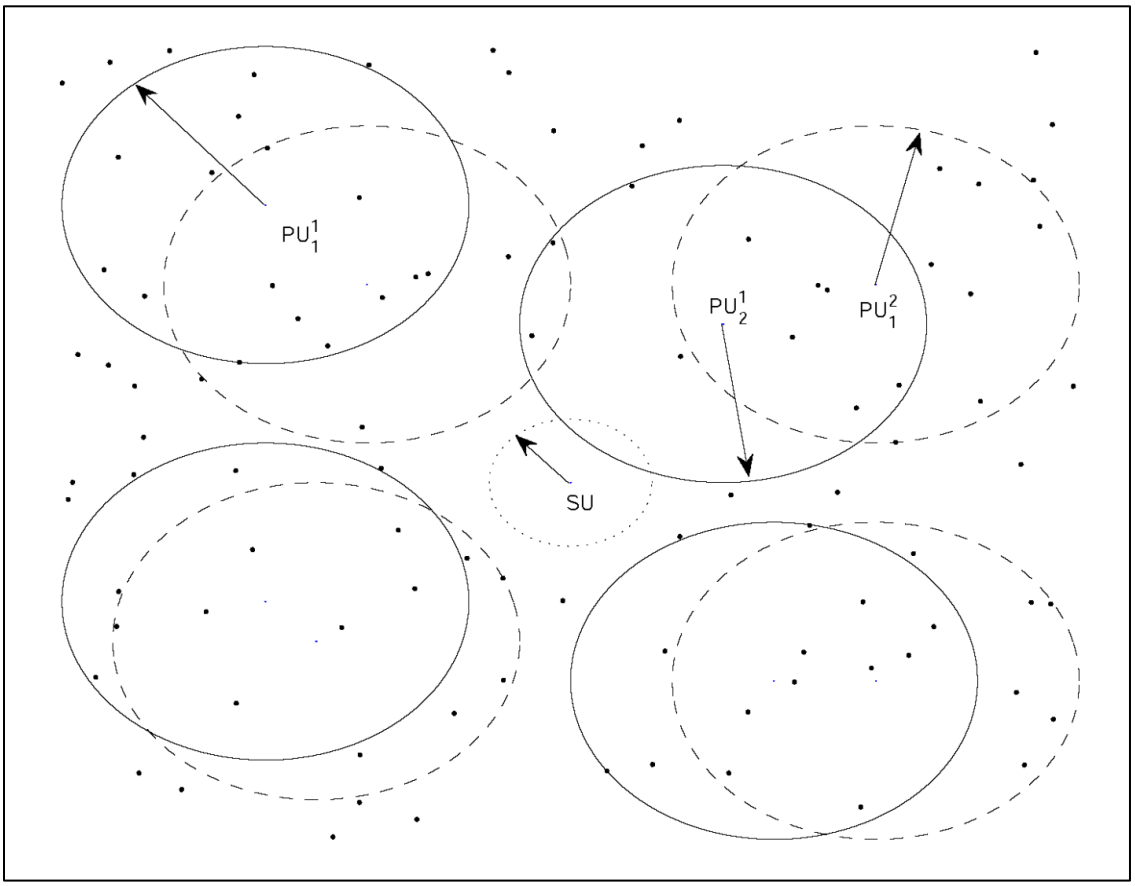

Figure 4.7: Schematic diagram for a cognitive radio network, with *M* primary users (PUs) networks with transmission radius *R*, and *N* secondary users (SUs) with transmission radius r_o distributed uniformly over a square area of side *L*.

For the k^{th} layer where all PUs are operating on f_k, let $\mathbb{C}^k$ represent the set of all nodes within the network, $\mathbb{P}_m^k$ represent the set of nodes lie within the coverage area of the m^{th}

primary users in the k^{th} layer, and $\mathbb{S}^k$ represent the set of nodes lying outside the primary users effect, i.e., $\mathbb{Q}^k = \mathbb{C}^k - \bigcup_{m=1}^{M} \mathbb{P}_m^k$. Let AF_{mk} denote the activity factor of $\mathbb{P}_m^k$ which is defined as the percentage, in terms of time, that PU_m^k is active, i.e., in the transmission mode.

Let $\Delta_{mk} = 1 - AF_{mk}$ represent the availability of a link that lies within the transmission range of PU_m^k and define a vector $\boldsymbol{\Delta}_{\mathbf{k}} = [\Delta_{1k}, \Delta_{2k}, \cdots, \Delta_{M_k k}]$.

4.3.2 Cognitive Adjacent Matrix

In this section we propose a novel probabilistic model for the adjacent matrix in cognitive radio networks denoted $\mathbf{A}(\boldsymbol{\Delta}_{\mathbf{k}})$. The i^{th} and j^{th} element $a_{ij,k}$ of the k^{th} layer *cognitive adjacent matrix* $\mathbf{A}(\boldsymbol{\Delta}_{\mathbf{k}})$ is set according to the probability that the link between node *i* and node *j* is available to establish a communication link using the frequency band f_k. For the k^{th} layer, i.e., frequency band f_k, with M_k independent and spatially-disjointed primary users, the element $a_{ij,k}$ of the matrix $\mathbf{A}(\boldsymbol{\Delta}_{\mathbf{k}})$ is given by

$$a_{ij,k} = \begin{cases} 0, & r_{ij} > r_k \\ 1, & r_{ij} \le r_k, v_i \in \mathbb{Q}^k \text{ and } v_j \in \mathbb{Q}^k \\ \Delta_{mk}, & r_{ij} \le r_k, v_i \in \mathbb{Q}^k \text{ and } v_j \in \mathbb{P}_m^k \\ \Delta_{mk}\Delta_{m'k}, & r_{ij} \le r_k, v_i \in \mathbb{P}_m^k \text{ and } v_j \in \mathbb{P}_{m'}^k \end{cases} \tag{4.1}$$

Note that $\mathbf{A}(\boldsymbol{\Delta}_{\mathbf{k}})$ is symmetric around the diagonal, i.e., $a_{ij,k} = a_{ji,k}$ each link $a_{ij,k}$ is assigned the value of the probability that the link is available for communication over the frequency band f_k. In this context $\lambda_i(\boldsymbol{\Delta}_{\mathbf{k}})$ denote the i^{th} *eigenvalues* of $\mathbf{A}(\boldsymbol{\Delta}_{\mathbf{k}})$.

4.3.3 Multi-Band Cognitive Natural Connectivity (MBCNC) Metric

In this section we present a new connectivity metric for multi-band cognitive radio networks, termed *multi-band cognitive natural connectivity* (MBCNC) and is denoted as $\bar{\lambda}(\mathbf{\Delta})$. The new metric is a generalization of the Cognitive Natural Connectivity discussed in Chapter 3. In MBCNC the associated weight to each edge in the graph can take any value between 0 and 1 representing the link availability. The associated weights are captured by the resulting single layer *cognitive adjacent matrix* $\mathbf{A}(\mathbf{\Delta_k})$ as shown above. For a given frequency band f_k, the cognitive natural connectivity metric is expressed as

$$\bar{\lambda}(\mathbf{\Delta_k}) = \log\left(\frac{1}{N}\sum_{i=1}^{N} e^{\lambda_i(\mathbf{\Delta_k})}\right) \tag{4.2}$$

Lemma 4.1

Let $f(\mathbf{\Delta_k}) = \left(\frac{1}{N}\sum_{i=1}^{N} e^{\lambda_i(\mathbf{\Delta_k})}\right)$ then for a given *k*, $f(\mathbf{\Delta_k})$ is a convex function in Δ_{mk}.

Proof: The proof follows the same steps in Appendix A.

Thus for a single layer indexed by *k* and having M_k PUs, the $\bar{\lambda}(\mathbf{\Delta_k})$ is a monotonically decreasing metric in Δ_{mk}. Consider the case of multi-band cognitive network and define the total adjacent matrix $\mathbf{A}(\mathbf{\Delta})$ as follows,

$$\mathbf{A}(\mathbf{\Delta}) = \max_k \left\{\mathbf{A}(\mathbf{\Delta^1}), \cdots, \mathbf{A}(\mathbf{\Delta^k}), \cdots, \mathbf{A}(\mathbf{\Delta^K})\right\} \tag{4.3}$$

where the maximization is taken element-wise on the entries of each matrix indexed by *k*.

Let $\lambda_i(\mathbf{\Delta})$ denote the eigenvalues of the matrix $\mathbf{A}(\mathbf{\Delta})$ then the MBCNC metric is given by

$$\bar{\lambda}(\mathbf{\Delta}) = \log\left(\frac{1}{N}\sum_{i=1}^{N} e^{\lambda_i(\mathbf{\Delta})}\right) \tag{4.4}$$

Since $\mathbf{A}(\mathbf{\Delta}) \geq \mathbf{A}(\mathbf{\Delta^k})$, where $\geq$ is an element-wise operator, and due to the convexity of $f(\mathbf{\Delta_k})$ then it is straightforward to show that

$$\bar{\lambda}(\mathbf{\Delta}) \geq \bar{\lambda}(\mathbf{\Delta_k}), \qquad \forall k \in \{1, \cdots, K\} \tag{4.5}$$

Thus the MBCNC metric can effectively characterize the connectivity of multi-band cognitive radio networks.

4.3.4 Simulations

In this section, the properties and the applications of the MBCNC metric as a measure for networks connectivity are discussed where different cognitive radio network topology and parameters are considered. In each simulation scenario, it is shown that the MBCNC is an efficient metric that can be used in all scenarios to characterize the network connectivity with a significant computational complexity reduction compared to the POFR metric.

POFR and MBCNC versus single layer Activity factor

Consider a network of size $5R \times 5R$ centered at the origin with $M = 12$ independent PUs, each having a transmission radius *R* and distributed over $K = 3$ different frequency bands f_1, f_2 and f_3. Each frequency band has $M_1 = M_2 = M_3 = 4$ spatially-disjointed PUs. However, PUs operating at different frequency bands could be spatially overlapped. The network consists also of $N = 200$ SUs that are uniformly distributed over the area with the assumption that f_1, f_2

and f_3 are close such that each SU has a transmission radius that is approximated as $r_k = r_o$ for $k = 1, 2$ and 3 and let r_o=0.5R.

Two scenarios are considered to establish a communication path between any two arbitrary SU nodes. In the first scenario, which is termed *single-band mode*, the network computes the CNC for each frequency band f_k with $k = 1, 2$ and 3, i.e., layer, independently and then the frequency band with the maximum CNC is selected to establish a communication link.

In the second scenario, which is termed multi-band *mode*, each SU node selects which frequency band f_k^* will be utilized to send its data to the neighbor node. The frequency band f_k^* is simply the frequency associated with the PU that has the smallest activity factor affecting the link. In this case a typical path would consist of different frequencies. This allows a higher connectivity but also requires spectrum sensing information of the entire available band.

In this simulation, the activity factors of the first layer operating at f_1 varies as $AF_{m1} = \{0, \cdots, 1\}$, with $m = \{1, \cdots, 4\}$, simultaneously for the $M_1 = 4$ PUs operating at this band. However, the other two frequency bands PUs are fixed as $AF_{m2} = 0.3$ and $AF_{m2} = 0.5$ with $m = \{1, \cdots, 4\}$. As shown in Figure 4.8, the POFR for SUs operating at f_1 decreases as the PUs' activity factor increases. As expected the POFR for SUs operating at f_2 or f_3 in single-band mode is constant independent of AF_{m1} and the latter is smaller since $AF_{m3} > AF_{m2}$. Note that POFR for a multi-band system, which uses links subjected to minimum activity factor in all bands, is shown to be better than POFR for any single band mode. It is also decreases as the AF^1 increases.

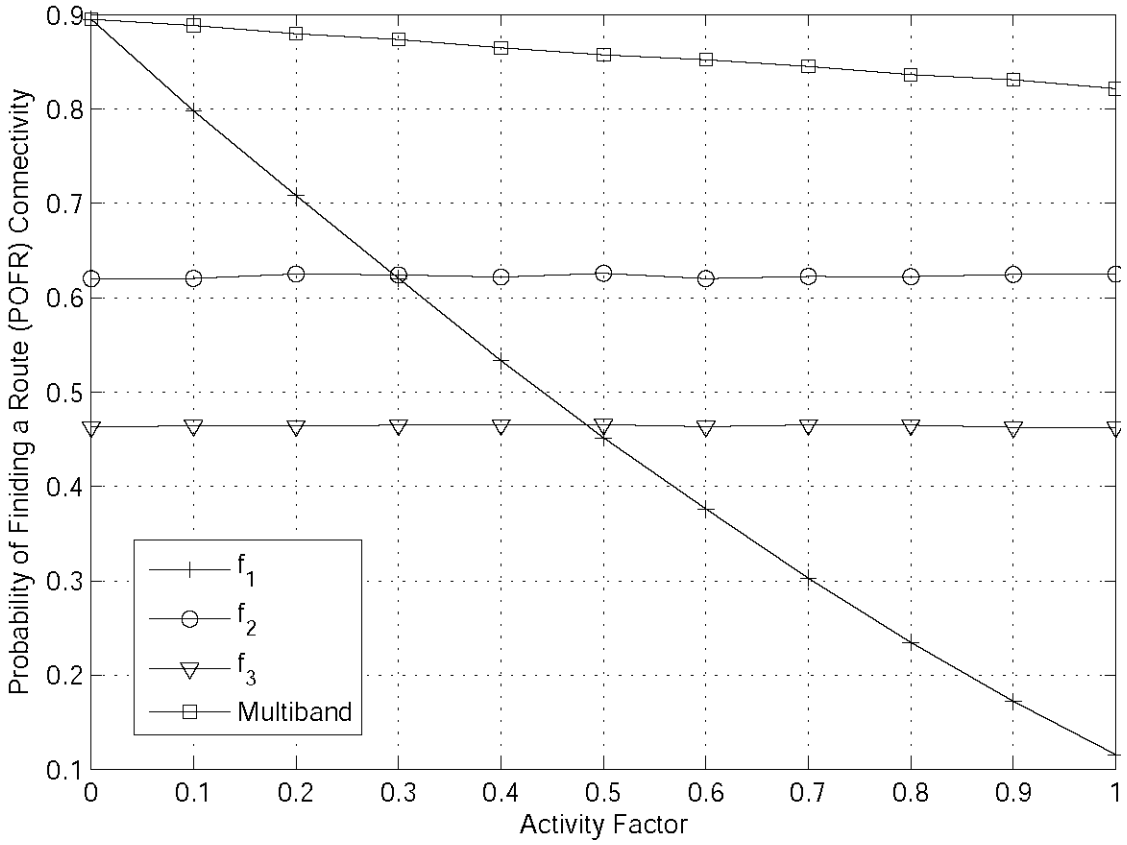

Figure 4.8: POFR in a multi-band CRN versus single-band PU activity factor.

Figure 4.9 presents the network connectivity using the natural connectivity metric where both single-band and multi-band modes are analyzed. As the activity factor of the f_1 layer increases, the CNC for SUs operating at f_1 decreases, and the CNC for *SUs* operating in the multi-band mode decreases as well. Both Figure 4.8 and Figure 4.9 which have the same monotonic decreasing behavior show that the MBCNC metric is an adequate measure for cognitive network connectivity. Note that MBCNC has a significant computational complexity reduction compared to POFR. Quantitatively, the average execution time for the MBCNC metric in this simulation is approximately $= 0.02$ of the average execution time for the POFR metric.

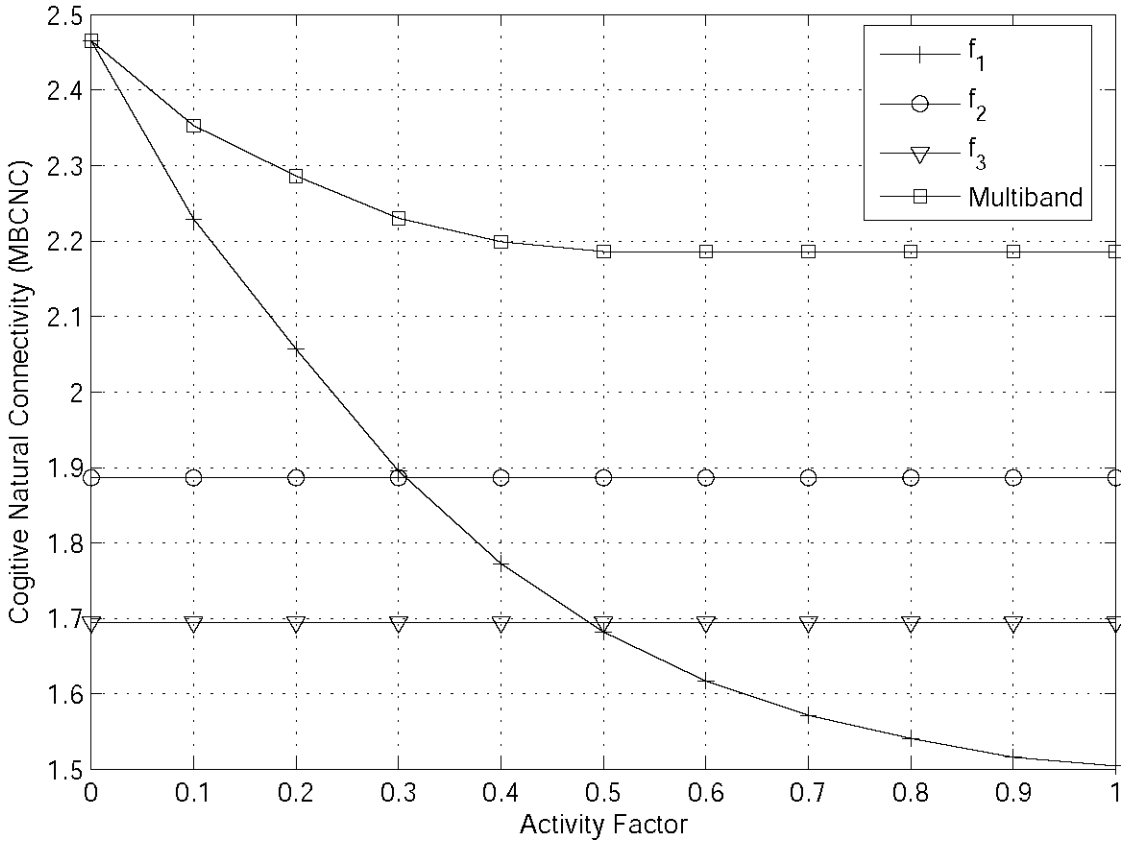

Figure 4.9: MBCNC versus PU activity factor in multi-band CRN

MBCNC and PUs Layers Transmission radius

Consider the cognitive network presented in the above example with network area $5R \times 5R$ and *M*=12 PUs divided into 3 layers, each having 4 PUs with frequency bands f_1, f_2 and f_3. In this example different frequency bands are considered as $f_1 < f_2 < f_3$. In this case the PUs transmission radius in each frequency band is assumed as follows, $R_1 = R$ for all PUs in f_1, $R_2 = 0.9R$, and $R_3 = 0.85R$ for f_2 and f_3 respectively. The PU's activity factor is kept fixed for all the 12 PUs as $AF = 0.5$. Figure 4.10 presents the MBCNC metric versus the number of SUs nodes in the network. As shown, in single-band mode when all SUs utilize f_3 where the

corresponding PUs have the smallest transmission radius, higher network connectivity is achieved compared with SUs layers using either f_1 or f_2 since R_1 and R_2 are greater than R_3. As expected, the largest network connectivity is achieved when the multi-band mode is considered where each SU chose the best available link among the three frequency bands.

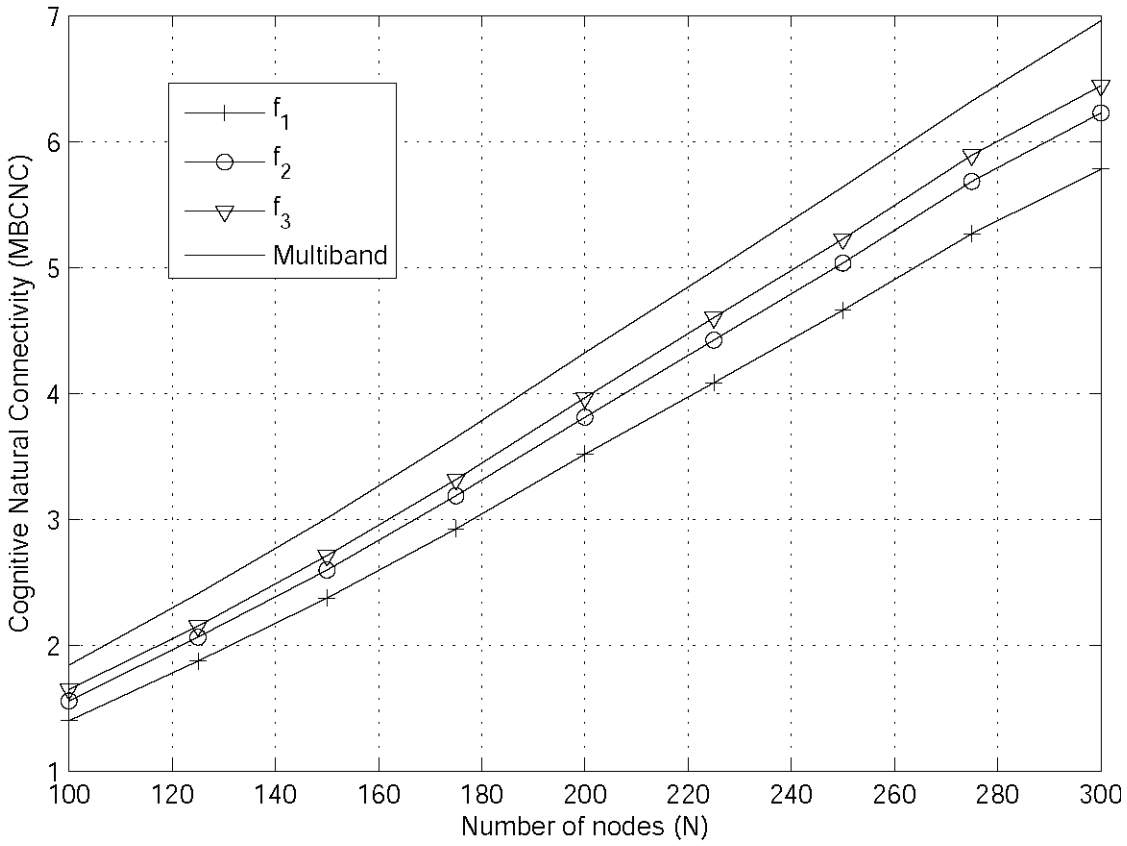

Figure 4.10: MBCNC vs. the number of SUs with fixed Activity factors $AF = 0.5$ and different PUs radii

MBCNC Averaged Over Random AF Realizations

Consider the network described above. In this section each PU among the 12 PUs is assigned a random value for the activity factor $AF_{mk} \in \{0,\cdots,1\}$. Both the single-band (CNC) and the multi-band (MBCNC) metrics are computed and averaged over 100 iterations. The metric is presented

in Figure 4.11 versus the number of SUs. As shown, the connectivity is approximately the same for the three frequencies f_1, f_2 and f_3 (single-band mode) since the three layers have identical parameters and hence an identical behavior when averaged over the random activity factor realizations.

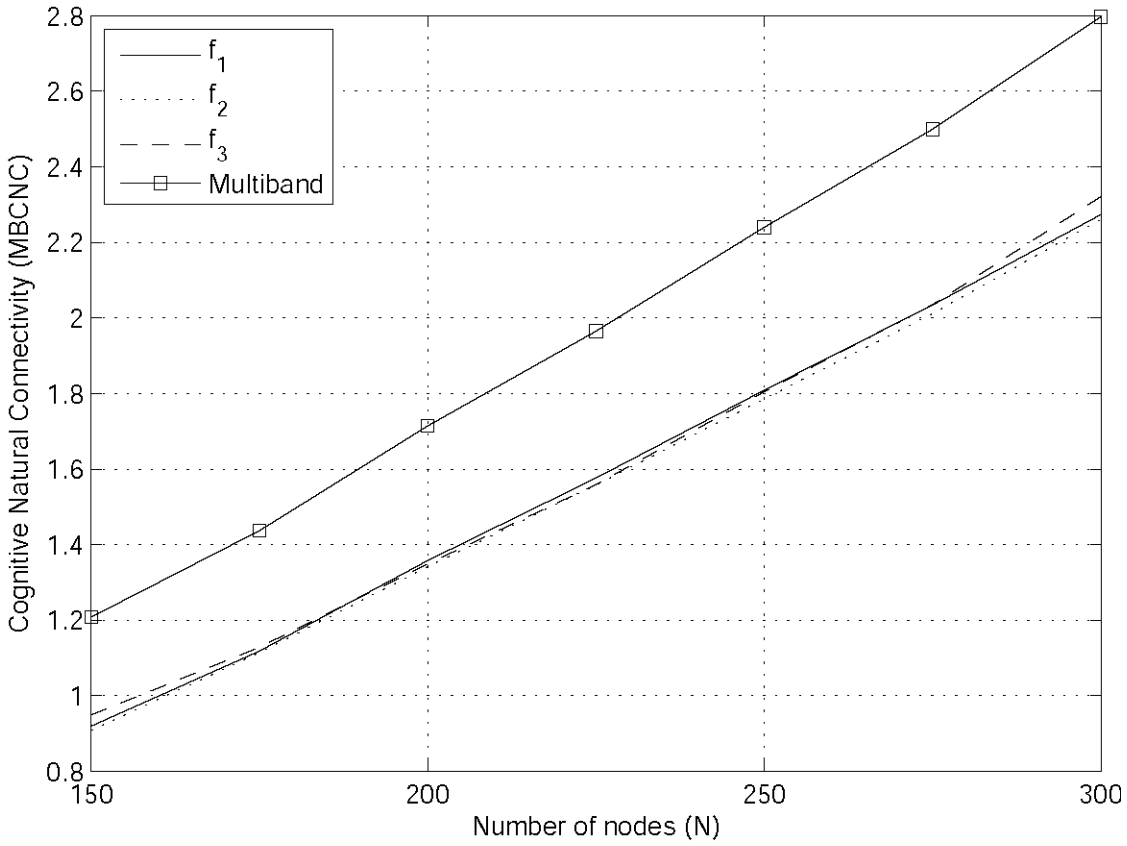

Figure 4.11: MBCNC for the single-band and multi-band CRNs vs. the number of SUs averaged over random AFs realizations.

MBCNC and SU Transmission Radius

Consider the network described above. In this section each PU among the 12 PUs is assigned a random value for the activity factor $AF_{mk} \in \{0, \cdots, 1\}$. In this section the effect of r_o on MBCNC is investigated. It is assumed that the transmission range of all SUs in the three frequency bands is

fixed to r_o. The MBCNC metric is computed at each radius $r_o \in \{0.15,\cdots,1\}R$ and averaged over 50 iterations where all activity factors are set to random value $\in [0,1]$ for each realization..

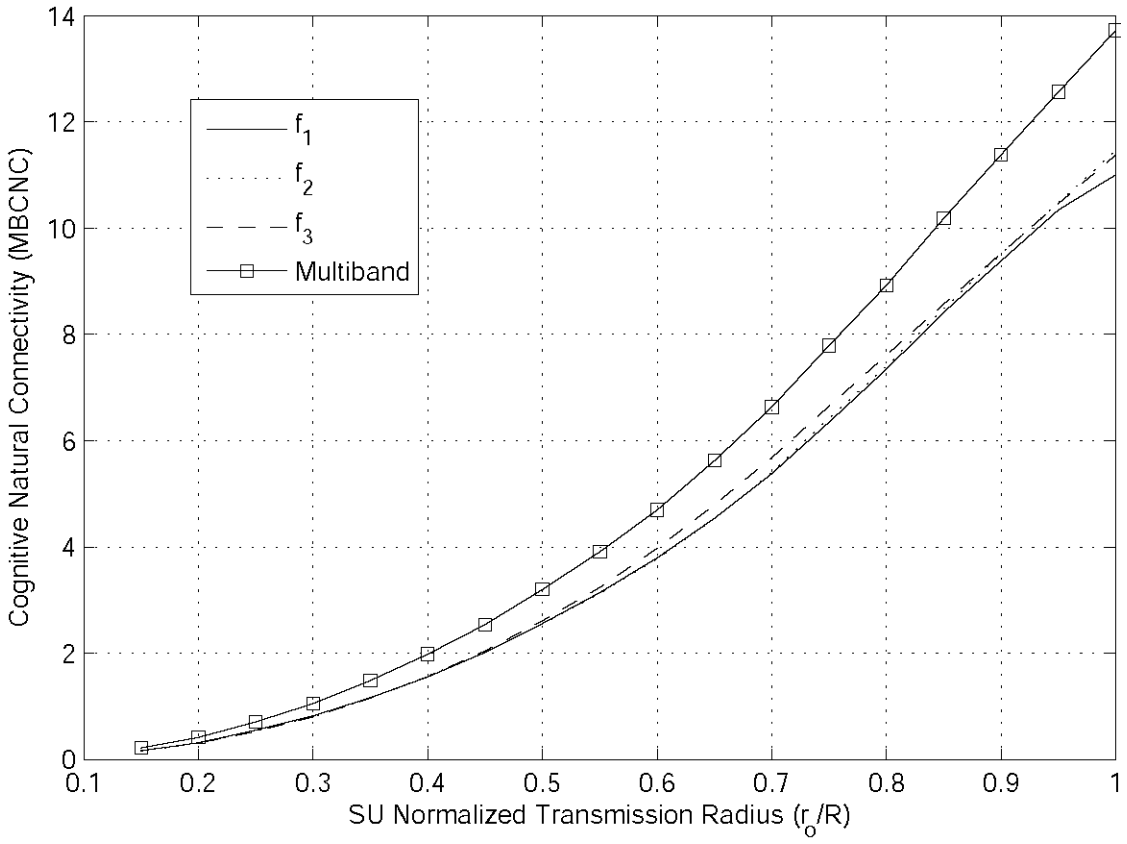

Figure 4.12: MBCNC for the single-band and multi-band CRNs versus the normalized SU transmission radius r_o/R averaged over AFs realizations.

The result is shown in Figure 4.12 where the three frequency bands deliver an identical performance. Clearly the multi-band mode has a higher connectivity compared to the single-band mode. In this example r_o can represent the power allocated to each SU node. As r_o increases, more nodes are connected and hence the network connectivity increases as shown in Figure 4.12.

The Convexity of MBCNC

Finally, we discuss the convexity of the CNC metric in the multi-band hybrid scenario. Due to the display limitations, we will consider two frequency band f_1 and f_2 each has 4 PUs. Figure 4.13 presents a 3-D plot of the MBCNC metric for the multi-band scenarios. As AF increases, the network's MBCNC decreases. Note that for a given activity factor AF_1, the MBCNC is monotonically decreasing with AF_2 and vice versa when AF_2 is fixed.

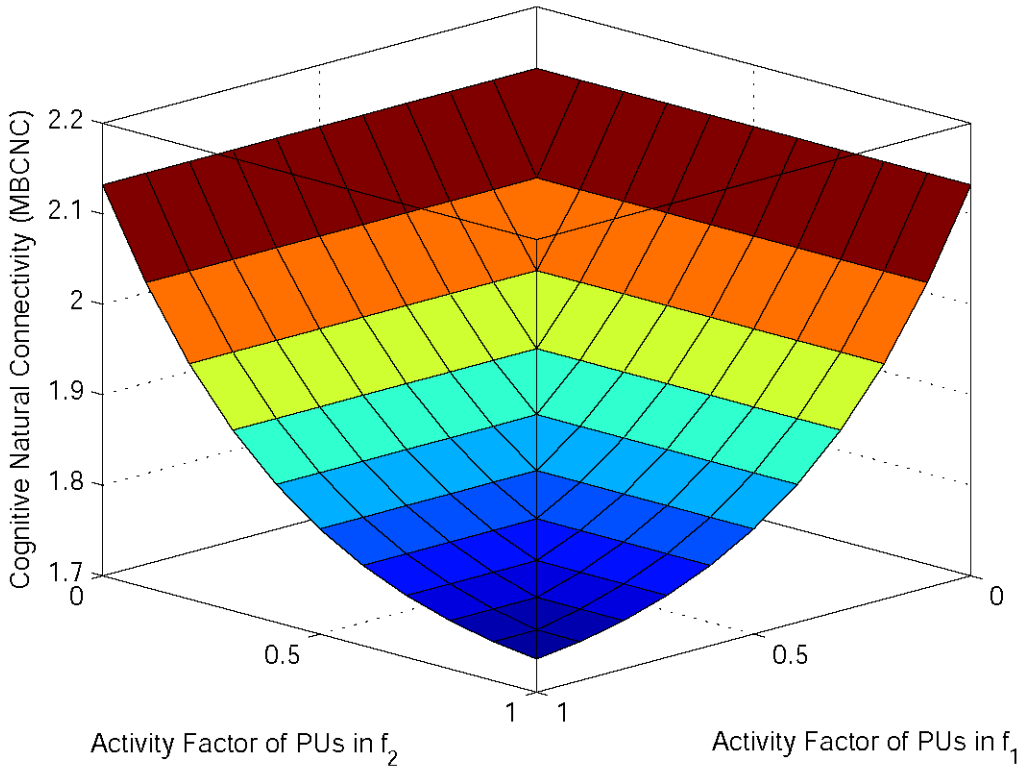

Figure 4.13: A 3-D plot of the MBCNC for the multi-band scenario vs. AF_1 and AF_2

4.4 Conclusion

In this chapter, we started by analyzing the connectivity of a practical CRN scenario, i.e. dual band capable cognitive radio networks. In such a scenario, the cognitive radio nodes have the capability of falling back to an unlicensed spectrum band (f_2) when they cannot access the primary spectrum band (f_1). We proposed two strategies to select routes which maximize the network connectivity, namely, single-frequency routing (SFR) and dual-frequency routing (DFR). We showed that dual-band CRNs deploying DFR will offer a slightly better connectivity than those deploying SFR. CRNs with better connectivity will be able to guarantee acceptable QoS and seamless communications to their CR nodes.

Next, we showed that the CNC metric can efficiently be utilized in the design of Dual-band cognitive radio networks, where it provides information on how a frequency-assignment scenario can be selected to maximize the resulting cognitive network connectivity.

Finally, we proposed an extension to the CNC metric for multi-band CRNs. It is shown that the metric is convex in the activity factors of the primary users. The proposed connectivity metric provides a simple and robust method to determine the cognitive radio network connectivity under various network scenarios. The proposed metric is a useful tool that can be used in studying the effect of different network parameters on the connectivity of cognitive networks and in designing CRNs routing algorithms.

Chapter 5

A Reduced Search Space Routing Algorithm for Large-Scale Cognitive Radio Networks

5.1 Introduction

Large-scale wireless networks have been an interesting area of research for the past decade, specifically since the appearance of the work of Gupta and Kumar [GUP-00] on the scalability of large-scale sensor networks. Many applications have been envisioned such as industrial monitoring, large scale disaster relief operations [UCH-12], large scale sensor networks, and high density mesh networks.

The high demand for wireless services and the limitations of the traditional large-scale networks have paved the road for a new area of research for large-scale networks using cognitive radio technology to enhance the system's performance and heighten its adaptability to the surrounding environment [LU-12].

Large-scale CRNs are characterized by a couple of special traits that can differentiate them from regular CRNs. First, they have a high SU node density. This implies that the complexity of the routing algorithm is significantly higher than the regular CRNs. For example, applying the Dijkstra's algorithm to find the optimal route in *N* nodes network, with a complexity of order

$\mathcal{O}(N^2)$, would highly increase the routing selection time which could lead to the loss of the available spectrum opportunity. Second, the high node degree increases the number of possibilities for a given node to choose the next hop node, leading to a high computational complexity. Third, due to the high node density, the link availabilities of neighbor nodes are highly correlated. These challenges require a new routing algorithm specially designed for large-scale CRNs which is both fast and efficient.

In this chapter, the problem of finding the shortest route between a source and a destination in a large-scale wireless ad hoc network is investigated. A novel and efficient technique to reduce the network search space size based on nodes location information is developed. Following the proposed technique, it is shown that the route found within the reduced search space has the same (or nearly the same) number of hops as that obtained when solving the problem considering the large-scale network as the number of nodes increases. Furthermore, the proposed technique provides a significant complexity reduction. The proposed algorithm is also applied to cognitive radio networks to analyze route throughput. Compared to the average link throughput obtained via solving the large-scale network, negligible throughput degradation is noticed and a remarkable complexity reduction is obtained. Finally, the analysis of the proposed algorithm using the similarity between the shortest path algorithm and the greedy forwarding algorithm is presented.

5.2 System Model and Performance Metrics

We adopt a two-dimensional network model, where N cognitive radio SU nodes are randomly distributed on a square area of size $L \times L$ following a uniform distribution in both x and y

directions. The PU transmitters are distributed in a non-overlapping fashion. We can assume, without loss of generality, that they operate using the same frequency. A disc propagation model is assumed such that R and r_o are the transmission ranges of the PU transmitter and CR nodes respectively. We assume a two state PU that operates according to a Markov chain such that q is the probability of an off channel.

As discussed in Chapter 2, routing metrics for CRNs can be classified according to the performance measure it aims to optimize. These performance measures include: end-to-end throughput, delay, interference, and route availability. Some routing metrics are designed mainly to optimize only one performance measure while others are designed to find a balance between some or all of these measures according to system application. In this chapter we are focusing on the design of a fast and efficient routing algorithm for large-scale CRNs. We will use the Expected Transmission Count (ETX) metric as an example. Any other routing metric, especially delay-based metrics, can be also used with either no or minor modifications to the proposed algorithm.

ETX is one of the early adapted metrics specially designed for ad hoc networks. It started with the observation that minimal hop count is not optimal for wireless networks. The metric is based on the channel loss ratio. It aims to predict the number of transmissions required to send a packet over a link. Let q be the expected delivery ratio, the likelihood that a packet arrives can be defined as $ETX = 1/q$. ETX can be easily adapted in the CRN's environment by assigning q as the probability of a channel to be vacant.

5.3 A Reduced Complexity Routing Algorithm for Large-Scale CRNs

Large-scale CRNs require new routing algorithms specially designed for those networks that are both fast and efficient. The assumption that each node has full spectrum knowledge is not feasible in large-scale CRNs because of scalability issues. In [LI-10], the authors used the idea of reducing the network size from N to n where $n \ll N$ such that it reduces the routing complexity, e.g., $\mathcal{O}(N^2)$ when using Dijkstra's algorithm. The idea is based on reducing the network size using clustering techniques. While this method is efficient in the case of large-scale ad hoc networks, it is not adequate for cognitive radio large-scale networks since the clustering technique depends on the channel parameters, i.e., channel availability, which is time variable in the case of CRN.

To develop a routing algorithm for large scale networks, two approaches can be used to reduce the network search space from N to n nodes. The first approach can be summarized as follows:

1. Find the minimum hop path between a source *S* and a destination *D* using the Dijkstra's algorithm while the PU activity is off.
2. For each node in the obtained route, consider all neighbors within one hop from each node to construct a sub-network of n nodes. For the n nodes network assign a weight for each link based on the PU activity factor, i.e., link availability according to the ETX metric for every channel state.
3. The shortest path is computed depending on the PU activity.

The main drawback of this method is that in the initialization stage the search is performed within the full network size N. For large-scale networks this is a time-consuming process, where the number of nodes ranges between hundreds and thousands of CR nodes. Furthermore, the initialization stage requires a full knowledge of the network topology which requires a large amount of spectrum sensing data exchanges between nodes.

The second approach is to develop a method to estimate the sub-nodes without the need to search the entire network for the shortest path between *S*-*D*. The proposed algorithm relies on the observation that the number of nodes in the CRN increases, while the asymptotic behavior of the shortest path between a source *S* and a destination *D* tends to be closer to the direct line that is geometrically connecting *S* and *D* in the two-dimensional space $\mathbb{R}^2$. This observation will also be interpreted later in the simulations section.

To further illustrate the previous observation, assume a square network area of side 6 units, with $N \in \{50,100,...,300\}$ nodes, each with a transmission range $r_o = 1$ unit. For each network realization, a random $S-D$ pair is selected and the shortest path with the minimum number of hops $\{L_1,..,L_i,...,L_k\}$ between $S-D$ is calculated. Let us define $P_{S,D}$ as the maximum displacement distance between the selected route and the line connecting $S-D$. Figure 5.1 shows the Cumulative Distribution Function (CDF) of the maximum perpendicular displacement distance $P_{S,D}$ for different network sizes. Figure 5.2 shows the probability that the distance between any node on the selected route and the $S-D$ line is less than r_o. It is noticed that as N increases, the probability that the shortest path lies closer to the $S-D$ line increases. For $N = 100$, the $CDF = 91\%,$ and for $N = 300$, the $CDF = 96\%$.

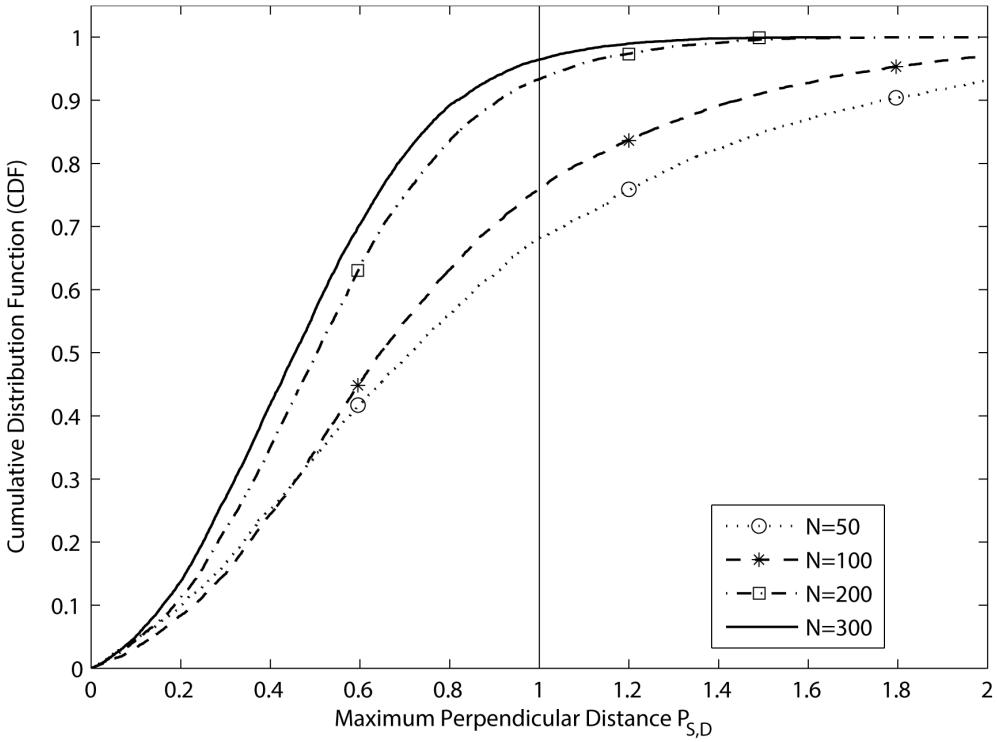

Figure 5.1: CDF of the maximum perpendicular distance $P_{S,D}$ for different network sizes N

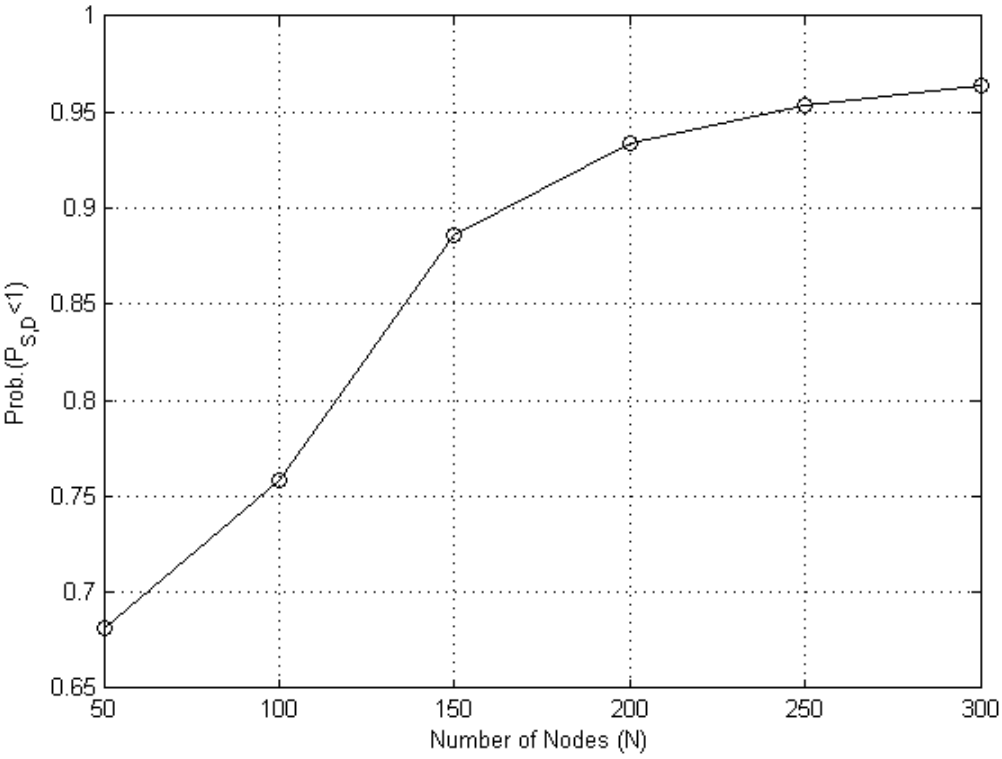

Figure 5.2: The probability that the distance between any node on the selected route and the *S-D* line is less than *r* versus network size *N*

The previous example shows that as *N* increases, the shortest path between *S*-*D* tends to be closer to the connecting line. This finding will be discussed further in the analysis section.

The proposed algorithm can be summarized as follows:

1. Using the *S*,*D* location information, find the length of the line connecting *S* and *D* (L_{SD}).
2. Draw a rectangular of dimensions $L_{SD} \times 2\, r_0$ as shown in Figure 5.3.
3. Construct a subset ψ from the nodes inside the rectangular and use it to construct a sub-graph G_{ψ}
4. Apply the ETX metric to G_{ψ} to find the shortest path between S-D.
5. Repeat 4 if the PUs activity factors are changed.

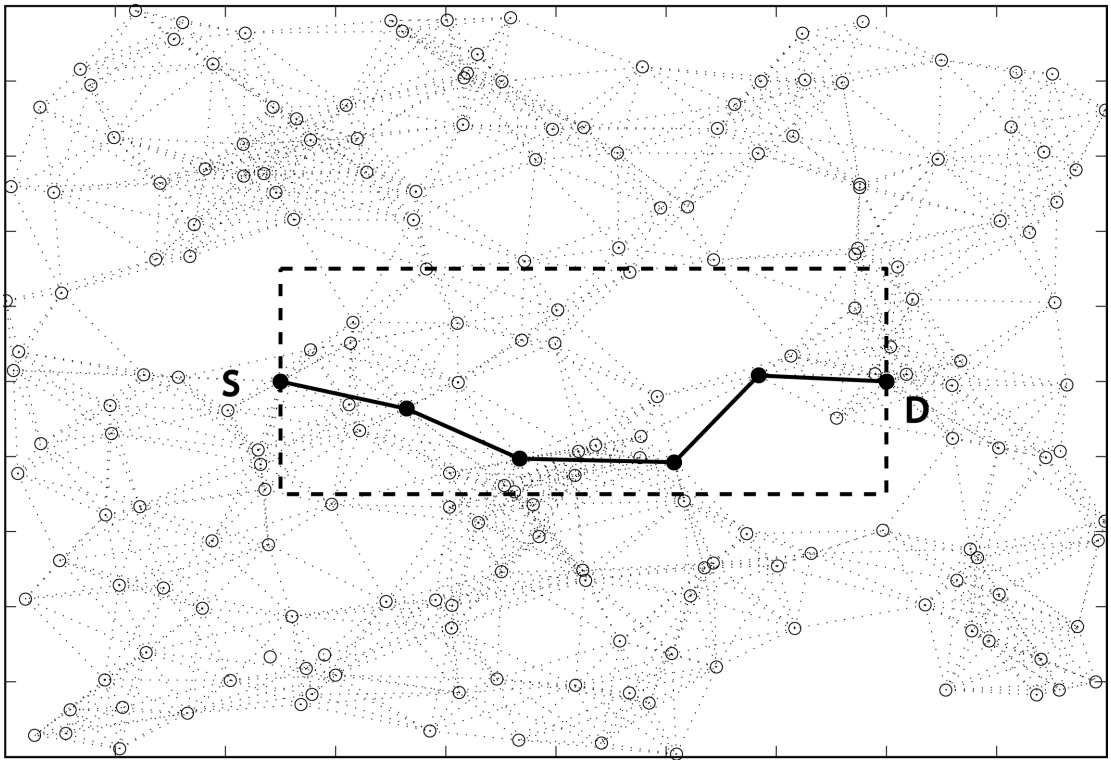

Figure 5.3: The subset ψ of position-based selected nodes

5.4 Simulation Results

Consider a network of N nodes (secondary users) uniformly distributed over a square region of area $A = L \times L$ where L is the side length. Let r_0 denote the communication radius of each user. In order to reduce the size and hence the complexity of the source-destination route finding problem, a new subset of nodes ψ is created. This subset contains the nodes belonging to a rectangular of dimensions $L_{SD} \times 2r_0$ where L_{SD} is the distance between the source node S and the destination node D. Figure 5.3 presents a simple illustrative diagram for the subset ψ along with solving a route finding problem within ψ between a randomly chosen source and destination.

In this section, the robustness of the proposed method in terms of the probability that the minimum hops route lies within the set ψ is analyzed. Consider a network of size N with each node being connected to its neighbor if they are within a distance r_0. Each edge weight is set to unity. For a given network realization with N nodes, the shortest path between a source S and a destination D is found using Dijkstra's algorithm. Let H_N represent the number of hops counted in the shortest path.

In order to reduce the problem size, consider a subset ψ that consists of nodes within the area $L_{SD} \times 2r_0$ as shown in Figure 5.3. Let n_ψ represent the number of nodes in ψ. The shortest path between S and D using ψ is obtained using Dijkstra's algorithm. Let H_{n_ψ} represent the shortest path length, in hops, found in ψ. The robustness of considering n_ψ instead of N, to

find the shortest path, can be measured by the probability of finding a route within ψ that has the same number of hops as that obtained when solving the complete network. Mathematically, this measure can be presented by (5.1)

$$P_H = Prob.\left(H_{n_\psi} = H_N\right) \tag{5.1}$$

In order to illustrate the behavior of P_H versus a different number of network size N, let $\delta = \alpha r_0$ represent a variable side-length of the rectangular representing ψ with $\alpha > 0$. The probability P_H versus the total number of nodes *N* is shown in Figure 5.4 with $\delta \in \{0.75\, r_0, r_0, 1.25\, r_0\}$.

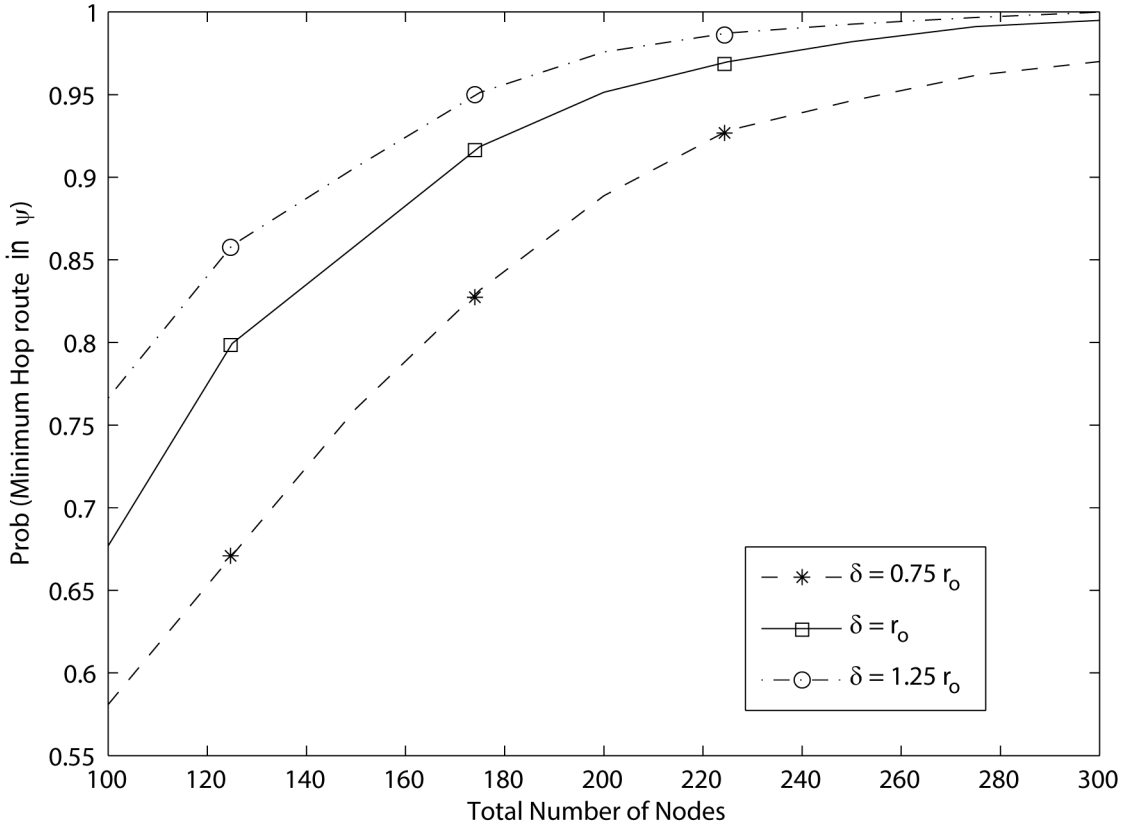

Figure 5.4: The probability that the shortest path, with $H_{n_\psi} = H_N$ lies within ψ versus a different number of network size N

As shown when N increases and for a given δ, with high probability that a route within ψ having H_N hops exists. Furthermore, for a given *N*, increasing the physical size of ψ, and hence n_ψ, increases the probability that a route exists within ψ that has H_N hops. For example, with *N*=200 and $\delta = r_0$, the shortest path of H_N hops lies within ψ with probability $P_H = 0.95$ and as N increases this probability approaches one.

Although the probability of successfully finding a minimum hops route within ψ is important, the size of the search space has a significant impact on the shortest path computation time.

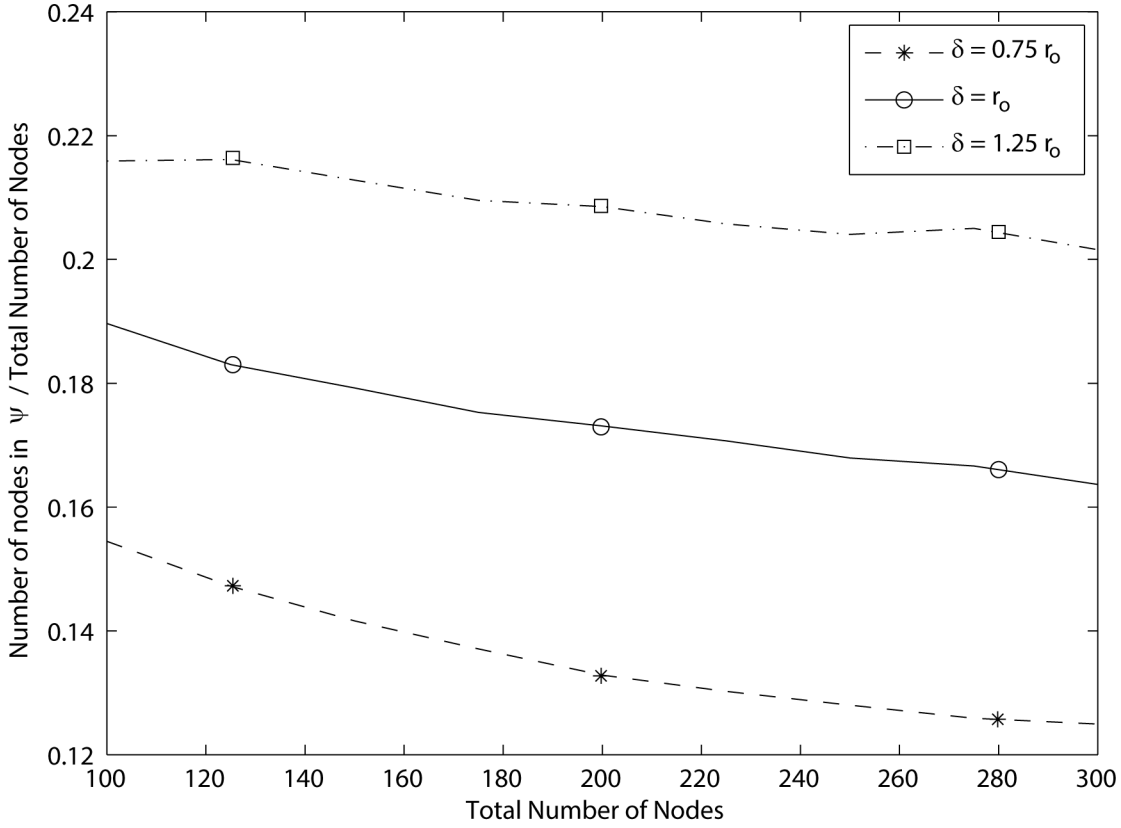

Figure 5.5: The ratio between the number of nodes in ψ and the total number of network nodes n_ψ / N

Figure 5.5 presents the ratio between n_ψ and N for different values of δ. As shown, when $\delta = r_0$ and over a wide range of $N \in \{100,125,\cdots,300\}$, the number of nodes within ψ to the total network node, n_ψ / N varies approximately from 0.19 to 0.16 indicating a significant reduction in the problem size. Furthermore, a tradeoff between the probability of finding the shortest path and the number of nodes n_ψ exists. In particular, from Figure 5.5 and when *N*=200 as δ increases from r_o to 1.25r_o the ratio n_ψ / N increases approximately from 0.17 to 0.21 leading to a higher computational complexity. On the other hand, the probability of finding the shortest path in ψ increases from 0.95 to 0.97, for *N*=200 as shown in Figure 5.4.

In this section, the proposed location-based technique developed above to form the subset ψ will be applied to the routing problem in cognitive radio networks. The network consists of N secondary users uniformly distributed over an area of $A = L \times L$ centered at the origin with r_0 representing the radius of communication for each user, and let $L = 6r_o$. Four primary users PU_i with $i = 1,\cdots,4$ are located at the points $(\pm L/4, \pm L/4)$ with radius of communication $L/4$ and equal users activity factors $AF_i = 0.6$ for $i = 1,\cdots,4$. A node i is connected to a node j if their inner distance is less than r_0. The weight of each edge in the network represents the delay encountered by the link. The delay represents the time required for packet retransmission which is inversely proportional to link availability. An edge affected by the primary user PU_i has a delay of $\frac{1}{(1-AF_i)}$, while an edge crossing the border of two primary users i and j assigned a delay $\frac{1}{(1-AF_i)}\frac{1}{(1-AF_j)}$.

After establishing the network edge weights, Dijkstra's algorithm is utilized to solve the N nodes problem for the shortest path, minimum delay, route between a randomly chosen source and destination. Assuming that all links communicate at the same data rate, the route throughput, T_N, is determined as the inverse of the total delay associated with the path. The same procedure is repeated while considering the subset ψ which is formed using the position-based algorithm described above. The throughput of the shortest path route found within ψ and denoted T_ψ is computed also as the inverse of the route delay. For the sake of comparison, the throughput T_ψ is normalized to T_N in order to realize the gain in throughput achieved when reducing the search space to ψ as

$$T = \frac{T_\psi}{T_N} \times 100\%. \tag{5.2}$$

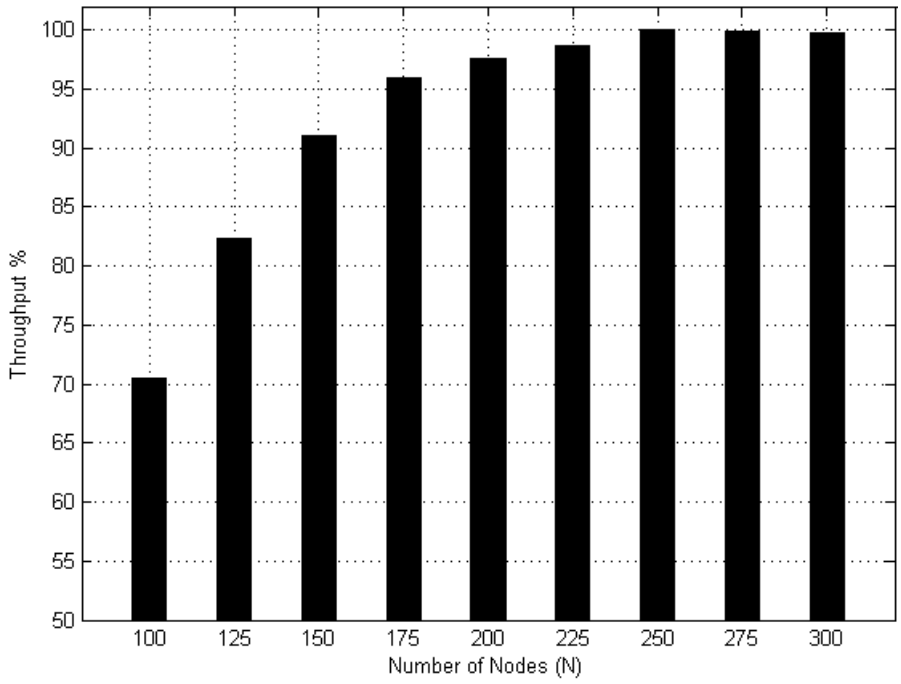

Figure 5.6: The percentage ratio of throughput calculated using n_ψ nodes and *N* nodes.

As shown in Figure 5.6, when $N = 100$ approximately $T = 70\%$ of the throughput can be achieved when applying the proposed technique within ψ. However, when *N* increases, and approaches large-scale network, the ratio increases. Quantitatively, when *N*=250 approximately $T = 99\%$ of the throughput obtained when solving the large network can be obtained when reducing the search space within ψ.

5.5 Geometrical analysis of the shortest Path Routing Algorithm

In this section we analyze the shortest path routing algorithm. Due to the similarity between the shortest path algorithm and the greedy forwarding algorithm analysis in [SRI-10], the analysis of the greedy forwarding algorithm will be used to study the behavior of the shortest path routing algorithm in location-based routing protocols.

Node Distributions

In wireless networks, the knowledge of inter-node distributions is essential from many points including protocol design and performance evaluation. Typically, it is assumed that nodes are distributed as a stationary Poisson Point Process (PPP). For a PPP network of density λ, the number of nodes in any given set Q of size $|Q|$ is a Poisson random variable with mean $\lambda|Q|$, and the numbers of nodes in disjointed sets are independent. While this assumption is a good approximation for the sake of analytical convenience, it suffers from certain shortcomings. Practical networks differ from Poisson networks in certain aspects. First, networks consist of a finite number of nodes in a given area. In this case, the nodal arrangement is a Binomial Point Process (BPP). Second, since the area or volume of deployment is necessarily finite then the

edge effect problem is present and the point process formed is non-stationary. This means that the network characteristics, as seen from a node's perspective, are not the same for all nodes. Third, the numbers of nodes in disjointed sets are not independent.

A BPP Ω is formed as a result of independently and uniformly distributing N points in a compact set W. For any set Q, the number of points in S, i.e., $\Omega(Q)$, is binomial (N, p) with $p = |Q \cap W| / |W|$. By this property, the number of nodes in disjointed sets is joined via a multinomial distribution. Accordingly, for disjointed sets $\{Q_1, Q_2, \cdots, Q_N\}$ and $n = \sum_{i=1}^{k} n_i$, we have

$$\Pr\left(\Omega(Q_1) = n_1, \cdots\cdots, \Omega(Q_k) = n_k\right) = \frac{n! \prod_{i=1}^{k} |Q \cap W| / |W|^{n_i}}{\prod_{i=1}^{k} n_i ! |W|^{n}} \tag{5.3}$$

If the number of nodes is known, the PPP realization may have more nodes than the actual number of nodes deployed or no nodes at all if the number of nodes is small. The PPP is clearly an inaccurate model when the number of nodes is known. Also, the independence of the number of nodes in disjointed areas assumption is an impractical assumption. These remarks motivated the need to study and accurately characterize finite uniformly random network, as in [SRI-10], using the BPP. The BPP model can also be applied to studying many different realistic networks such as mobile ad hoc and sensor networks and wireless networks with infrastructure.

In [SRI-10], the distribution of the Euclidean distance to the n^{th} nearest point from an arbitrary reference point is studied for a *d*-dimensional isotropic BPP. Consider the BPP Ω with N points uniformly randomly distributed in a compact set $W \subset \mathbb{R}^d$. Let R_n denote the random variable

representing the Euclidean distance from an arbitrary reference point x to the n^{th} nearest node of the BPP, and let $b_d(x,r)$ denote the *d*-dimensional ball of radius r centered at x as in Figure 5.7.

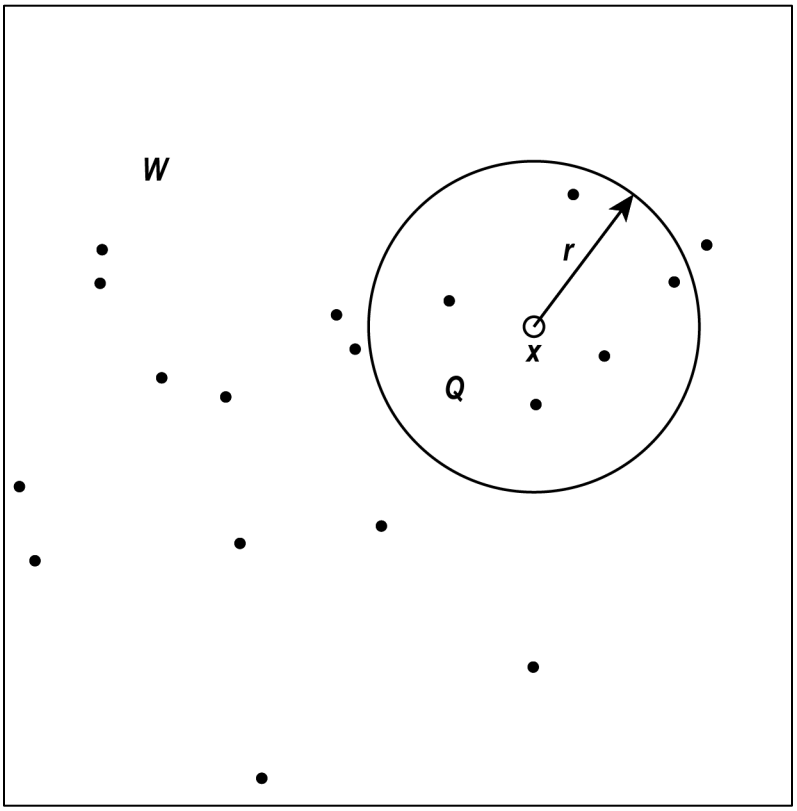

Figure 5.7: A BPP with *N* = 20 points in an arbitrary compact set *W*.

The CDF of R_n is the probability that there are less than n points in $b_d(x,r)$

$$\overline{F}_{R_n}(r) = \sum_{k=0}^{n-1} \binom{N}{k} p^k (1-p)^{N-k}, \qquad 0 \le r \le R \tag{5.4}$$

Where

$$p = \frac{|b_d(x,r) \cap W|}{|W|} \tag{5.5}$$

Greedy Forwarding Protocol

This protocol maximizes the expected progress of a packet toward its destination. There is a high similarity between the shortest path algorithm and the greedy forwarding routing algorithm. The results developed in this section will be used to study the Shortest path algorithm in the next section.

Consider a network with N nodes, each with a transmission range r_o, uniformly distributed in an area A. Assume that several packets need to be forwarded from a Source (S) to a destination node (D). The nodes adopt a greedy forwarding strategy in which each relay node X_i that gets a packet relays it to its farthest neighbor in a sector of angle $\phi \in [0 \le \phi \le \pi]$, i.e. along $\pm\phi/2$ around the $X_i - D$ axis as in Figure 5.8.

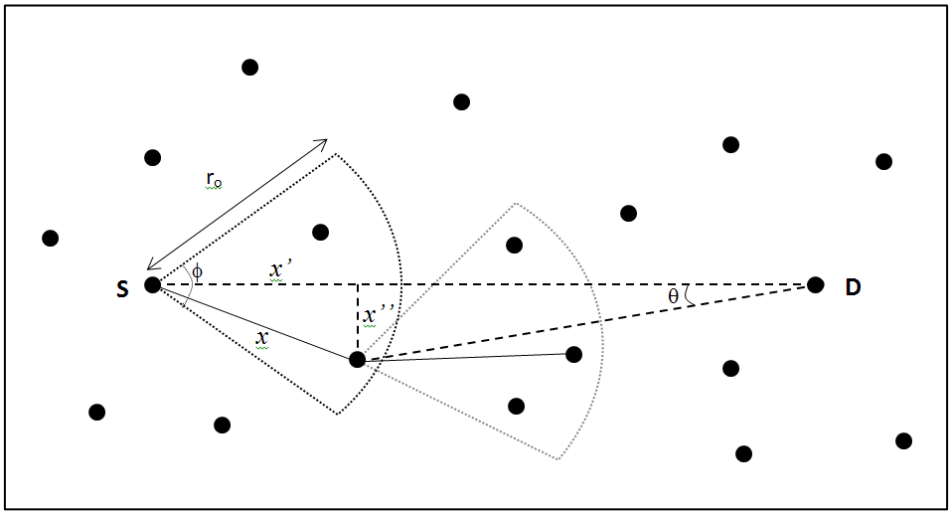

Figure 5.8: Greedy forwarding protocol.

For a large ϕ, the direction of the farthest neighbor in the sector may be off the $X_i - D$ axis, while for a small ϕ, there may not be enough nodes inside the sector. There is an optimum ϕ that maximizes the expected progress of packets toward D.

A similar problem is studied in [BAC-06] for an interference-limited PPP, in which the authors evaluate the optimal density of transmitters that maximizes the expected progress of a packet. In [HAE-05a], the energy required to deliver a packet over a certain distance for various routing strategies in a PPP is calculated. In [TAK-84], the optimal transmission radius that maximizes the expected progress of a packet is determined for different transmission protocols in a PPP wireless network.

Following the analysis in [SRI-10], let us define three quantities for each hop on the path between S and D: x as the link length, x' as the projection of the link x on the *S-D* line, and x'' as the vertical displacement per hop from the *S-D* line as in Figure 5.8. The mean distance to the farthest neighbor in the sector can be written as [SRI-10],

$$E[x] = \sum_{k=0}^{n-1} \binom{N}{k} p^k (1-p)^{N-k} \frac{2rk}{2k+1} \tag{5.6}$$

where

$$p = \frac{\text{Node Transmission Area}}{\text{Total Network Area}} = \frac{\phi r^2}{A} \tag{5.7}$$

The expected progress of a packet is given by [SRI-10] as,

$$E[x'] = E[x]E[\cos(\theta)] \tag{5.8}$$

Where θ is uniformly distributed over $[-\phi/2, \phi/2]$. The expected packet progress can be expressed as

$$E[x'] \le \frac{2}{\phi} \sin\left(\frac{\phi}{2}\right) \sum_{k=0}^{n-1} \binom{N}{k} p^k (1-p)^{N-k} \frac{2rk}{2k+1} \tag{5.9}$$

The expected vertical displacement per hop $\left(E\left[x''\right]\right)$ can be approximated as

$$E\left[x''\right]=\sqrt{\left(E\left[x\right]\right)^2-\left(E\left[x'\right]\right)^2} \tag{5.10}$$

Now, we move forward to evaluate the expected maximum distance between any node on the selected route and the $S-D$ line. First, the Expected distance between two arbitrary nodes inside a rectangular area of sides a and b is analyzed in [PHI-07] as

$$\begin{aligned}E\left[\left\|S,D\right\|\right]=&\frac{a^2}{6b}\ln\left(\frac{b}{a}+\sqrt{1+\frac{b^2}{a^2}}\right)+\frac{b^2}{6a}\ln\left(\frac{a}{b}+\sqrt{1+\frac{a^2}{b^2}}\right)\\&+\frac{1}{15}\left(\frac{b^3}{a^2}+\frac{a^3}{b^2}+\left(3-\frac{a^2}{b^2}-\frac{b^2}{a^2}\right)\sqrt{a^2+b^2}\right)\end{aligned} \tag{5.11}$$

For the special case of $a=b$, this is reduced to

$$\begin{aligned}E\left[\left\|S,D\right\|\right]&=\left(\frac{1}{3}\ln\left(1+\sqrt{2}\right)+\frac{1}{15}\left(2+\sqrt{2}\right)\right)a\\&\approx 0.5214\,a\end{aligned} \tag{5.12}$$

The maximum distance between a node on the selected route and the *S-D* line, i.e. the worst case scenario, will occur when the first $m/2$ links are at 45^o away from the *S-D* line and the next $m/2$ links are at $\pi/4$ toward the S-D line. For a network of size $A=a^2$, the expected number of hops between S and D can be approximated by

$$Hops_{ave}=\frac{E\left[\left\|S,D\right\|\right]}{E\left[x'\right]}=\frac{0.5214\,a}{E\left[x'\right]} \tag{5.13}$$

Let us define $P_{S,D}$ as the maximum perpendicular displacement distance between the selected route and the line connecting S and D. The expected maximum perpendicular displacement can be expressed as

$$E\left[P_{S,D}\right] = \frac{Hops_{ave}}{2} \cdot E\left[x''\right] = 0.2607a\frac{E\left[x''\right]}{E\left[x'\right]} \tag{5.14}$$

To further understand the previous results, consider a square area network of side length equal to 6 units, with $N \in \{50,100,...,300\}$ nodes, each with a transmission range $r = 1$ unit, and let the greedy forwarding angle ϕ vary from $0 \le \phi \le \pi$. Figure 5.9 shows that the expected packet progress $E\left[x'\right]$ sharply increases as the forwarding angle ϕ increases until it reaches a maximum ϕ_N^* after which the expected packet progress $E\left[x'\right]$ slightly decreases. It is noticed that each network size N has a different optimum ϕ_N^* and as N increases, the ϕ_N^* angle decreases.

Figure 5.10 shows the optimum Expected Packet Progress $E\left[x'\right]^*$ versus the network size N. It is noticed that as N increases, i.e. the node density increases, the optimum Expected Packet Progress $E\left[x'\right]^*$ increases and approaches r_o. This happens because as N increases, the optimum forwarding angle ϕ_N^* decreases and the route gets closer to the $S-D$ line.

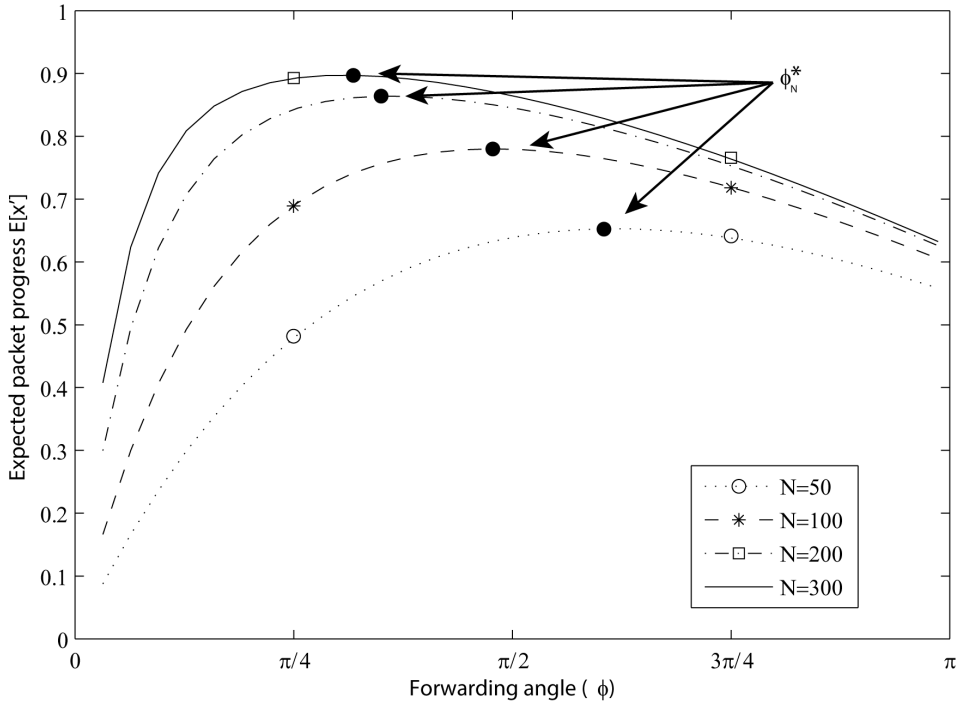

Figure 5.9: Expected Packet Progress $E\left[x'\right]$ versus the forwarding angle ϕ for different values of N. The circular markers, mark the optimum forwarding angle ϕ_N^* for each network size.

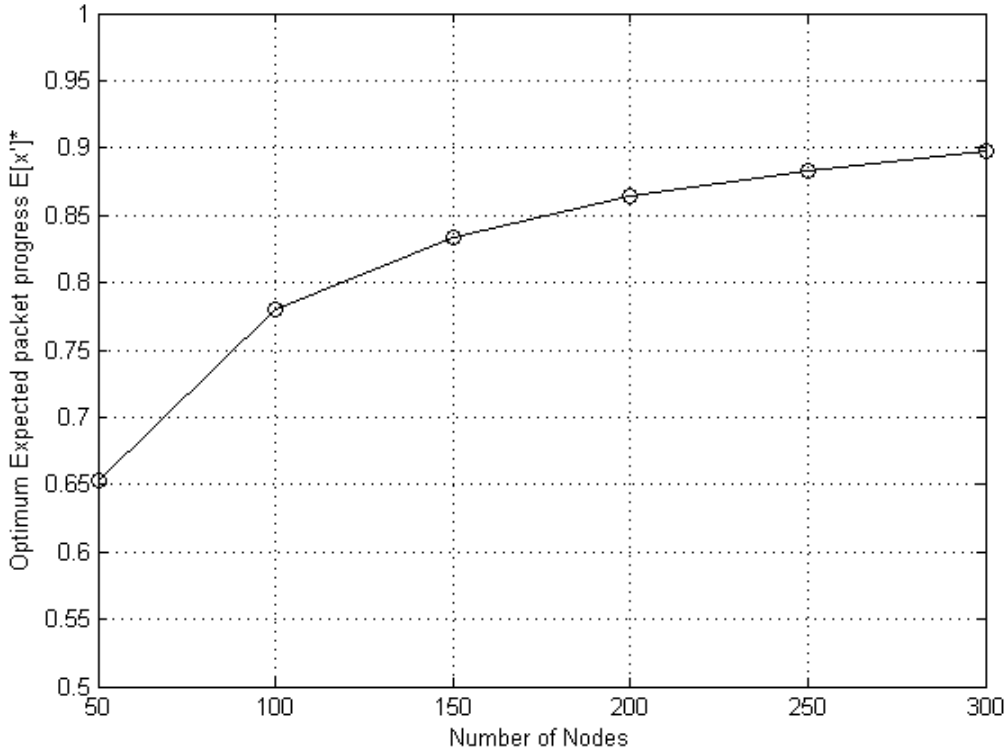

Figure 5.10: Optimum Expected Packet Progress $E\left[x'\right]^*$ versus the network size N.

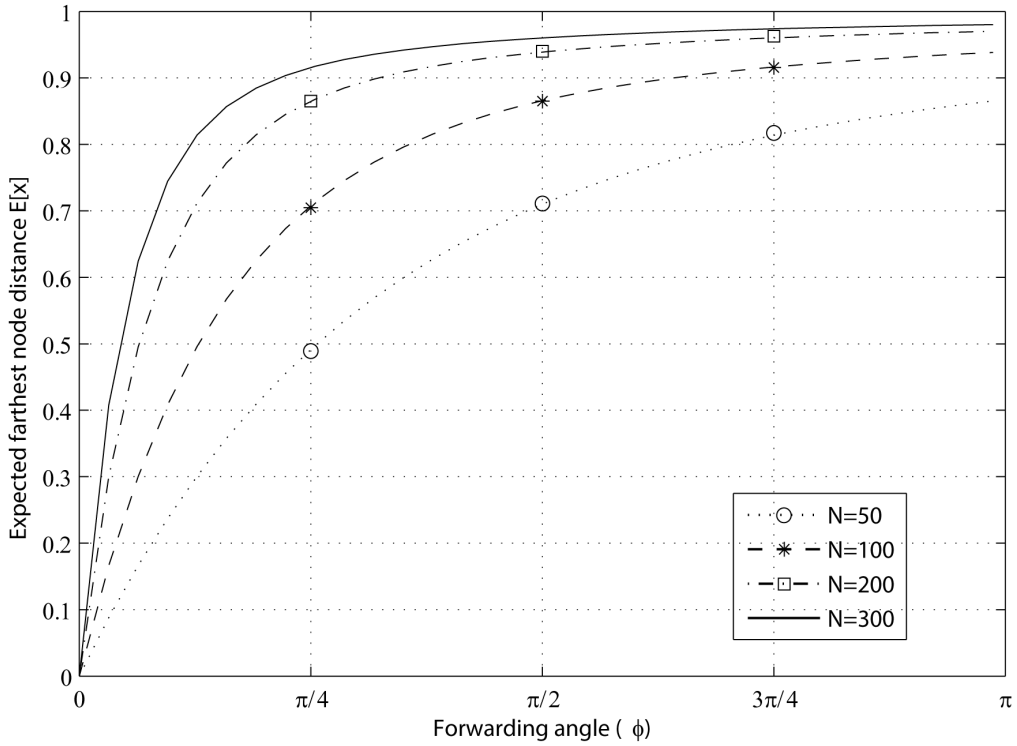

Figure 5.11: Expected Farthest node distance $E[x]$ versus forwarding angle ϕ for different network sizes N.

Figure 5.11 shows the expected farthest node distance $E[x]$ versus the forwarding angle ϕ for different network sizes N. $E[x]$ increases as the forwarding angle increases.

Figure 5.12 shows the optimum farthest node distance $E[x]^*$, for different network sizes N. For larger N, $E[x]^*$ approaches r_o.

Figure 5.13 shows the optimum expected vertical displacement per hop $E[x'']^*$ versus the network size N. It is clear that as N increases, the $E[x'']^*$ decrease. This shows that the routes' node spread from the $S-D$ line is decreased.

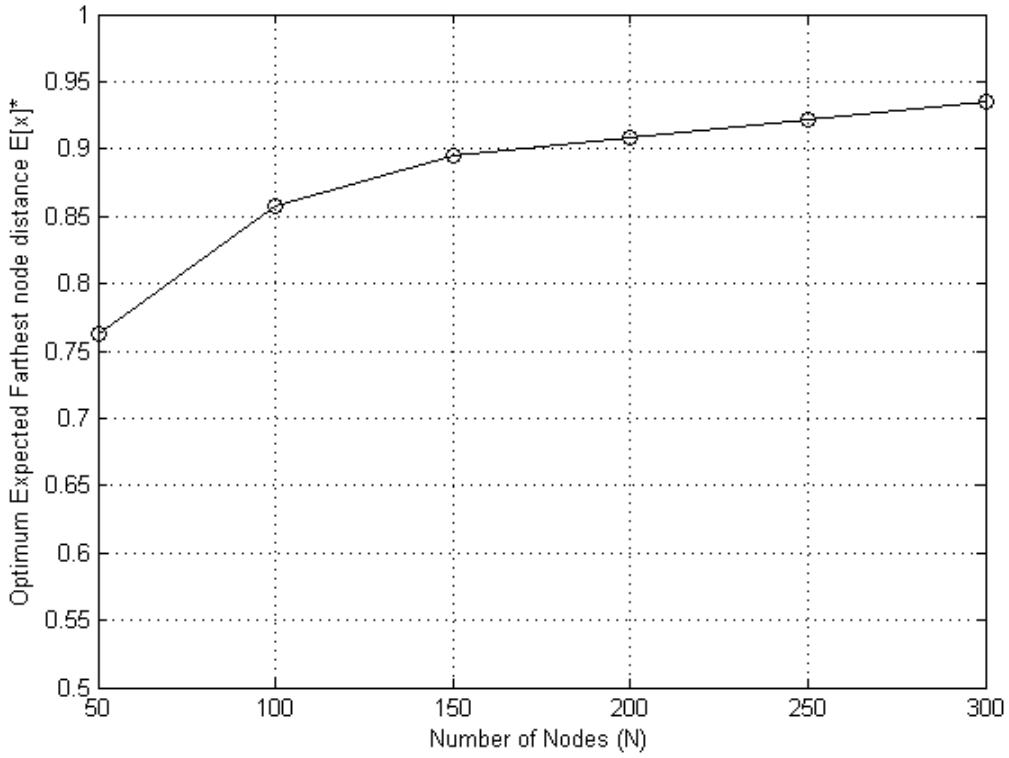

Figure 5.12: Optimum farthest node distance $E\left[x\right]^{*}$ versus the network size N.

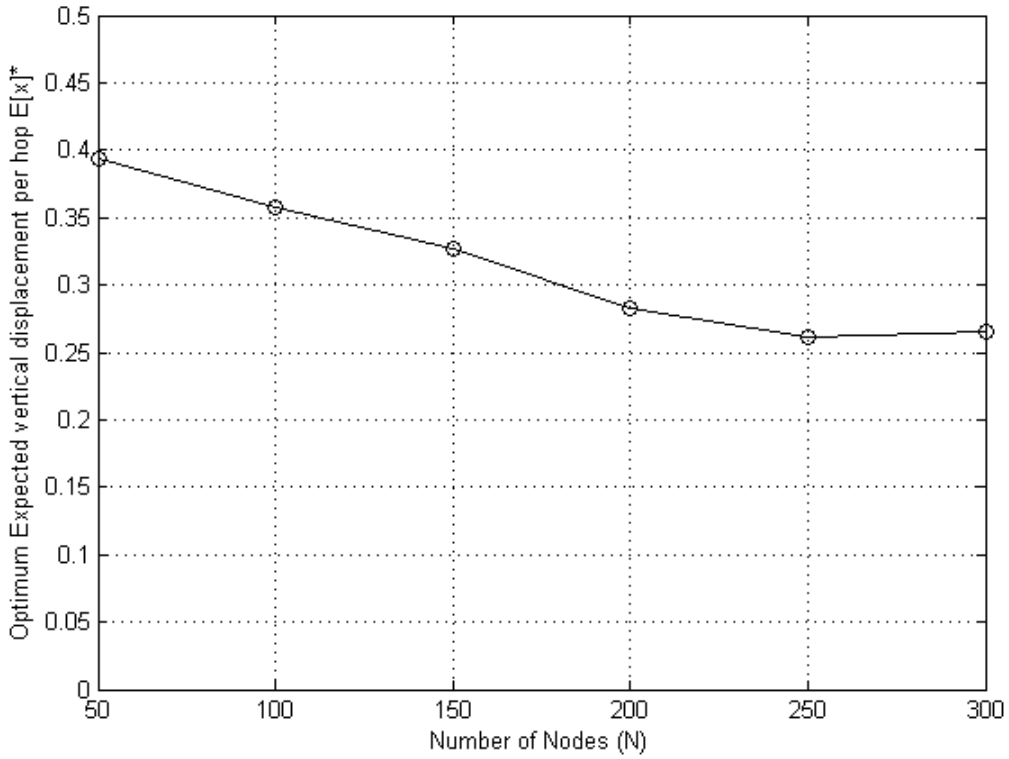

Figure 5.13: Optimum Expected vertical displacement per hop $E\left[x''\right]^{*}$ versus the network size N.

Detailed Analysis of the Shortest Path Routing Algorithm

A shortest path route of m links (hops) $\{L_1,..,L_i,...,L_m\}$ is formed between S, D using Dijkstra's algorithm. Let us define $\|L_{S,D}\|$ as the Euclidean distance between S and D. Let $\|L_i\|$ be the Euclidean length of the i^{th} link on the shortest path between S, D.

Following the same notation used to analyze the greedy forwarding algorithm, let $\|L_i'\|$ be the length of the projected link L_i on $S-D$, and let $\|L_i''\|$ be the perpendicular displacement from $S-D$ per hop.

To evaluate the performance of the shortest path routing algorithm and compare it to the results of the greedy forwarding algorithm discussed in the previous section, the following simulation was conducted using the same parameters used in the previous section. Assume a rectangular network area of side 6 units, with $N \in \{50,100,...,300\}$ nodes, each with a transmission range $r_o = 1$ unit. For each network realization, a random S and D are selected and the shortest path with the minimum number of hops $\{L_1,..,L_i,...,L_m\}$ between $S-D$ is calculated.

Figure 5.14 shows the probability density function of $\|L_i\|$ for different network sizes. It is noticed that the peak of the PDF is close to the value of the nodes' transmission range r_o.

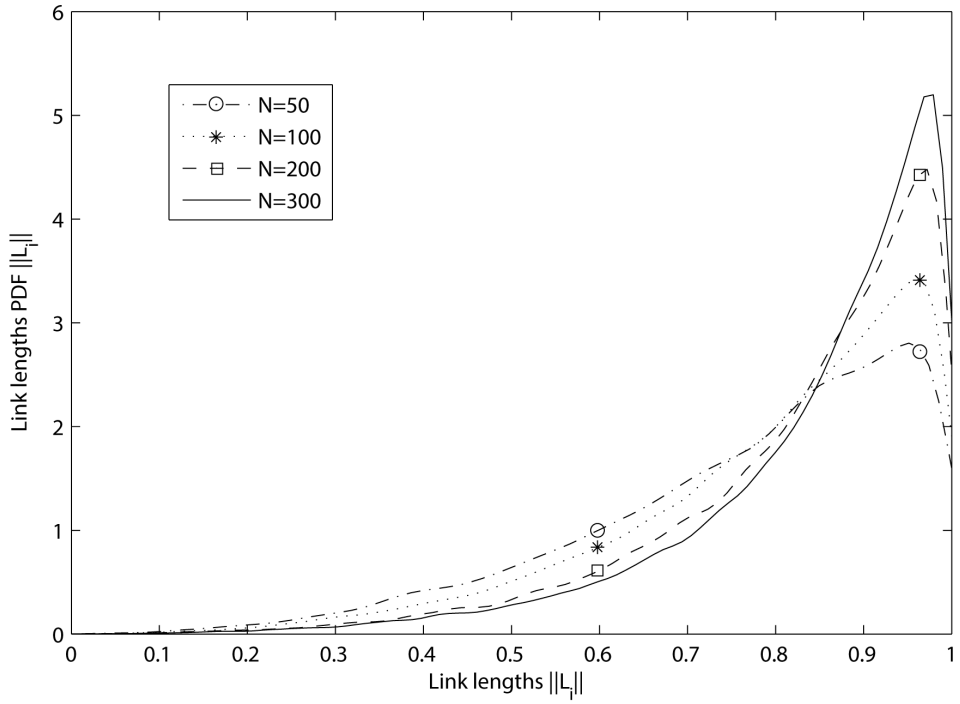

Figure 5.14: The probability density function of the link lengths $\|L_i\|$ for different network sizes N.

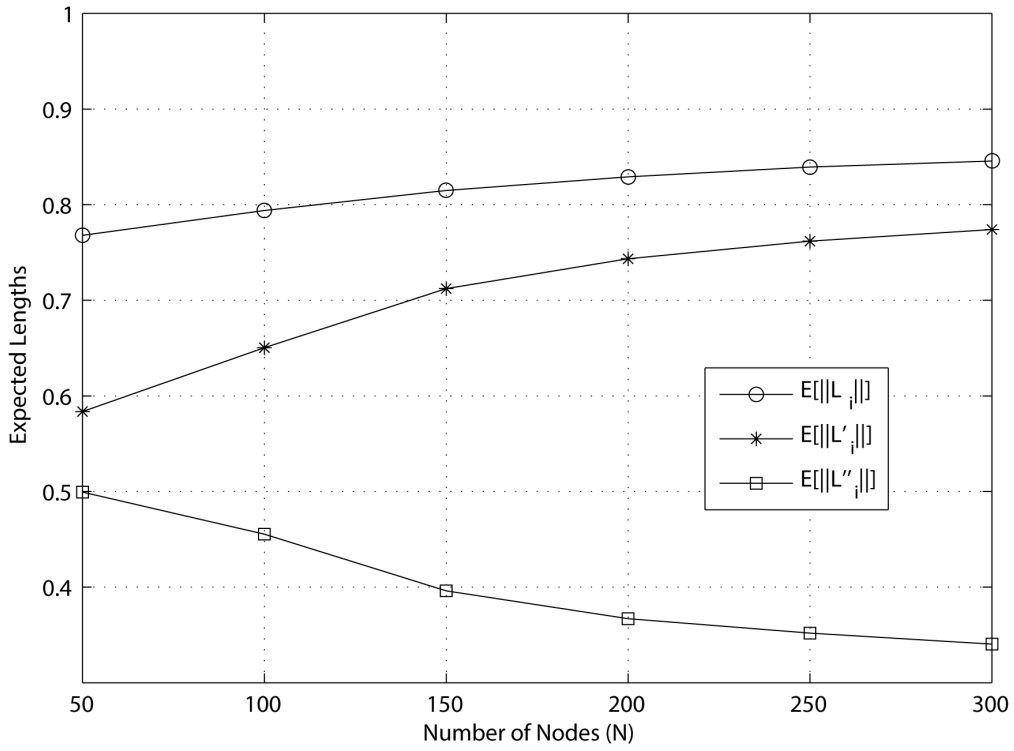

Figure 5.15: Mean link length, mean projected path length, and mean perpendicular displacement per hop versus the network size.

Figure 5.15 shows the mean link length $E\left[\left\|L_i\right\|\right]$, the mean projected path length $E\left[\left\|L_i'\right\|\right]$, and the mean perpendicular displacement per hop $E\left[\left\|L_i''\right\|\right]$ versus different network size. The mean link length and the mean projected path length increase as the number of nodes increases, while the mean perpendicular displacement per hop decreases as N increases. The shortest path algorithm follows the same trend as the greedy forwarding algorithm.

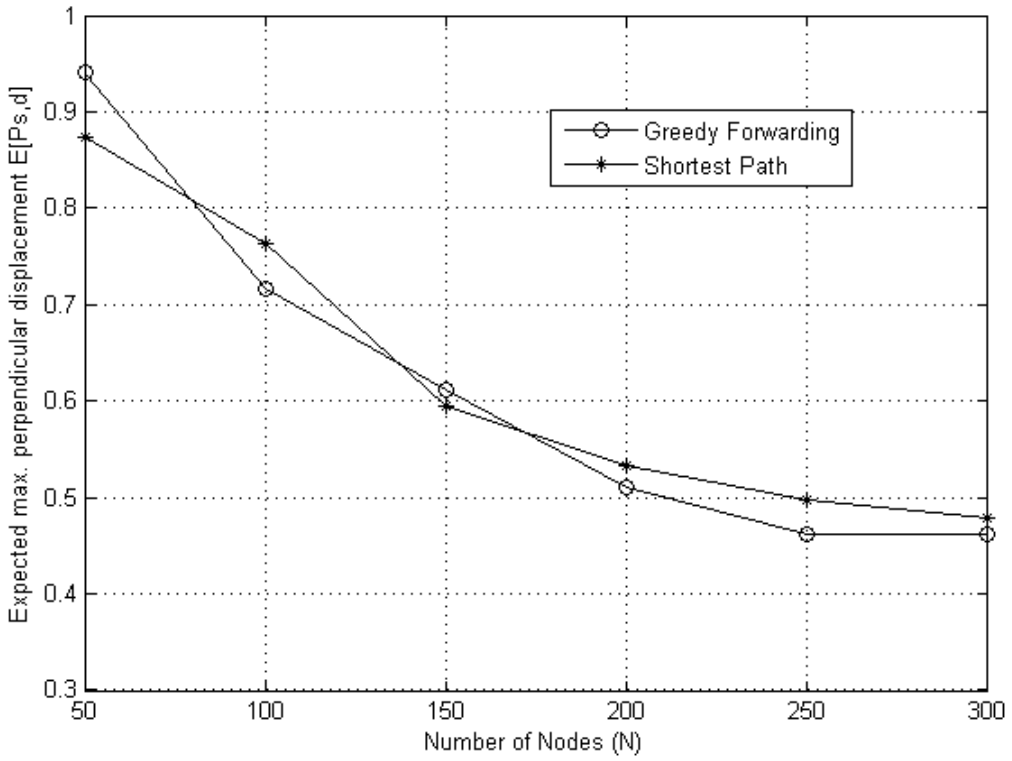

Figure 5.16: Expected maximum perpendicular displacement for both the greedy routing algorithm and the shortest distance algorithm versus network size *N*.

Figure 5.16 compares between the expected maximum perpendicular displacement for both the greedy routing algorithm and the shortest distance algorithm. For the greedy routing algorithm, equation (5.14) is used to evaluate the $E\left[P_{S,D}\right]$, while the results from Figure 5.15 are used to evaluate the $E\left[P_{S,D}\right]$ for the shortest path algorithm.

5.6 Conclusion

In this chapter, the problem of finding efficient routes in a large-scale network was analyzed. We proposed a position-based routing algorithm that reduces the node search space. The location information is assumed to be shared between nodes and updated as needed. For large-scale networks, the proposed technique significantly reduces the problem complexity and provides negligible performance degradation when compared to the performance of the complete network search space. The algorithm's performance was mathematically analyzed and compared to the greedy routing algorithm. The algorithm was then applied to cognitive radio networks to evaluate link throughput.

Chapter 6

A Novel CNC-based Routing Protocol and Future Cognitive Radio Applications

6.1 Cognitive Natural Connectivity-based Distributed Routing Protocol for CRNs

6.1.1 Introduction

A main challenge in designing routing protocols for cognitive radio networks is the balance between long term stability and short term performance measure such as the end-to-end delay. Recently various routing protocols have been proposed for CRNs, as discussed before in Chapter 2. Gymkhana [ABB-10] is a notable distributed connectivity-aware routing protocol which searches for stable routes in a given CRN using the second smallest eigenvalue of the Laplacian matrix, i.e. algebraic connectivity, as a measure of connectivity.

In Chapters 3 and 4, we proposed new connectivity metrics for both single-band and multi-band cognitive radio networks. We also discussed the application of the CNC metric in designing centralized connectivity-aware routing algorithms for CRNs. In this section, we propose a distributed connectivity-aware routing algorithm for CRNs based on the CNC metric.

6.1.2 System model

Consider the multi-hop cognitive radio network with *M* primary users and *N* secondary users (nodes) described in Section 4.3.1. Each node has the capability to setup a communication link with its neighbor nodes using one of *K* spectrum bands denoted $\{f_1, \cdots, f_K\}$. Each SU has a transmission range of r_k. Let M_k represent the number of PUs operating at the band f_k with a total number of PUs given by $M = \sum_{k=1}^{K} M_k$. In this work it is assumed that the M_k PUs are spatially-disjointed for all $k \in \{1, \cdots, K\}$ with transmission range R_{ik} for the i^{th} PU operating on the k^{th} frequency. Note that the transmission range of PUs and SUs is inversely proportional to the used frequency band. However, if adjacent frequencies are used then the effect of the frequency difference on the radius can be neglected.

6.1.3 Cognitive Natural Connectivity Routing (CNCR) metric

Selecting stable routes in CRNs can be a challenging task. For example, stable routes can be formed by avoiding routing packets through secondary nodes in areas affected by PUs activity. While this may be possible in some cases, it will highly increase the overall end-to-end delay. On the other hand, using the shortest hop route may also indicate that the route will be under the influence of many PUs and this will, again, increase the end-to-end delay.

In this section we will use the Cognitive Natural Connectivity (CNC) metric to design a distributed routing protocol for multi-band, multi-PUs CRNs that maximizes the route stability and minimizes the end-to-end delay.

The proposed CNC based routing protocol consists of two main phases: a route discovery phase and a route evaluation phase. In the Route discovery phase, the protocol collects key information related to the nodes which could be used to form a route between a Source (*S*) and a Destination (*D*). In the route evaluation phase, the *quality* of the different candidate routes are evaluated using the CNC based routing metric.

Each route consists of a source, a destination and a number of intermediate secondary nodes, each having access to *K* frequency bands. Each route can be expressed as a layered graph. The concept of layered graphs is discussed in detail in Section 2.6.1. In this layered graph, the number of layers is set to be equal to the number of the available frequency channels. For any layer, a horizontal edge between node *i* and node *i+1* indicates that the two nodes can communicate over the given frequency. The associated weights on the horizontal edges are the PUs availability values. The vertical edge indicates that a node can switch between different frequencies.

For a given S-D path, let us define the Cognitive Natural Connectivity Routing metric (CNCR) for a path l as follows:

$$CNCR_l = \frac{CNC_l}{CNC_{sp}} \times \frac{H_{sp}}{H_l}$$

where CNC_l is the cognitive natural connectivity metric of the path l layered graph, CNC_{sp} is the cognitive natural connectivity metric of the shortest path route layered graph, H_l is the hop-count of the path l, and H_{sp} is the shortest path hop-count.

The proposed CNCR metric is a hybrid metric which attempts to balance between the long-term route stability and the short-term end-to-end delay requirements. If the shortest path route is affected by many PUs activities, then a more stable route l^* but slightly longer, may be a better stable option than the shortest path route. The best case scenario is when the shortest path route is affected by the least PUs activities.

6.1.4 A CNC based Routing Protocol for Multi-band CRNs

The proposed routing protocol consists of two main phases: a route discovery phase and a route evaluation phase. The proposed protocol is based on the fact that each SU maintains a list of the PUs which are affected by using different means of spectrum sensing methods or spectrum database sharing schemes previously described in Chapter 2.

The route discovery process is carried based on the AODV protocol. It starts with a route request (RREQ) broadcasted by the source to neighbors on each channel not affected by a PU activity and ends with a route set up after the reception of a route reply (RREP) from the destination. Each node returns a list of the available frequencies as well as the PUs affecting its transmission and their activity factors.

In the route evaluation phase, a destination (*D*) uses the information contained in the received RREQs to classify paths on the basis of their CNCR metric and to select one of them for routing. The path selection is sent back with a Route Reply (RREP) packet on the reverse path toward the source (*S*).

6.1.5 Simulations

To evaluate the proposed CNC based routing protocol, a discrete-time MATLAB simulation is developed. Consider *M*=12 PUs and *N*=100 SUs randomly distributed over a square area of 500m X 500m. The 12 PUs are distributed over 3 frequency channels such that PUs in the same channel do not intersect. PUs follow an On-Off pattern with activity factors equal to $AF_i, i = 1,....,M$. A log-normal propagation model is used. The PU power levels are adjusted such that each has a transmission radius $R_1 = 80,\ R_2 = 90,\ R_3 = 100$ m for PUs operating on $\{f_1, f_{2,} f_3\}$ respectively. SU packet generation follows a Poisson distribution with a transmission rate equal to 1 Mbps. The SUs power level is adjusted such that each has a transmission radius of 50 m. SUs use a CSMA-based MAC protocol to access the channel. For each simulation, 10 runs were conducted.

In the following simulations, we compare the performance of our CNC-based routing protocol (CNCR) with both AODV and Gymkhana. AODV is based on the hop-count and Gymkhana is based on the algebraic connectivity λ_2 . For the simplicity of presenting the results, we assume all PU Activity Factors are equal.

In the first simulation, we compare the average SU throughput and the average end-to-end delay for different PU activity factors, for the three protocols. Source-Destination pairs were selected at random. Figure 6.1 shows the SU throughput, normalized to SU throughput for PU $AF = 0$, for different PU activity factors. Figure 6.2 shows the end-to-end delay, normalized to the end-to-end delay for PU at $AF = 0$, for different PU activity factors.

Figure 6.1 shows that, for the three protocols, as the PU AF increases, the SU throughput decreases. Figure 6.2 shows that as the PU AF increases, the end-to-end delay increases. Since AODV relies only on the hop-count, AODV provides the lowest throughput and the highest delay between the three protocols. CNCR performs better than Gymkhana since it is designed to choose more stable routes with limited end-to-end delay.

In the second simulation, we compare the average Secondary User throughput and end-to-end delay for a different number of active PUs, $M \in \{6,9,12,15\}$ PUs equally distributed over 3 frequencies, with constant $AF = 0.3$, for the three protocols. Figure 6.3 shows the SU throughput, normalized to SU throughput at $M = 6$, for a different number of PUs. Figure 6.4 shows the end-to-end delay, normalized to SU throughput at $M = 6$, for a different number of PUs.

Figure 6.3 shows that, for the three protocols, as the number of PUs increases, the SU throughput decreases. Figure 6.4 shows that as the number of PUs increases, the end-to-end delay increases. Again, since AODV relies only on the hop-count, AODV provides the lowest throughput and the highest delay between the three protocols. CNCR performs better than Gymkhana since it chooses more stable routes with limited end-to-end delay.

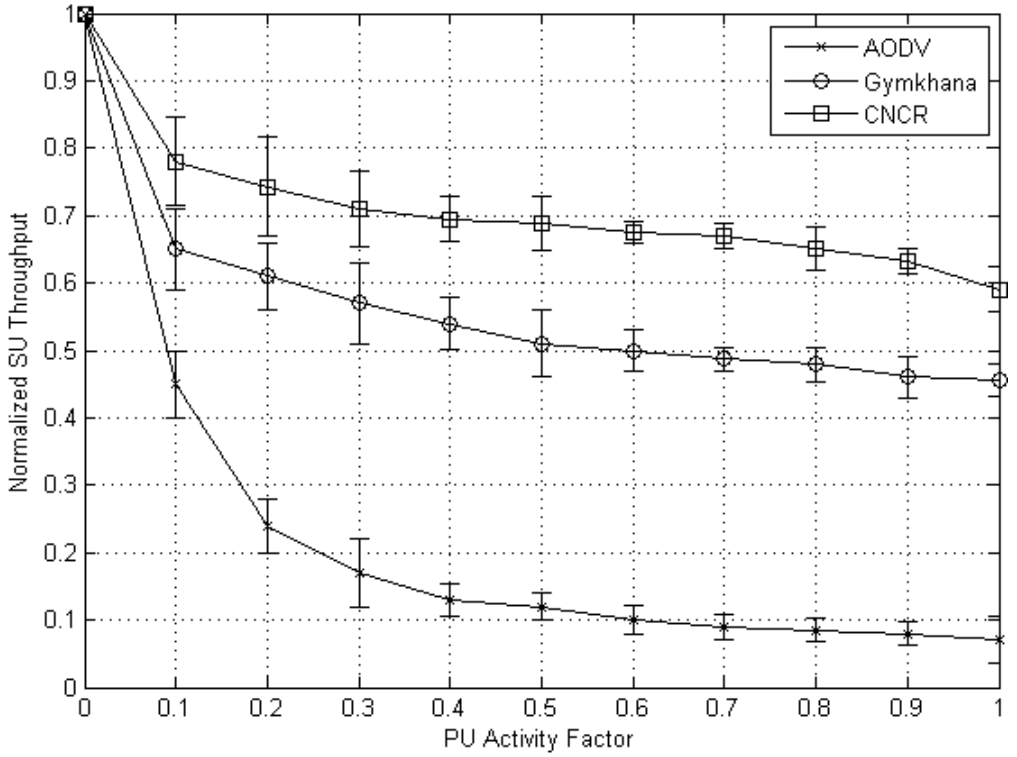

Figure 6.1: The effect of PU activity factor on the SU throughput

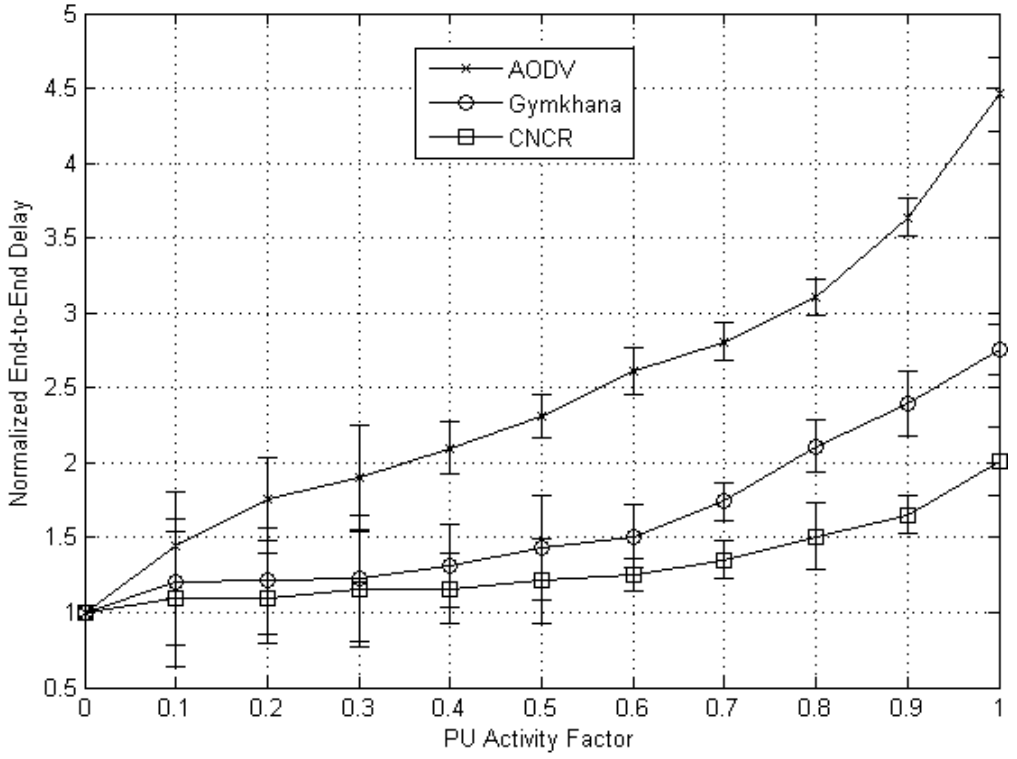

Figure 6.2: The effect of PU activity factor on the SU end-to-end delay

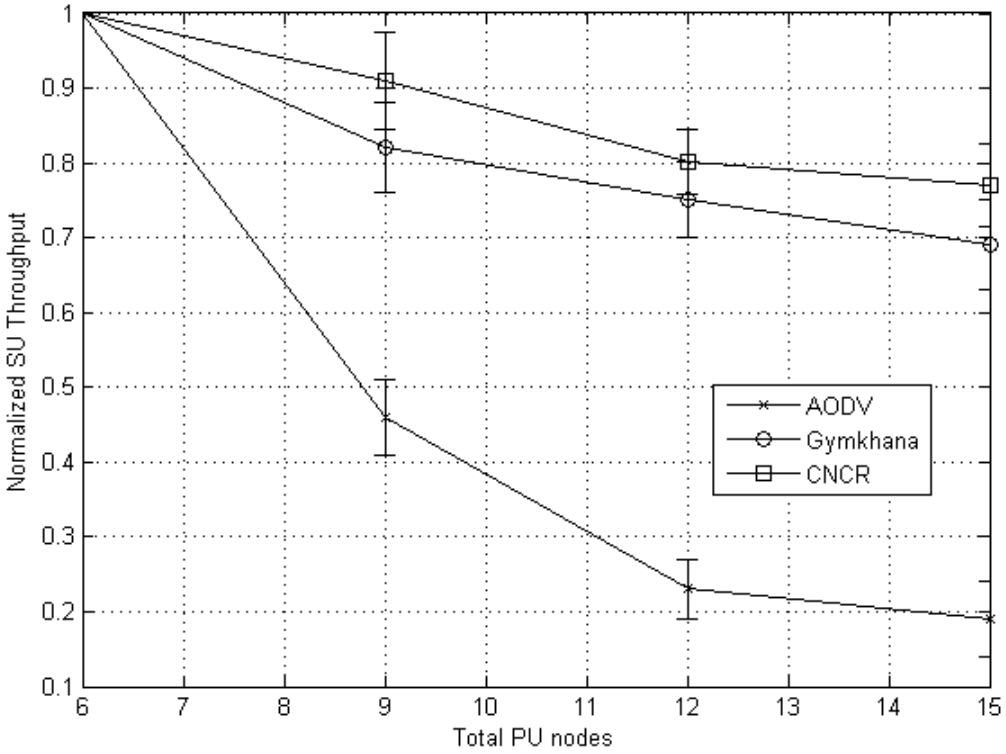

Figure 6.3: The effect of the number of PUs on the SU throughput

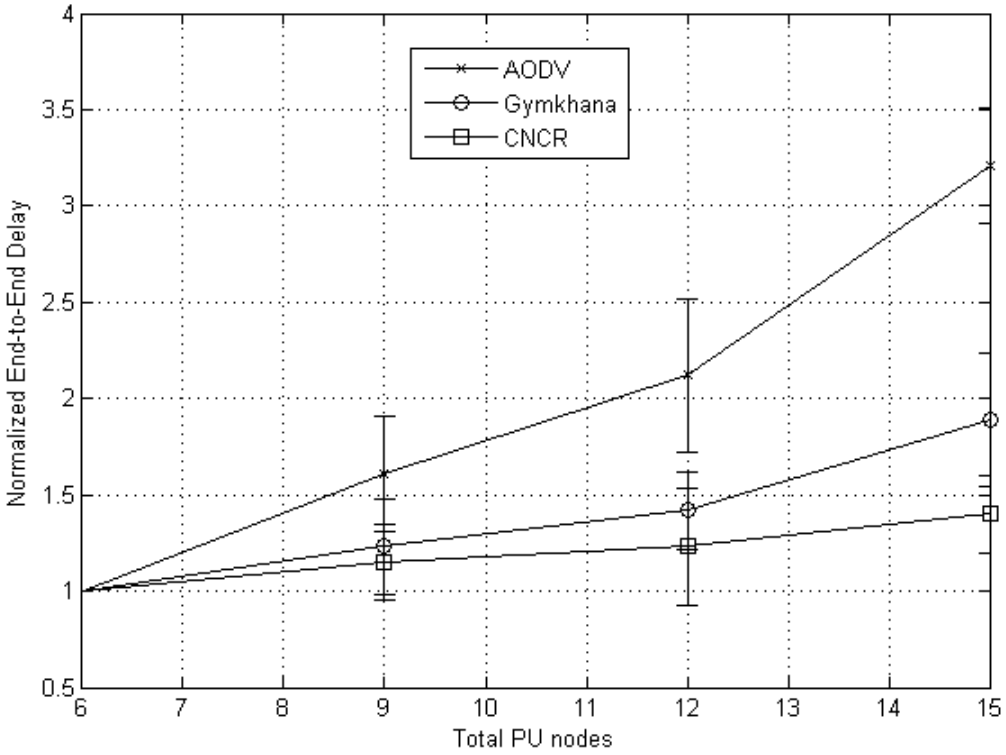

Figure 6.4: The effect of the number of PUs on the SU end-to-end delay

6.2 Cognitive Radio Wi-Fi Networks

One of the promising applications of the cognitive radio technology is CR-based Wi-Fi networks. A wave of Wi-Fi standards are currently emerging including IEEE 802.11af, a standard for WLAN in TV white spaces, and IEEE 802.22, a standard for wireless regional area networks (WRAN) in TV white spaces. CR-based Wi-Fi networks enable: (1) increase in spectrum efficiency through better utilization of the current spectrum band usage, (2) increase in the network capacity by enabling access to more under-utilized spectrum bands.

In this section, we will use a Wi-Fi based Cognitive Radio testbed named CORAL, to measure the interference in the 2.4 GHz ISM and to demonstrate the use of Cognitive Radio technology for Wi-Fi networks in the ISM band. This work could be extended in the future by using a testbed capable of accessing different spectrum bands, e.g. 700 MHz white spaces, 2.4 GHz and 5.1 GHz bands.

6.2.1 Introduction to Cognitive Radio Testbeds

Experiments in wireless networking in general, and in CRNs in particular, are inherently complex, typically time-consuming to set up, and hard to repeat by other researchers. For these reasons, simulation has been the methodology of choice for researchers in the wireless networking domain. However, there is a growing awareness of the fact that simulators make several simplifying assumptions to model many essential characteristics of real systems. This could lead to missing hidden interoperability problems or making poor performance assessment due to inaccurate models of user behavior (e.g. the statistical properties of the

traffic) and the characteristics of the space that the systems operate within, especially in a new research area like cognitive radio networks [PAW-11].

There are several cognitive radio testbeds that are available for researchers such as Universal Software Radio Peripheral (USRP) [ETT-14], COgnitive RAdio Learning (CORAL) [SYD-10], and others. A full list of the available CR testbeds can be found in [GUS-10]. They mainly differ in their operating frequency, computational complexity, and operation mode (stand-alone or PC based).

6.2.2 COgnitive RAdio Learning (CORAL) Platform

CORAL is a cognitive radio platform for research and commercial applications developed by the Communication Research Center (CRC) [SYD-10]. The radio is based on the IEEE 802.11 standard and operates in the ISM 2.4 and 5 GHz bands. The system consists of two elements: the physical radio interface, containing a modified Wi-Fi Router-radio called the WIFI-CR, and the network software, called the Cognitive Radio Network Management System (CR-NMS). The intelligence of the wireless network of Access Points (AP) and Client radios resides in the CR-NMS since it contains the cognitive control algorithms, the Cognitive Engine (CE), which manages the WIFI-CR terminals.

6.2.3 Testing Environment and Results

A field measurement experiment was conducted at the Ottawa downtown area to measure the interference in the ISM band in an urban area. We used 16 Access Points (AP), placed according to Figure 6.5.

The experiment lasted for 6 hours including the lunch time to pick the maximum interference caused by microwave ovens. The output of the field test are two sets of databases, one with the Wi-Fi interference data and the other is the spectrum analyzer data both collected by the 16 APs. The Wi-Fi interface database includes node ID, time, sensor MAC address, channel number, GPS location, source address, destination address, and other information. The spectrum analyzer data includes the interference level in dBm sampled each 200 mSec with a frequency resolution 1 MHz between 2.4 GHz and 2.5 GHz.

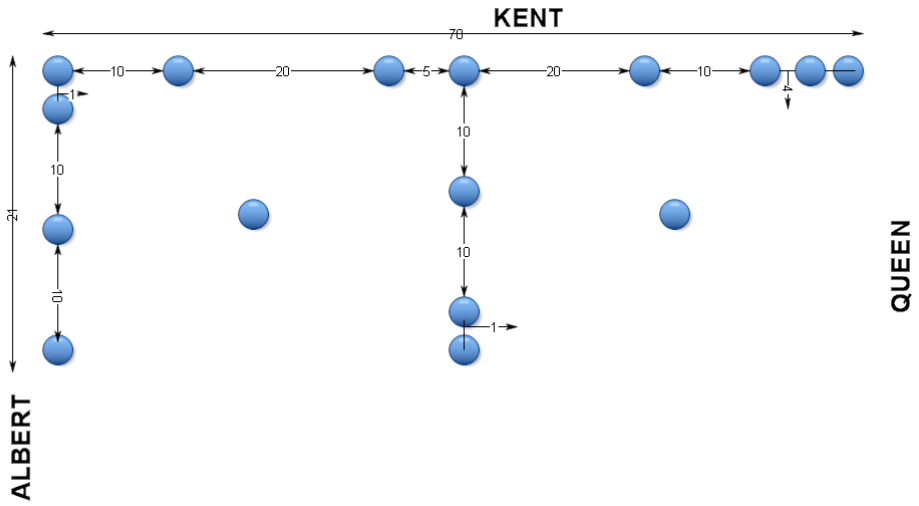

Figure 6.5: Node placement map

We also developed a MATLAB toolbox that we used to interact with the CORAL platform. The MATLAB toolbox has two main modules, an input interface module and an output interface module. The input interface is used to import the spectrum measurements from the CORAL hardware. The output interface is used to control the packet transmission parameters such as power level, channel frequency, rate, and packet type.

Figure 6.6 shows a sample of the spectrum analyzer interference in the 2.4 GHz ISM band. The interference power levels are measured using the CORAL internal energy detector.

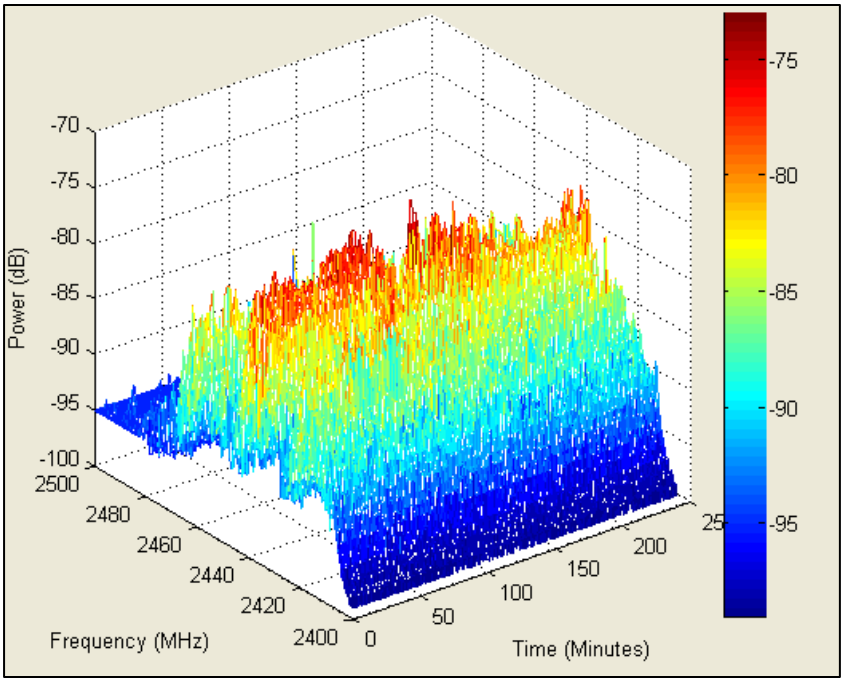

Figure 6.6: A 3-D representation of the spectrum analyzer data

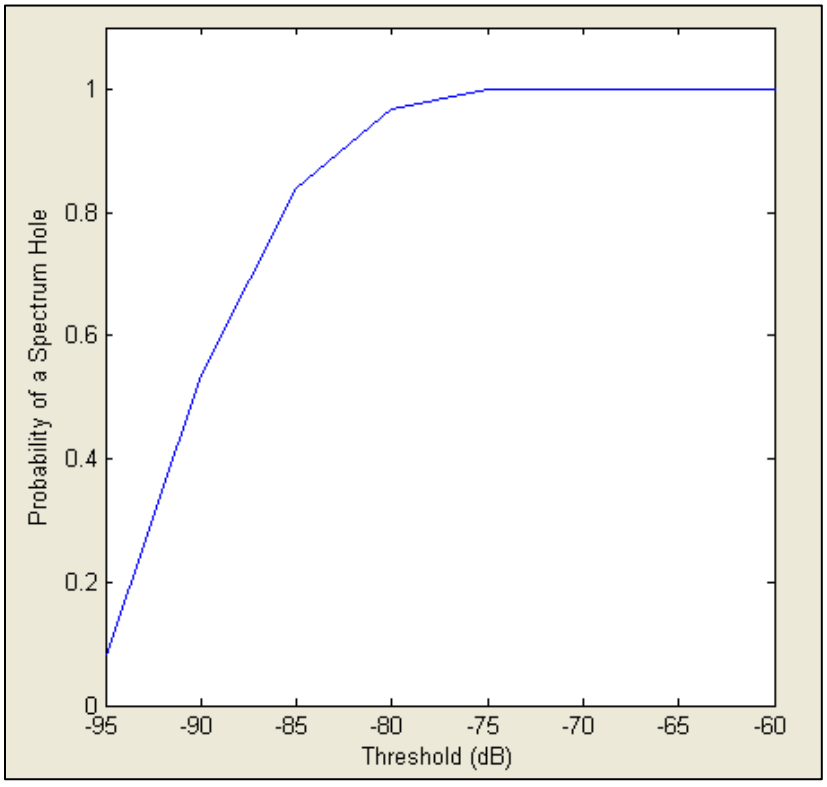

Figure 6.7: Threshold level vs. spectrum holes

Figure 6.7 shows the receiver's characteristics curve. It gives the probability of finding a spectrum opportunity for a given detection threshold.

One application of CRNs in Wi-Fi systems is a Wi-Fi network in which the existing Wi-Fi users are the PUs and the new nodes are the secondary cognitive nodes. This model can be applied in many applications where there are two levels of access priorities. For example, it could be applied in a first responders' radio access network in which first responders own the spectrum access rights and have the highest priority while they allow the public to use their network when they are in an idle state.

6.3 Conclusion

In this chapter we proposed a distributed connectivity-aware routing protocol based on the CNC metric presented in Chapters 3 and 4. Using MATLAB simulations, the proposed protocol outperformed the Gymkhana and AODV protocols in both throughput and end-to-end delay. Next, a future application of CRNs in Wi-Fi networks was discussed. Finally, CORAL CR testbed was used to demonstrate some practical aspects of CRNs.

Chapter 7

Conclusions and Future Research

7.1 Concluding Remarks

In this thesis, the routing problem in cognitive radio networks is studied with emphasis on connectivity-based routing algorithms. The limited available spectrum and the inefficiency in the spectrum usage necessitate a new communication paradigm shift from a fixed resources allocation model to a dynamic allocation model using the cognitive radio technology. The time-varying nature of communications links in multi-hop CRNs creates a dependency between the CRN availability and the PU network activity factor. The connectivity of multi-hop CRNs has been studied for some special cases in the past.

A new connectivity metric, named CNC, is developed as a tool to measure the network connectivity in CRNs. CNC metric was analyzed in both single and multi-Primary-user scenarios. Through the mathematical and numerical analysis presented, it is shown that the metric provides a qualitative, low numerical complexity, and a robust connectivity measure when compared to traditional connectivity.

We analyzed the connectivity of a practical CRN scenario named dual band capable cognitive radio networks. We proposed two strategies to select the route which maximizes the network connectivity, namely, single-frequency routing and dual-frequency routing. We showed that

dual-band CRNs deploying DFR have a slightly better connectivity than those deploying SFR. Finally, we proposed an extension to the CNC metric for multi-band CRNs.

We proposed a position-based routing algorithm for large scale CRNs which reduces the node search space. For large-scale networks, the proposed algorithm significantly reduces the problem complexity and provides negligible performance degradation when compared to the performance of the complete network search space.

We proposed a distributed connectivity-aware routing protocol for Cognitive Radio Networks. The protocol is based on the Cognitive Natural Connectivity metric we developed in Chapters 3 and 4. Finally, we demonstrated the main concept of Cognitive Wi-Fi networks using a Cognitive Radio testbed named CORAL.

7.2 Future Research

Based on the investigations and findings in this thesis, there are several areas that can be considered for future research. These areas can be summarized as follows:

- A hybrid routing algorithm for CRNs can be designed to address more than one routing metric at the same time. For example, it can address routing packets over highly stable routes while minimizing the consumed power per packet.
- A hardware implementation of the cognitive solutions would provide significant insights into its performance and ways in which it can be improved. Deployments in several environments such as urban, rural, forests, etc. can illustrate the suitability of the proposed cognitive solutions for different applications.
- Design delay-sensitive CRNs routing protocols for critical missions. A good application would be in the public safety applications as well as in disaster relief missions.
- A cross-layer optimization analysis and protocol design would be a very interesting area of research as an extension to this work. Especially on how to couple MAC, routing, and transport layer protocols in order to maximize the CRN performance.
- Extending this work to mobile CRNs especially for inter-vehicular communications.

References

[ABB-10] A. Abbagnale, F. Cuomo, "Gymkhana: A Connectivity-Based Routing Scheme for Cognitive Radio Ad Hoc Networks," Proceedings of the IEEE Conference on Computer Communications Workshops (INFOCOM 2010), pp.1-5, March 2010.

[ABB-12] A. Abbagnale and F. Cuomo, "Leveraging the Algebraic Connectivity of a Cognitive Network for Routing Design," IEEE Transactions on Mobile Computing, vol.11, no.7, pp.1163-1178, July 2012.

[AKY-09] I. F. Akyildiz, W.-Y. Lee, and K. R. Chowdhury, "CRAHNs: Cognitive radio ad hoc networks," Elsevier Ad Hoc Networks Journal, vol. 7, no. 5, pp.810 - 836, 2009.

[BAN-03] N. Bansal and Z. Liu, "Capacity, delay and mobility in wireless ad-hoc networks," Proceedings of the 22nd Conference of the IEEE Computer and Communications (INFOCOM 2003), pp.1553-1563, March 2003.

[BAC-06] F. Baccelli, B. Blaszczyszyn, and P. Mühlethaler, "An Aloha protocol for multihop mobile wireless networks," IEEE Transactions on Information Theory, vol.52, no.2, pp.421-436, February 2006.

[BEN-14] M. Di Benedetto, "Cognitive radio and networking for heterogeneous wireless networks", Springer International Publishing, Switzerland, 2014.

[CAC-09] A. S. Cacciapuoti, M. Caleffi, and L. Paura, "Reactive Routing for Mobile Cognitive Radio Ad Hoc Networks," Ad Hoc Networks Journal, vol.10, no.5, pp.803–815, 2012.

[CES-10] M. Cesana, F. Cuomo, and E. Ekici, "Routing in cognitive radio networks: Challenges and solutions," Elsevier Ad Hoc Networks Journal, vol. 9, no. 3, pp.228-248, 2011.

[CHE-07a] G. Cheng, W. Liu, Y. Li, W. Cheng, "Spectrum Aware On-Demand Routing in Cognitive Radio Networks," Proceedings of the 2nd IEEE International Symposium on New Frontiers in Dynamic Spectrum Access Networks, DySPAN 2007, pp.571-574, April 2007.

[CHE-07b] G. Cheng, W. Liu, Y. Li, W. Cheng, "Joint On-Demand Routing and Spectrum Assignment in Cognitive Radio Networks,", Proceedings of the IEEE International Conference on Communications, ICC '07, pp.6499-6503, June 2007.

[CHO-09] K.R. Chowdhury and M. Di Felice, "SEARCH: A routing protocol for mobile cognitive radio ad-Hoc networks," IEEE Sarnoff Symposium, pp.1-6, March 2009.

[CUO-10] F. Cuomo, A. Abbagnale, and A. Gregorini, "Impact of primary users on the connectivity of a cognitive radio network," Proceedings of the 9th IFIP Annual Mediterranean Ad Hoc Networking Workshop, Med-Hoc-Net 2010, pp.1-8, June 2010.

[CVE-95] D. Cvetkovic, M. Doob, H. Sachs," Spectra of Graphs- Theory and Application", 3rd edition, Heidelberg, Leipzig, 1995.

[DAR-03] DARPA XG WG, The XG Vision RFC v1.0, 2003.

[DIN-09] L. Ding, T. Melodia, S. Batalama, M.J. Medley, "ROSA: distributed joint routing and dynamic spectrum allocation in cognitive radio ad hoc networks", Proceedings of the 12th ACM international conference on Modeling, analysis and simulation of wireless and mobile systems (MSWiM 2009), pp.13-20, Canary Islands, Spain, 2009.

[EST-00] E. Estrada, "Characterization of 3D molecular structure", Chemical Physics Letters, vol. 319, pp. 713–718.

[ETT-14] M. Ettus, Ettus Research LLC, http://www.ettus.com, last accessed on 30 December, 2014.

[FCC-03] Federal Communication Commission, "Facilitating opportunities for flexible, efficient, and reliable spectrum use employing cognitive radio technologies, notice of proposed rulemaking and order," FCC, pp.03–322, December 2003.

[FCC-08] FCC, FCC 08-260, Unlicensed Operation in the TV Broadcast Bands, November 2008.

[FRA-08] M. Franceschetti and R. Meester, "Random Networks for Communication: from Statistical Physics to Information Systems", New York: Cambridge University Press, 2008.

[GAD-11] M. M. Gad, M. El-Khamy, H. T. Mouftah, "Dual Band Connectivity of Cognitive Radio Networks", Proceedings of the 4th International Conference on Cognitive Radio and Advanced Spectrum Management, CogART 2011, Article No. 20, Barcelona, Spain, October 2011.

[GUP-00] P. Gupta, and P. R. Kumar, "The capacity of wireless networks," IEEE Transactions on Information Theory, vol.46, no.2, pp.388-404, March 2000.

[GUS-10] O. Gustafsson, et. Al, "Architectures for cognitive radio testbeds and demonstrators - An overview," Proceedings of the 5th International Conference on Cognitive Radio Oriented Wireless Networks & Communications (CROWNCOM 2010), pp.1-6, June 2010.

[HAB-13] K. Habak, M. Abdelatif, H. Hagrass, K. Rizc, and M. Youssef, "A Location-Aided Routing Protocol for Cognitive Radio Networks," in International Conference on Computing, Networking and Communications (ICNC), pp.729,733, January 2013.

[HAE-05a] M. Haenggi, "On routing in random Rayleigh fading networks," IEEE Transactions on Wireless Communications, vol.4, no.4, pp.1553-1562, July 2005.

[Hou-07] Y. Hou, Y. Shi, H. Sherali, "Optimal Spectrum Sharing for Multi-Hop Software Defined Radio Networks," Proceedings of the IEEE 26th IEEE International Conference on Computer Communications (INFOCOM 2007), pp.1-9, May 2007.

[Hou-08] Y. Hou, Y. Shi, H. Sherali, "Spectrum Sharing for Multi-Hop Networking with Cognitive Radios," IEEE Journal on Selected Areas in Communications, vol.26, no.1, pp.146-155, January 2008.

[JAM-07] A. Jamakovic and S. Uhlig, "On the relationship between the algebraic connectivity and graph's robustness to node and link failures," Proceedings of the 3rd EuroNGI Conference on Next Generation Internet Networks, pp.96-102, May 2007.

[JEO-11] S-W. Jeon, N. Devroye, M. Vu, S-Y. Chung, and V. Tarokh, "Cognitive networks achieve throughput scaling of a homogeneous network," Proceedings of the 7th International

Symposium on Modeling and Optimization in Mobile, Ad Hoc, and Wireless Networks (WiOPT 2009), pp.1-5, June 2009.

[JIA-14] R. Jia, J. Zhang,X. Wang, X. Tian, Q. Zhang, "Scaling laws for heterogeneous cognitive radio networks with cooperative secondary users," Proceedings of the IEEE INFOCOM, pp.871-879, April 2014.

[JON-05] F.K. Jondral, "Software-defined radio: basic and evolution to cognitive radio", EURASIP Journal on Wireless Communications and Networking, no. 3, Article ID 652784, 9 pages, 2005.

[KHA-09] H. Khalife, N. Malouch, S. Fdida, "Multihop cognitive radio networks: to route or not to route," IEEE Network Magazine, vol.23, no.4, pp.20-25, July 2009.

[LE-09] L. B. Le, K. Jagannathan, and E. Modiano, "Delay analysis of maximum weight scheduling in wireless Ad Hoc networks," Proceedings of the 43rd Annual Conference on Information Sciences and Systems, CISS 2009, pp.389-394, March 2009.

[LI-10] Y. Li, D. Zou, H. Wang, Z. Zhou, Y. Liu, and Y. Qiao, "LOR: Localized Opportunistic Routing in Large-Scale Wireless Network," IEEE Global Telecommunications Conference (GLOBECOM 2010), pp.1-5, December 2010.

[LIA-11] Y. Liang; K. Chen; G. Li; P. Mahonen, "Cognitive radio networking and communications: an overview," IEEE Transactions on Vehicular Technology, vol.60, no.7, pp.3386-3407, September 2011.

[LU-12] D. Lu, X. Huang, P. Li, and J. Fan, "Connectivity of large-scale Cognitive Radio Ad Hoc Networks," Proceedings of the IEEE INFOCOM 2012 conference, pp.1260,1268, March 2012.

[MA-08] M. Ma, D. Tsang, "Joint Spectrum Sharing and Fair Routing in Cognitive Radio Networks," Proceedings of the 5th IEEE Consumer Communications and Networking Conference (CCNC 2008), pp.978-982, January 2008.

[MA-08] H. Ma, L. Zheng, X. Ma, Y. luo, "Spectrum Aware Routing for Multi-Hop Cognitive Radio Networks with a Single Transceiver," Proceedings of the 3rd International Conference on Cognitive Radio Oriented Wireless Networks and Communications (CrownCom 2008), pp.1-6, May 2008.

[MAR-12] J. Marinho and E. Monteiro, "Cognitive radio: survey on communication protocols, spectrum decision issues, and future research directions," Wireless Networks, vol.18, no.2, pp.147–164, 2012.

[McH-07] M. McHenry, E. Livsics, T. Nguyen, N. Majumdar, "A Description of the August 2006 XG Demonstrations at Fort A.P. Hill", XG Dynamic Spectrum Access Field Test Results", IEEE Communications Magazine, Vol. 45, no. 6, pp.51-57 June 2007.

[MIT-00] J. Mitola III, "Cognitive radio: an integrated agent architecture for software defined radio," Ph.D. dissertation, Computer Communication System Laboratory, Department of Teleinformatics, Royal Institute of Technology (KTH), Stockholm, Sweden, May 2000.

[NEE-05] M. J. Neely and E. Modiano, "Capacity and delay tradeoffs for ad hoc mobile networks," IEEE Transactions on Information Theory, vol.51, no.6, pp.1917-1937, June 2005.

[OVE-95] M. Overton and R. Womersley, “Second derivatives for optimizing eigenvalues of symmetric matrices “, SIAM Journal on Matrix Analysis and Applications, vol. 16, pp.697-718, 1995.

[PAT-11] K. Patil, R. Prasad, K. Skouby, “A Survey of Worldwide Spectrum Occupancy Measurement Campaigns for Cognitive Radio,” International Conference on Devices and Communications (ICDeCom), pp.1-5, February 2011.

[PAW-11] P. Pawelczak, K. Nolan, L. Doyle, D. Ser Wah Oh; Cabric, “Cognitive radio: Ten years of experimentation and development,” IEEE Communications Magazine, vol.49, no.3, pp.90-100, March 2011.

[PEF-08] I. Pefkianakis, S. Wong, S. Lu, “SAMER: Spectrum Aware Mesh Routing in Cognitive Radio Networks,” Proceedings of the 3rd IEEE Symposium on New Frontiers in Dynamic Spectrum Access Networks, DySPAN 2008, pp.1-5, October 2008.

[PEN-07] J. Pena, I. Gutman, J. Rada, “Estimating the Estrada index”, Linear Algebra and its Applications, Vol. 427, pp.70-76,November 2007.

[PHI-07] J. Philip, “The probability distribution of the distance between two random points in a box”, TRITA MAT, vol.7, no.10, December 2007.

[PYO-07] C.W. Pyo, M. Hasegawa, “Minimum weight routing based on a common link control radio for cognitive wireless ad hoc networks”, Proceedings of the 2007 International Conference on Wireless Communications and Mobile Computing (IWCMC ’07), pp.399-404, 2007.

[REN-10] W. Ren, Q. Zhao, and A. Swami, "On the Connectivity and Multihop Delay of Ad Hoc Cognitive Radio Networks," Proceedings of the IEEE International Conference on Communications (ICC), pp.1-6, May 2010.

[REN-11] W. Ren, Q. Zhao, and A. Swami; "On the Connectivity and Multihop Delay of Ad Hoc Cognitive Radio Networks", IEEE Journal on Selected Areas in Communications, vol.29, no.4, pp.805-818, April 2011.

[SAM-08] A. Sampath, L. Yang, L. Cao, H. Zheng, B.Y. Zhao, "High throughput spectrum-aware routing for cognitive radio based ad-hoc networks", Proceedings of the International Conference on Cognitive Radio Oriented Wireless Networks and Communications (CROWNCOM), May 2008.

[SEE-07] F. Seelig, "A Description of the August 2006 XG Demonstrations at Fort A.P. Hill," Proceedings of the 2nd IEEE International Symposium on New Frontiers in Dynamic Spectrum Access Networks (DySPAN), pp.1-12, April 2007.

[SHA-04] G. Sharma and R. Mazumdar, "Scaling laws for capacity and delay in wireless ad hoc networks with random mobility," Proceedings of the 2004 IEEE International Conference on Communications, vol.7, pp.3869-3873, June 2004.

[SHA-07] G. Sharma, R. Mazumdar, N. B. Shroff,"Delay and Capacity Trade-Offs in Mobile Ad Hoc Networks: A Global Perspective," IEEE/ACM Transactions on Networking, vol.15, no.5, pp.981-992, October 2007.

[SHI-08] Y. Shi, Y. Hou, "A Distributed Optimization Algorithm for Multi-Hop Cognitive Radio Networks," Proceedings of the IEEE 27th Conference on Computer Communications (INFOCOM 2008), 13-18 April 2008.

[SRI-10] S. Srinivasa, M. Haenggi, "Distance Distributions in Finite Uniformly Random Networks: Theory and Applications," IEEE Transactions on Vehicular Technology, vol.59, no.2, pp.940-949, February 2010.

[SUN-13] H. Sun, A. Nallanathan, C.-X. Wang, and Y. Chen, "Wideband spectrum sensing for cognitive radio networks: a survey," IEEE Wireless Communications, vol. 20, no. 2, pp.74–81, 2013.

[SYD-10] J. Sydor, A. Ghasemi, S. Palaninathan, W. Wong, "Cognitive, Radio-Aware, Low-Cost (CORAL) Research Platform," Proceedings of the 2010 IEEE Symposium on New Frontiers in Dynamic Spectrum, pp.1-2, April 2010.

[TAK-84] H. Takagi and L. Kleinrock, "Optimal Transmission Ranges for Randomly Distributed Packet Radio Terminals," IEEE Transactions on Communications, vol.32, no.3, pp.246-257, March 1984.

[UCH-12] N. Uchida, K. Takahata, and Y. Shibata, "Network Relief Activity with Cognitive Wireless Network for Large Scale Disaster," Proceedings of the 26th International Conference on Advanced Information Networking and Applications Workshops (WAINA 2012), pp.1043-1047, March 2012.

[VU-07] M. Vu, N. Devroye, M. Sharif, and V. Tarokh, "Scaling Laws of Cognitive Networks," Proceedings of the 2nd International Conference on Cognitive Radio Oriented Wireless Networks and Communications (CrownCom 2007), pp.2-8, August 2007.

[WAN-06] Q. Wang, H. Zheng, "Route and spectrum selection in dynamic spectrum networks," Proceedings of the 3rd IEEE Consumer Communications and Networking Conference (CCNC), pp.625-629, 8-10 January 2006.

[WU-12] J. Wu, M. Barahona, Y. jin Tan, and H. Zhong Deng, "Robustness of random graphs based on graph spectra," Chaos: An Interdisciplinary Journal of Nonlinear Science, vol. 22, no. 4, pp.1-7, 2012.

[XIE-10] M. Xie, W. Zhang, K. Wong, "A geometric approach to improve spectrum efficiency for cognitive relay networks," IEEE Transactions on Wireless Communications, vol.9, no.1, pp.268-281, January 2010.

[YOU-14] M. Youssef, M. Ibrahim, M. Abdelatif, Lin Chen, A. V. Vasilakos, "Routing Metrics of Cognitive Radio Networks: A Survey," IEEE Communications Surveys & Tutorials, vol.16, no.1, pp.92-109, First Quarter 2014.

[XIN-05a] C. Xin, B. Xie, C.C. Shen, "A novel layered graph model for topology formation and routing in dynamic spectrum access networks," Proceedings of the First IEEE International Symposium on New Frontiers in Dynamic Spectrum Access Networks (DySPAN), pp.308-317, November 2005.

[XIN-05b] C. Xin, L. Ma, C.-C. Shen, "A path-centric channel assignment framework for cognitive radio wireless networks", Mobile Networks and Applications, vol. 13, no. 5, 463–476, July 2008.

[XU-08] Y. Xu and W. Wang, "The Speed of Information Propagation in Large Wireless Networks," Proceedings of the 27th IEEE Conference on Computer Communications (INFOCOM), April 2008.

[YAN-08] Z. Yang, G. Cheng, W. Liu, W. Yuan, W. Cheng, "Local coordination based routing and spectrum assignment in multi-hop cognitive radio networks", Mobile Networks and Applications, vol. 13, no. 1-2, 2008.

[YIN-08a] C. Yin, L. Gao, and S. Cui, "Scaling Laws for Overlaid Wireless Networks: A Cognitive Radio Network vs. a Primary Network," Proceedings of the IEEE Global Telecommunications Conference (GLOBECOM), pp.1-5, November 2008.

[YIN-08b] L. Ying, S. Chao, and R. Srikant, "Optimal Delay–Throughput Tradeoffs in Mobile Ad Hoc Networks," IEEE Transactions on Information Theory, vol.54, no.9, pp.4119-4143, September 2008.

[YUC-09] T. Yucek and H. Arslan, "A survey of spectrum sensing algorithms for cognitive radio applications," IEEE Communications Surveys & Tutorials, vol.11, no.1, pp.116-130, 2009.

[ZHE-06] R. Zheng, "Information Dissemination in Power-Constrained Wireless Networks," Proceedings of the 25th IEEE International Conference on Computer Communications (INFOCOM), pp.1-10, April 2006.

[ZHO-09] X. Zhou, L. Lin, J. Wang, X. Zhang, “Cross-layer routing design in cognitive radio networks by colored multigraph model”, Wireless Personal Communications, vol. 49, no. 1, 2009.

[ZHU-08] G. M. Zhu, I. Akyildiz, G.S. Kuo, “STOD-RP: A Spectrum-Tree Based On-Demand Routing Protocol for Multi-Hop Cognitive Radio Networks,” Proceedings of the IEEE Global Telecommunications Conference (GLOBECOM), pp.1-5, November 2008.

Appendix A

Derivations of Theorem 3.1

$f(\boldsymbol{\Delta})$ is a non-decreasing function when $\Delta_m \geq 0$

Consider the derivative of $f(\boldsymbol{\Delta}) = \sum_{i=1}^{N} e^{\lambda_i(\boldsymbol{\Delta})}$ with respect to Δ_m as follows.

$$\frac{\partial f(\boldsymbol{\Delta})}{\partial \Delta_m} = \sum_{i=1}^{N} e^{\lambda_i(\boldsymbol{\Delta})} \frac{\partial \lambda_i(\boldsymbol{\Delta})}{\partial \Delta_m} \tag{A.1}$$

In the following, and for simplicity, $\mathbf{A}$ and λ_i will be used instead of $\mathbf{A}(\boldsymbol{\Delta})$ and $\lambda_i(\boldsymbol{\Delta})$ respectively.

Let $\mathbf{v}_i$ represent the i^{th} eigenvector of $\mathbf{A}$, i.e.,

$$\mathbf{A}\mathbf{v}_i = \lambda_i \mathbf{v}_i.$$

Taking the derivative of both sides and multiplying by $\mathbf{v}_i^T$, where $(\cdot)^T$ is the transpose operator, results in [OVE-95]

$$\frac{\partial \lambda_i}{\partial \Delta} = \mathbf{v}_i^T \frac{\partial \mathbf{A}}{\partial \Delta} \mathbf{v}_i. \tag{A.2}$$

Let $\mathbf{B} = \partial \mathbf{A} / \partial \Delta$, then the i^{th} and j^{th} element of the symmetric matrix $\mathbf{B}$ denoted as b_{ij} is given as,

$$b_{ij} = \begin{cases} 1, & a_{ij} = \Delta; \\ 0 & \text{Otherwise.} \end{cases}$$

Assume there are $2K$ nonzero elements in $\mathbf{B}$ as,

$$\sum_{i=1}^{N}\sum_{j=1}^{N} b_{ij} = 2K.$$

Then $\mathbf{B}$ can be written as the sum of *K* symmetric matrices, $\mathbf{B}_k$, each with only two nonzero elements as

$$\mathbf{B} = \sum_{k=1}^{K} \mathbf{B}_k.$$

Substituting (A.2) into (A.1) results in

$$\begin{aligned} \frac{\partial f(\Delta)}{\partial \Delta} &= \sum_{i=1}^{N} e^{\lambda_i} \mathbf{v}_i^T \left(\sum_{k=1}^{K} \mathbf{B}_k \right) \mathbf{v}_i, \\ &= \sum_{k=1}^{K} \left(\sum_{i=1}^{N} e^{\lambda_i} \mathbf{v}_i^T \mathbf{B}_k \mathbf{v}_i \right). \end{aligned} \tag{A.3}$$

In order to show that $\frac{\partial f(\Delta)}{\partial \Delta} \geq 0$, it is sufficient to prove that $\sum_i e^{\lambda_i} \mathbf{v}_i^T \mathbf{B}_k \mathbf{v}_i \geq 0$ for any k.

Assume that $\mathbf{B}_k(m,n) = \mathbf{B}_k(n,m) = 1$ are the nonzero m^{th} and n^{th} element of the symmetric matrix $\mathbf{B}_k$ then,

$$\sum_{i=1}^{N} e^{\lambda_i} \mathbf{v}_i^T \mathbf{B}_k \mathbf{v}_i = 2\, \mathbf{w}_m\, \mathbf{E}\, \mathbf{w}_n^T, \tag{A.4}$$

where $\mathbf{w}_m$ is the m^{th} row vector of the $\mathbf{V}$ and $\mathbf{E}$ is a diagonal matrix defined as $\mathbf{E} = \text{diag}(e^{\lambda_1}, \cdots, e^{\lambda_N})$. Define a symmetric matrix $\mathbf{A}_E$ as

$$\mathbf{A}_E = 2\,\mathbf{V}\,\mathbf{E}\;\mathbf{V}^T,$$

then (A.4) can be written as

$$\sum_{i=1}^{N} e^{\lambda_i}\mathbf{v}_i^T\mathbf{B}_k\mathbf{v}_i = \mathbf{A}_E(m,n),$$

where $\mathbf{A}_E(m,n)$ is the m^{th} and n^{th} element of the matrix $\mathbf{A}_E$. In order to prove the *lemma*, it is sufficient to show that $\mathbf{A}_E(m,n) \geq 0$.

Staring from the eigenvalue decomposition of the adjacent matrix $\mathbf{A}$ and for any positive integer $r \geq 0$ we have

$$\mathbf{A}^r = \mathbf{V}\,\mathbf{\Lambda}^r\,\mathbf{V}^T.$$

Dividing by the factorial of *r* and summing results in,

$$\sum_{r=0}^{\infty}\frac{\mathbf{A}^r}{r!} = \mathbf{V}\left(\sum_{r=0}^{\infty}\frac{\mathbf{\Lambda}^r}{r!}\right)\mathbf{V}^T. \tag{A.5}$$

Since $\mathbf{A} \geq 0$ is a nonnegative matrix, i.e., $a_{ij} \geq 0$, then

$$\sum_{r=0}^{\infty}\frac{\mathbf{A}^r}{r!} \geq 0. \tag{A.6}$$

Also since $\mathbf{\Lambda}$ is a diagonal matrix and the summation is performed element-wise then,

$$\left(\sum_{r=0}^{\infty}\frac{\mathbf{\Lambda}^r}{r!}\right)=\text{diag}(e^{\lambda_1},\cdots,e^{\lambda_N})=\mathbf{E}. \tag{A.7}$$

Substituting (A-6) and (A-7) into (A-5) results in

$$\mathbf{V}\,\mathbf{E}\,\mathbf{V}^T\geq 0, \tag{A.8}$$

equivalently, $\mathbf{A}_E(m,n)\geq 0$ and hence

$$\sum_{i=1}^{N}e^{\lambda_i}\mathbf{v}_i^T\mathbf{B}_k\mathbf{v}_i\geq 0 \tag{A.9}$$

Substituting back into (A.3) we get

$$\frac{\partial f(\mathbf{\Delta})}{\partial \Delta_m},\qquad \Delta_m\geq 0.$$

Convexity of $f(\mathbf{\Delta})$

A necessary and sufficient condition for the convexity of $f(\mathbf{\Delta})$ is the non-negativity of its second derivative, i.e.,

$$\frac{\partial^2 f(\mathbf{\Delta})}{\partial \Delta_m^2}\geq 0$$

For simplicity, in the following analysis f, λ_i, and $\mathbf{A}$ will be used instead of $f(\mathbf{\Delta})$, $\lambda_i(\mathbf{\Delta})$, and $\mathbf{A}(\mathbf{\Delta}))$ respectively.

The first and second derivative of $f(\mathbf{\Delta})$ with respect to Δ_m are given as follows

$$\frac{\partial f}{\partial \Delta_m}=\sum_{i=1}^{N}e^{\lambda_i}\frac{\partial \lambda_i}{\partial \Delta_m},$$

and

$$\frac{\partial^2 f}{\partial \Delta_m^2} = \sum_{i=1}^{N} \left[e^{\lambda_i} \frac{\partial^2 \lambda_i}{\partial \Delta_m^2} + e^{\lambda_i} \left(\frac{\partial \lambda_i}{\partial \Delta_m} \right)^2 \right]. \tag{A.10}$$

Let $\mathbf{v}_i$ represent the i^{th} eigenvector of $\mathbf{A}$, *i.e.* $\mathbf{A}\mathbf{v}_i = \lambda_i \mathbf{v}_i$.

Taking the derivative of both sides and multiplying by $\mathbf{v}_i^T$, where $(\cdot)^T$ is the transpose operator, results in [OVE-95]

$$\frac{\partial \lambda_i}{\partial \Delta_m} = \mathbf{v}_i^T \frac{\partial \mathbf{A}}{\partial \Delta_m} \mathbf{v}_i. \tag{A.11}$$

One further step results in [OVE-95]

$$\frac{\partial^2 \lambda_i}{\partial \Delta_m^2} = \mathbf{v}_i^T \frac{\partial^2 \mathbf{A}}{\partial \Delta_m^2} \mathbf{v}_i + 2 \sum_{s \neq i}^{N} \frac{(\mathbf{v}_i^T \frac{\partial \mathbf{A}}{\partial \Delta_m} \mathbf{v}_s)^2}{\lambda_i - \lambda_s}. \tag{A.12}$$

Note that $\partial^2 \mathbf{A} / \partial \Delta_m^2 = 0$. Substituting (A.11) and (A.12) into (A.10) results in

$$\frac{\partial^2 f}{\partial \Delta_m^2} = \sum_{i=1}^{N} \sum_{s \neq i}^{N} 2\, e^{\lambda_i} \frac{(\mathbf{v}_i^T \frac{\partial \mathbf{A}}{\partial \Delta_m} \mathbf{v}_s)^2}{\lambda_i - \lambda_s} + \sum_{i=1}^{N} e^{\lambda_i} \left(\mathbf{v}_i^T \frac{\partial \mathbf{A}}{\partial \Delta_m} \mathbf{v}_i \right)^2$$

It is clear that the second term in the right hand side of the above equation is nonnegative since

$$e^{\lambda_i} \left(\mathbf{v}_i^T \frac{\partial \mathbf{A}}{\partial \Delta_m} \mathbf{v}_i \right)^2 \geq 0$$

Consider the first term in the right hand side and let

$$F(i,s) = 2\, e^{\lambda_i} \frac{(\mathbf{v}_i^T \frac{\partial \mathbf{A}}{\partial \Delta_m} \mathbf{v}_s)^2}{\lambda_i - \lambda_s},$$

then with $i \neq s$

$$F(i,s)+F(s,i)=2\,e^{\lambda_i}\,\frac{(\mathbf{v}_i^T\,\frac{\partial\mathbf{A}}{\partial\Delta_m}\,\mathbf{v}_s)^2}{\lambda_i-\lambda_s}+2\,e^{\lambda_s}\,\frac{(\mathbf{v}_s^T\,\frac{\partial\mathbf{A}}{\partial\Delta_m}\,\mathbf{v}_i)^2}{\lambda_s-\lambda_i},$$

Since $\partial\mathbf{A}/\partial\Delta_m$ is a symmetric matrix then

$$\mathbf{v}_i^T\,\frac{\partial\mathbf{A}}{\partial\Delta_m}\,\mathbf{v}_s=\mathbf{v}_s^T\,\frac{\partial\mathbf{A}}{\partial\Delta_m}\,\mathbf{v}_i.$$

Resulting in

$$F(i,s)+F(s,i)=2\,\frac{e^{\lambda_i}-e^{\lambda_s}}{\lambda_i-\lambda_s}\left(\mathbf{v}_i^T\,\frac{\partial\mathbf{A}}{\partial\Delta_m}\,\mathbf{v}_s\right)^2\geq 0.$$

Consequently,

$$\frac{\partial^2 f(\mathbf{\Delta})}{\partial\Delta_m^2}\geq 0,$$

thus $f(\mathbf{\Delta})$ is a convex function of Δ_m.

Appendix B

Confidence Intervals Computation

A Confidence Interval (CI) is used to quantify the uncertainty in any collected sample of data. It is defined as the estimated range of values within which a generated data lies with a specified probability. Simulated results such as Route availability, end-to-end delay, and reliability are measured by taking the mean of a successive of *n* runs, with different simulation seed to ensure that there no correlation in the presented results. All simulation runs have the same environment (identical) although they are independent from each other.

As an example, the result for the Route Availability (RA) is considered, where the *n* independent results are represented by RA_1, RA_2, $\cdot \cdot \cdot$, RA_n where RA_i represents the Route availability for a given SU network obtained from simulation run *i*. The mean of all the reliability simulation measurements is therefore given by

$$\overline{RA} = \frac{1}{n}\sum_{i=1}^{n} RA_i \tag{B.1}$$

However, the mean of the independent simulation runs RA provides a single numerical value for the estimate of the expected value of $E\left[RA\right] = \mu_s$. In order to evaluate the quality of the estimate provided by $\overline{RA}$ for the simulation results, it is necessary to compute the variance σ_s^2. The variance is given by the following equation

$$\sigma_s^2 = \frac{1}{n-1}\sum_{i=1}^{n}\left(RA_i - \overline{RA}\right)^2 \tag{B.2}$$

Small σ_s^2 indicates that the results are tightly clustered around $\overline{RA}$ and we can be confident the $\overline{RA}$ is close to the E[RA]. On the other hand, if σ_s^2 is large, the results are widely dispersed around $\overline{RA}$ and we are less confident that $\overline{RA}$ is close to E[RA]. Instead of seeking a single value to estimate the E[RA], we can specify an interval of values that is highly likely to contain the true value of the parameter.

A probability of $1-\sigma_s$ is defined, an interval $\left[L(RA),\ U(RA)\right]$ is found such the probability is given by

$$P\left[L(RA) \le \mu_s \le U(RA)\right] = 0.95 \tag{B.3}$$

This interval contains the true value of the parameter with probability 0.95. Such an interval is a 95% CI.

Using Standard deviation and t-distribution table (since the number of measurements used is less than 30), the lower and upper limits of the CI are calculated using

$$L(RA) = \overline{RA} - \frac{t_{\left[\frac{0.05}{2}, d_f\right]} \times \sigma_s}{\sqrt{n}} \tag{B.4}$$

$$U(RA) = \overline{RA} + \frac{t_{\left[\frac{0.05}{2}, d_f\right]} \times \sigma_s}{\sqrt{n}} \tag{B.5}$$

where *n* is the number of measurements, d_f is the degree of freedom and is equal to *n*−1, σ_s is the standard deviation of the measurements.